

2010

Collection of endmembers and their separability for spectral unmixing in rangeland applications

Rolfson, David

Lethbridge, Alta. : University of Lethbridge, Dept. of Geography, 2010

<http://hdl.handle.net/10133/2527>

Downloaded from University of Lethbridge Research Repository, OPUS

**COLLECTION OF ENDMEMBERS AND THEIR SEPARABILITY FOR
SPECTRAL UNMIXING IN RANGELAND APPLICATIONS**

DAVID ROLFSON

Bachelor of Science, University of Lethbridge, 2007

A Thesis

Submitted to the School of Graduate Studies
of the University of Lethbridge
in Partial Fulfilment of the
Requirements for the Degree

MASTER OF SCIENCE

Department of Geography
University of Lethbridge
LETHBRIDGE, ALBERTA, CANADA

© David Rolfson, 2010

ABSTRACT

Rangelands are an important resource to Alberta. Due to their size, mapping rangeland features is difficult. However, the use of aerial and satellite data for mapping has increased the area that can be studied at one time. The recent success in applying hyperspectral data to vegetation mapping has shown promise in rangeland classification. However, classification mapping of hyperspectral data requires existing data for input into classification algorithms. The research reported in this thesis focused on acquiring a seasonal inventory of *in-situ* reflectance spectra of rangeland plant species (endmembers) and comparing them to evaluate their separability as an indicator of their suitability for hyperspectral image classification analysis. The goals of this research also included determining the separability of species endmembers at different times of the growing season.

In 2008, reflectance spectra were collected for three shrub species (*Artemisia cana*, *Symphoricarpos occidentalis*, and *Rosa acicularis*), five rangeland grass species native to southern Alberta (*Koeleria gracilis*, *Stipa comata*, *Bouteloua gracilis*, *Agropyron smithii*, *Festuca idahoensis*) and one invasive grass species (*Agropyron cristatum*). A spectral library, built using the SPECCHIO spectral database software, was populated using these spectroradiometric measurements with a focus on vegetation spectra.

Average endmembers of plant spectra acquired during the peak of sample greenness were compared using three separability measures – normalized Euclidean distance (NED), correlation separability measure (CSM) and Modified Spectral Angle Mapper (MSAM) – to establish the degree to which the species were separable. Results

were normalized to values between 0 and 1 and values above the established thresholds indicate that the species were not separable. The endmembers for *Agropyron cristatum*, *Agropyron smithii*, and *Rosa acicularis* were not separable using CSM (threshold = 0.992) or MSAM (threshold = 0.970). NED (threshold = 0.950) was best able to separate species endmembers.

Using reflectance data collected throughout the summer and fall, species endmembers obtained within two-week periods were analyzed using NED to plot their separability. As expected, separability of sample species changed as they progressed through their individual phenological patterns. Spectra collected during different solar zenith angles were compared to see if they affected the separability measures. Sample species endmembers were generally separable using NED during the periods in which they were measured and compared. However, *Koeleria gracilis* and *Festuca idahoensis* endmembers were inseparable from June to mid-August when measurements were taken at solar zenith angles between 25° – 30° and 45° – 60°. However, between 30° and 45°, *Bouteloua gracilis* and *Festuca idahoensis* endmembers, normally separable during other solar zenith angles, became spectrally similar during the same sampling period.

Findings suggest that the choice of separability measures is an important factor when analyzing hyperspectral data. The differences observed in the separability results over time also suggest that the consideration of phenological patterns in planning data acquisition for rangeland classification mapping has a high level of importance.

ACKNOWLEDGEMENTS

In acknowledgement of those who have helped and supported me throughout my work, the following thanks are deserved. I wish to thank my supervisor, Dr. Karl Staenz, co-supervisor, Dr. Craig Coburn, and committee members, Drs. Philippe Teillet and Anne Smith, for their help, expertise, and encouragement. I thank Dr. Robert Gauthier for agreeing to be the external examiner. I wish to include thanks to the staff at the Alberta Terrestrial Imaging Corporation (ATIC) for the provision of equipment, office space and assistance, namely: Dr. Jinkai Zhang, Dr. Nadia Rochdi, and Peter Eddy. Also, a big thank-you to everyone who helped me with the data collection: Kent Schonknecht, Christian Lutz, Trevor Armstrong, and Brian and Nicole (my brother and sister). Finally, I'm grateful to Brian, Matt, Dad and Mom for providing room and board when required, as well as encouragement. Finally, I am grateful to my wife, Jenni, and her support and encouragement through everything.

TABLE OF CONTENTS

ABSTRACT.....	III
ACKNOWLEDGEMENTS.....	V
LIST OF TABLES.....	IX
LIST OF FIGURES.....	X
LIST OF ABBREVIATIONS AND ACRONYMS.....	XII
1. INTRODUCTION.....	1
1.1 Background.....	3
1.2 Range Management.....	4
1.2.1 Invasive Species.....	5
1.3 Remote Sensing.....	7
1.3 Spectroradiometer.....	11
1.4 Endmembers.....	13
1.5 Spectral Mixture Analysis.....	14
1.6 Spectral Library.....	16
1.7 Phenology.....	18
1.8 Objectives.....	20
1.9 Hypotheses.....	21
2. METHOD.....	22
2.1 Species Selection.....	22
2.2 Study Area.....	23
2.3 Materials and Measurement Method.....	27
2.3.1 Equipment and Software.....	27
2.3.2 Sampling Procedure.....	32

2.4 Spectral Database.....	36
2.4.1 Database Organization.....	37
2.5 Endmember Creation.....	38
2.5.1 Digital Image Classification.....	40
2.5.2 Spectra Pre-processing.....	41
2.6 Separability Analysis of Green Plant Spectra.....	43
2.6.1 Euclidian Distance.....	44
2.6.2 Correlation Similarity Measure.....	44
2.6.3 Spectral Angle Mapper.....	45
2.7 Separability Analysis Incorporating Phenology.....	46
3. RESULTS.....	48
3.1 Collected Spectra and Spectral Library.....	48
3.2 Classification of Digital Images.....	50
3.3 Species Endmember Separability.....	53
3.4 Role of Phenology.....	58
4. DISCUSSION.....	64
4.1 Endmembers.....	64
4.2 Performance of Separability Measures.....	64
4.3 Spectral Separability.....	65
4.4 Phenology.....	68
5. CONCLUSIONS.....	70
6. FUTURE OUTLOOK.....	73
7. REFERENCES.....	75
APPENDICES.....	81
Appendix A: Summary of Field Measurements.....	81

Appendix B: Separability Over Time: Normalized Euclidean Distance Plots 83

LIST OF TABLES

Table 2.1: Rangeland species used for this study.....	31
Table 2.2: Measurement days arranged by comparison groups.....	47
Table 3.1: Confidence levels of sample spectra collected in the field.....	48
Table 3.2: Confusion analysis results.....	51
Table 3.3: Abbreviations used for identifying species in separability plots.....	54
Table 4.1: Phenology grouping of rangeland species and their phenological indicators.....	68

LIST OF FIGURES

Figure 1.1: Comparison of multispectral, hyperspectral, and laboratory spectra ...	9
Figure 1.2: A simplified description of a hyperspectral image	10
Figure 1.3: Blue grama reflectance spectra: green to senesced.....	19
Figure 2.1: The nine plant species studied for this thesis.....	23
Figure 2.2: Locations of study plots.....	24
Figure 2.3: LC study area.....	25
Figure 2.4: LRC study plots.....	26
Figure 2.5: The Galt site.....	26
Figure 2.6: The ASD FieldSpec 3 was used for all field measurements.....	27
Figure 2.7: A reference panel measurement.....	28
Figure 2.8: Screenshot of the Sun Position Calculator.....	30
Figure 2.9: Example of tripod and optical assembly and set-up.....	32
Figure 2.10: June grass after removal of surrounding vegetation.....	33
Figure 2.11: Photo of sample containing reference marks of spike heads.....	35
Figure 2.12: The organization of the database file structure.....	37
Figure 2.13: Example of jump in spectra at 1000nm.....	43
Figure 3.1: Detail of the SPECCHIO data form.....	49
Figure 3.2: Detail of the SPECCHIO metadata form.....	50
Figure 3.3: Classification examples using the SVM classification.....	52
Figure 3.4: Comparison of endmembers derived from the averages of spectral reflectances.....	53
Figure 3.5: Separability analysis results: CSM results.....	55

Figure 3.6: Separability analysis results: MSAM results.....	56
Figure 3.7: Separability analysis results: NED results.....	57
Figure 3.8: Wild rose, western wheatgrass, and crested wheatgrass spectra compared.....	58
Figure 3.9: Separability of the sample species: July.....	59
Figure 3.10: Comparison of band amplitudes of blue grama, Idaho fescue, June Grass, and crested wheatgrass.....	61
Figure 3.11: Comparison of band amplitudes of wild rose, western wheat grass, and crested wheatgrass.....	62
Figure 3.12: Separability of the sample species: September.....	63

LIST OF ABBREVIATIONS AND ACRONYMS

ASD – Analytical Spectral Devices
ASRD – Alberta Sustainable Resource Development
ASU – Arizona State University
AVIRIS – Airborne Visible and Infra-Red Imaging Spectrometer
CFOV – canopy field of view
CHRIS – Compact High Resolution Imaging Spectrometer
CSM – Correlation Similarity Measure
EO-1 – Earth Observing 1
FOV – field of view
GFOV – ground field of view
ID – identification number
LC – Lethbridge College
LRC – Lethbridge Research Centre
MNT – Minimum Noise Transfer
MSAM – Modified Spectral Angle Mapper
MSFF – Mars Space Flight Facility
NED – Normalized Euclidean Distance
NOAA – National Oceanic and Atmospheric Administration
NIR – near infra-red
NSPC – NOAA Sun Position Calculator
PRISMA – PRecursores IperSpettrale della Missione Applicativa
PTFE – polytetrafluoroethylene
ROI – region of interest
SAM – Spectral Angle Mapper
SMA – Spectral Mixture Analysis
SPC – Sun Position Calculator
SPOT – Satellite Pour l’Observation de la Terre
SVM – Support Vector Machine
SWIR – short-wave infra-red
USGS – United States Geological Survey
UTC – Coordinated Universal Time
VNIR – visible and near infra-red

Abbreviations for the plant species studied:

BG – blue grama
CW – crested wheatgrass
IF – Idaho fescue
JG – June grass
NT – needle and thread grass
SB – snowberry
SS – silver sagebrush
WR – wild rose
WW – western wheatgrass

1. INTRODUCTION

Rangelands are an important contributor to Alberta's economy and to its environmental health. Approximately 95,500 km², or 16%, of Alberta's land area is made up of rangeland (Castelli *et al.*, 2005). One of the most important uses of Alberta's rangelands is by ranchers for feeding their livestock. Ranching in Alberta is a \$30 billion industry¹ and up to 20% of the feed used for livestock comes from using rangeland areas for grazing. While providing feed to domestic livestock is important for Alberta's economy, rangelands also host a diverse collection of native plant and animal life (Mitchell and Somoliak, 1971; Owens and Myres, 1973; Olsen, 1994). A variety of unique plant and animal species live in Alberta's rangelands, including some that are endangered: the burrowing owl (*Speotyto cunicularia*), the peregrine falcon (*Falco peregrinus*), big sagebrush (*Artemisia tridentata*), and stiff yellow paintbrush (*Castilleja septentrionalis*) for example. The health of rangelands is important as it affects the ecological and economic well being of the plants, animals, and economies that depend on its sustainable management.

Maps are an invaluable source of information when it comes to planning for the future of rangeland areas. Mapping large areas, such as rangelands, is both costly and time-consuming (Booth and Tueller, 2003; Ustin *et al.*, 2004; Marsett *et al.*, 2006). One tool that has shown a degree of success in mapping large areas is remote sensing, which is the gathering of information about a target of interest without being in physical contact. Remotely sensed data can be acquired as digital images of the Earth's surface using sensors, mounted on a satellite or an airplane, that measure the intensity of reflected solar

¹ "Why Conserve Rangelands: Economic Vitality." Southern Alberta Land Trust Society. Accessed 25 July, 2010 <http://www.salts-landtrust.org>

radiation. Since the images are of a large area and are acquired from low Earth orbit, species identification is more difficult using these data than it would be on the ground. On top of the difficulty of telling species apart, plants are living organisms that react to their environment and are subject to changes in their physical appearance and to patterns of growth and spread as they compete and interact with each other. When mapping vegetation, rangeland managers (ranchers, parks stewards, conservation groups, etc.) are often interested in detecting the presence of one or more specific plant species. These species may include invasive plants (Underwood *et al.*, 2003; Lawrence *et al.*, 2006), native plants used for grazing (Marsett *et al.*, 2006), and/or indicator species (Rosentreter, 2001; Hunt *et al.*, 2003).

Invasive plant species are those coming from outside the local environment and are often introduced by human activities. If the plants are aggressive enough, they can quickly replace the plants that are native to the area, disrupting the diversity of the native plant population. Changes made to the plant population also affect native animal populations as food and shelter can become scarce (Sutter and Brigham, 1998; Heidinga and Wilson, 2002).

Indicator plant species are plants that are useful for gathering information about other aspects of an environment. One example of an indicator is sagebrush (of genus *Artemisia*), where its presence signals a specific climate, soil type and depth, and suggests what other plant or animal species are likely to be found in the vicinity (Rosentreter, 2001). If indicator species are detectable in an area, more data become available to profile that area, saving some of the time and resources required for field

campaigns that provide the same information (Dickinson and Dodd, 1976; Rosentreter, 2001).

The research conducted for this thesis was focussed on separating plant species by their reflectance. Reflectance data from a selection of plant species common to Southern Alberta were collected. The ability to distinguish between sample species reflectances was determined. The ability to differentiate between species using reflectance data gathered in the field may be useful in developing methods of rangeland monitoring and research using large-area hyperspectral data sets.

1.1 Background

Remote sensing has enhanced the ability to study vegetation by providing a synoptic view of the target of interest. Data acquired may give insight to the target vegetation's health and abundance, as well as information about the physical surroundings that may be contributing to its overall condition, including litter content and species encroachment (Asner and Lobell, 2000; Dennison and Roberts, 2003; Bennouna *et al.*, 2004; Kuemmerle *et al.*, 2006; Cheng *et al.*, 2007).

Rangelands are an important part of the environment as they reduce soil erosion by capturing and retaining moisture in their roots, sustain animal life by providing food and shelter, and act as ecological buffer zones (Lund, 2007). Rangelands are also vital to human activities. For example, 70% of the food consumed by domesticated grazing animals worldwide comes from rangelands.

Hunt *et al.* (2003) describe rangelands as areas of non-forested, native vegetation and highlight grasslands, savannas, and shrublands as examples. James *et al.* (2003)

stated that most rangeland areas are part of arid and semiarid environments and, therefore, are very sensitive to climatic and anthropogenic influences. They mention that there is a lack of commonly accepted methods of monitoring rangelands. Without common guidelines rangeland managers are left to their own arbitrary and subjective operation of stewardships and application of environmental protocols (James *et al.*, 2003; West, 2003).

1.2 Range Management

Range management is the planning and application of land use policies and practices specifically for improving the health and productivity of rangeland areas (Dyksterhuis, 1955; Stoddart, 1967). Management groups may work toward policies that have preservationist or conservationist goals or may lean toward modification of the land to increase its productivity or promote other uses on it (Smyth and Dumanski, 1993). When creating policies aimed at achieving their goals, management groups often turn to scientific research. In policy development, scientific researchers contribute to the areas of problem identification, strategy formulation in problem solving, setting standards and implementing policy, and monitoring and evaluating existing strategies (Norse and Tschirley, 2000). Information is needed to properly implement each step toward the creation of new, and the evolution of existing, policies. There are a number of important topics in which policies are being developed and in which rangeland composition and health play a large role (Rasmussen and Brunson, 1996; Pyke and Herrick, 2003).

Optimal management of rangeland systems has been a goal of conservation groups, researchers, and producers for a number of years (Stoddart, 1967), prompting

research in ecosystem modeling (Hanson *et al.*, 1988; Welk, 2004). Hunt *et al.* (2003) provided an overview of the potential impacts that remote sensing technologies can have on range management, including estimating biomass production, land cover monitoring, invasive species detection, and gauging the susceptibility of land to erosion. Modeling using remote sensing products and tools has been introduced to rangeland managers to assist them in decision making (Butterfield and Malstrom, 2006; Marsett *et al.*, 2006). In some cases the use of remote sensing products has resulted in more productive and healthier vegetation. For example, Butterfield and Malmstrom (2006) introduced the use of Landsat data to assist in land management decisions and weed control for livestock grazing operations. As a result, the larger operations saw a considerable improvement in their ability to control weeds, which led to an increase in forage quality.

Improvements to rangeland management practices have required researching and developing new monitoring methods in order to track rangeland dynamics. Knapp *et al.* (1990) compared large-scale aerial photographs to ground-based measurements of vegetation cover. They found that false-colour infrared photographs were better than true-colour photographs for identifying trees and cactus, and resulted in a more accurate vegetation inventory of the Organ Pipe Cactus National Monument. Moreover, Harris *et al.* (2003) successfully combined multispectral, hyperspectral and geographic information system (GIS) data to monitor grazing gradients for an area of rangeland.

1.2.1 Invasive Species

Invasive plants are introduced in a number of ways, including agricultural practices, establishing transportation corridors and unintended transmission through

travel. Once an invasive species is established in an area, it may expand geographically to new areas, carried by animals or the wind. The introduction of a new species to an area can have lasting effects. When left unchecked, (by controlled grazing and other practices) invasive plants can overrun a native population (Ogden and Rejmanek, 2005), thus reducing the diversity of plant life which then affects animal life due to decreased availability of food and/or cover (Sutter and Brigham, 1998).

Invasive species have been found to negatively affect a region's agricultural economy as well. One of the main issues of importance to rangeland managers is the ability to detect the presence and extent of invasive plant species so that they can be controlled. A study using data collected in the 1990s found that yellow star thistle (*Centaurea solstitialis*), an invasive plant in Idaho, was estimated to have cost that state's economy approximately \$12.7 million per year (Julia *et al.*, 2007). On the United States Department of Agriculture website, a document from the Maine Department of Environmental Protection introduces the problems of invasive plant species in the United States and Canada, specifically citing the hundreds of thousands of dollars spent annually by a handful of states to control invasive plant populations². It is estimated that damages and losses caused by invasive plant species in the U.S. alone total approximately \$137 billion per year (Pimentel *et al.*, 2002).

There is little information on the extent of the impacts that invasive species have on Alberta's economy. However, the Public Lands and Forests Division of Alberta alone spends between \$350,000 and \$500,000 per year on controlling invasive species in forests and rangeland areas. Other interested parties, such as the Alberta Association of

² "Costs of Invasive Species." Maine Department of Environmental Protection. Accessed May 4, 2010: <http://www.maine.gov/dep/blwq/topic/invasives/invcost.pdf>

Agricultural Fieldmen, have expressed concern over the current lack of control of invasive species populations due to a lack of resources (McClay *et al.*, 2004). Some problem species in Alberta's rangelands include: crested wheatgrass (*Agropyron cristatum*), downy brome (*Bromus tectorum*), purple loosestrife (*Lythrum salicaria*), Russian thistle (*Salsola pestifer*), and leafy spurge (*Euphorbia esula*).

Hyperspectral imagery has been used to detect invasive plants with a high accuracy in a number of cases (Underwood *et al.*, 2003; Lass *et al.*, 2005; Lawrence *et al.*, 2006). A method was developed to detect and monitor Chinese tallow (*Triadica sebifera*), an invasive plant to Louisiana, using sub-pixel modeling of hyperspectral image data from the Hyperion sensor (Ramsey *et al.*, 2005). Spectral unmixing results using the Compact Airborne Spectrographic Imager 2 (CASI-2) data showed an ability to consistently estimate and map yellow star-thistle populations on a regional scale in California (Miao *et al.*, 2006). Cheng *et al.* (2007) used the Minimum Noise Transform (MNT; Green *et al.*, 1988) and Spectral Angle Mapper (SAM; Kruse *et al.*, 1993) to analyze Airborne Visible and Infra-Red Imaging Spectrometer (AVARIS; Clark *et al.*, 1995) imagery and were successful in identifying kudzu (*Pueraria montana*) in Georgia.

1.3 Remote Sensing

Remotely sensed data about the Earth's surface are acquired using an active or a passive means (Jensen, 2007). Active remote sensing involves sending electromagnetic energy from a source and measuring a return signal. RADAR, which uses microwave energy, is an example of an active sensor. Passive remote sensing measures electromagnetic energy that is either emitted or reflected from a target. Optical sensors

are passive sensors that measure radiation in the visible to near infra-red (VNIR; 350 nm – 1000 nm) and short-wave infra-red (SWIR; 1000 nm – 2500 nm) ranges of the electromagnetic spectrum. The data are used to produce a digital image where each pixel is assigned the measured values from a specific area of the target surface.

Optical remote sensors are further classified by the size and number of wavelength ranges (bands) the electromagnetic spectrum their detectors measure and whether the bands are contiguous. Multispectral sensors use a few wide bands (3 or more bands 60 nm wide or more per band), which are not contiguous. Hyperspectral sensors have many narrow bands (a few hundred bands approximately 10 nm wide), which are contiguous (Jensen, 2007). For each pixel in an acquired digital image there is a set of values from the bands detected by the sensor used.

Optical sensors measure radiance, but surface reflectance is used for more reliable and repeatable results when analyzing target characteristics. Reflectance (r) is obtained by dividing radiance (L) by the magnitude of incident radiation, or irradiance (I) (Price, 1994)

$$r = \frac{L}{I}. \quad (1)$$

A graphical profile of target reflectance is created when the band values of a pixel are plotted. This is called a spectral signature or target spectrum. Multispectral sensor data will produce a spectral signature with very little detail while hyperspectral sensor data will result in a spectral signature with a high degree of detail (Jensen, 2007). Thus, when hyperspectral data is plotted, unique features in the spectrum are distinguishable and may be used as diagnostic features when comparing different target spectra. Figure

1.1 shows the difference between the spectral signatures produced using multispectral and hyperspectral data. Figure 1.2 is a simplified visualization of how hyperspectral data is acquired.

As rangelands often contain a large number of plant species, hyperspectral data holds more promising for accurate species mapping (Parker Williams and Hunt, 2004; Hutto *et al.*, 2006; Cheng *et al.*, 2007). Hyperspectral remote sensing technologies are useful for mapping because they can accurately classify a variety of targets in a mixed target setting, such as rangelands (Hirano *et al.*, 2003; Hunt *et al.*, 2003; Underwood *et al.*, 2003). Through continued research and development of technologies and analysis methods, hyperspectral remote sensing may become an integral part of invasive species monitoring in rangelands.

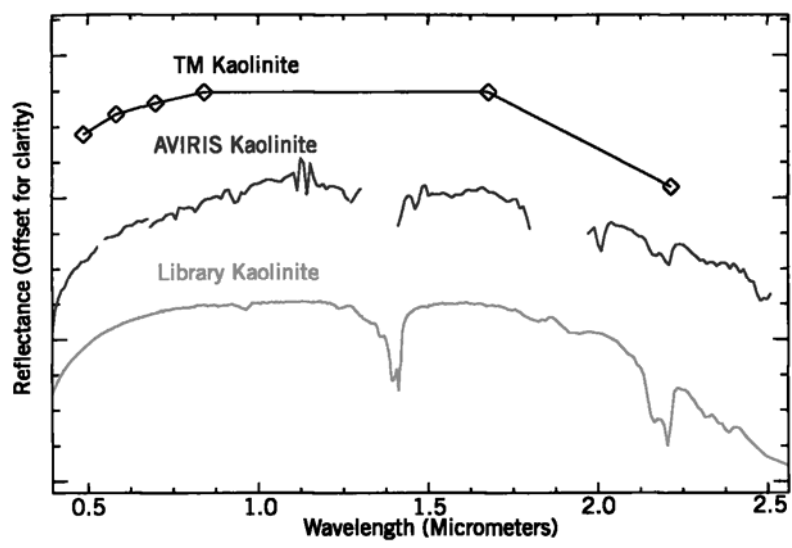


Figure 1.1: Comparison of spectra acquired with the multispectral sensor, Thematic Mapper (TM) on Landsat 5 (top), hyperspectral sensor AVIRIS (middle) and a laboratory measurement (bottom) (Chevrel, 2002).

Remotely sensed data are also collected *in-situ* at ground level using sensors that can be carried by a person or mounted on a vehicle such as a boom truck. *In-situ* means “in place” and, thus, implies that measurements and data are collected at the target site. Sensors used for *in-situ* data collection may include imaging sensors that collect images like those collected by sensors on board an aircraft or a spacecraft. They may also consist of spot measurements, which do not create an image, but merely a spectroradiometric measurement in the sensor’s field-of-view (FOV).

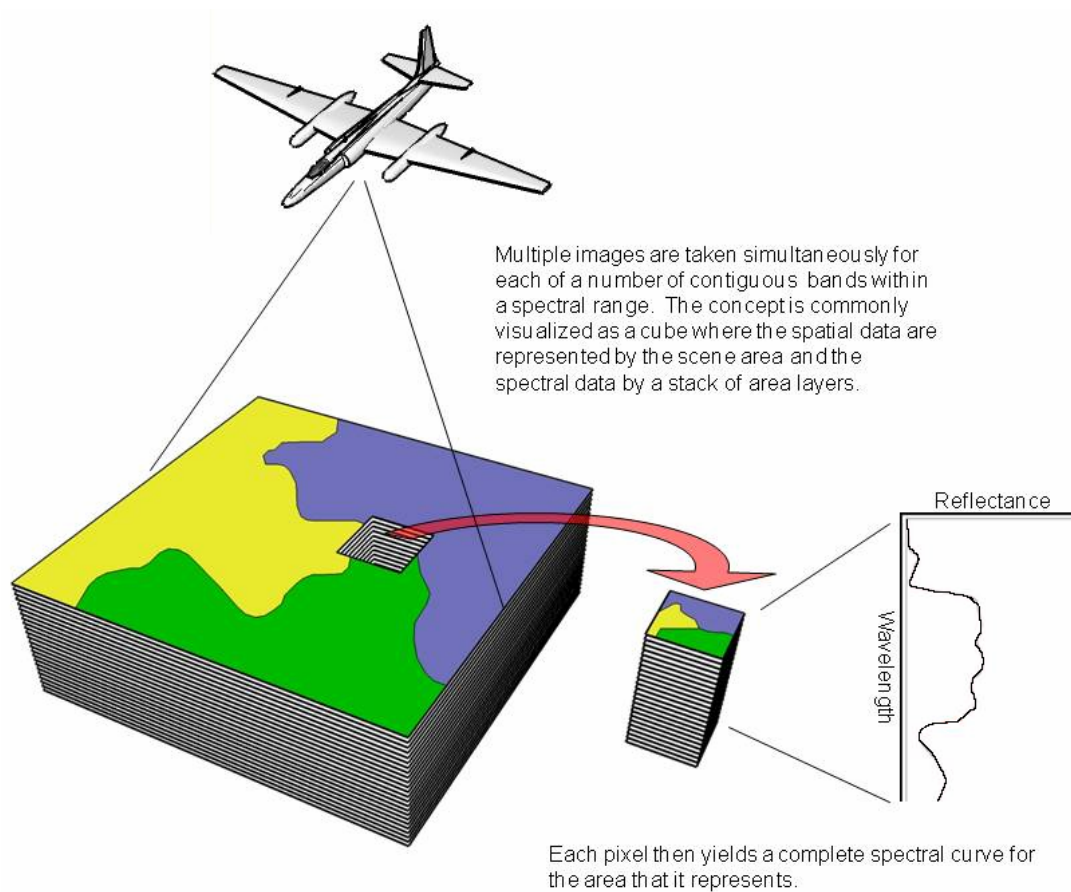


Figure 1.2: A simplified description of a hyperspectral image (Text modified from Jensen, 2007).

Hyperspectral data must be calibrated from raw digital counts to radiance and then combined with irradiance data to generate reflectance spectra at the sensor (Jensen, 2007). Computation of reflectance at the surface requires correcting for the effects of the atmosphere as well as the slope and aspect of the target area. The difference emerges with higher spectral resolution and band contiguity offered by hyperspectral sensors. While they allow greater flexibility in data analysis, they also require a more comprehensive approach to collect and interpret the data that are produced (Kerekes and Baum, 2003; Jensen, 2007).

The use of hyperspectral sensors, such as AVIRIS and Hyperion on the Earth Observing-1 (EO-1) satellite, is helping to improve the accuracy of land cover identification and discrimination (Underwood *et al.*, 2003). This higher level of spectral detail has allowed scientists to accurately detect specific species in areas of mixed vegetation. For example, AVIRIS has been used in determining differences in plant species found in California's chaparral communities (Dennison and Roberts, 2003) and detecting leafy spurge cover in Wyoming (Hunt and Parker Williams, 2006). Mirik *et al.* (2005a and b) used Probe-1 hyperspectral imagery to estimate biomass and nutritional values of forage in Yellowstone National Park, Wyoming.

1.3 Spectroradiometer

Spectroradiometers are instruments which are specially designed to measure radiant energy (radiance and irradiance). As hyperspectral imaging is still at an experimental stage when applied to Earth imaging, the data produced are often validated using measurements from a non-imaging ground-based spectroradiometer. Figure 1.1 also illustrates the high level of detail in spectra measured using a laboratory

spectroradiometer (Chevrel, 2002). Because conditions of data collection were different (e.g. illumination, sensor movement and stability, target to sensor distance, influence of adjacent targets) some spectrum features may differ, even while measuring the same target material. However, the diagnostic features are still present which will allow an accurate classification of the target material.

Portable or field spectroradiometers have made spectral data collection in the field a much easier process and have allowed for a higher degree of control over how a target is measured, especially when measurement of a specific, single target is desired (Shibayama *et al.*, 1986). For example, these instruments have been used to determine water quality in rice paddies in Japan (Shibayama *et al.*, 1993) and testing measurement methods for acquiring endmember data associated with crop cover (Peddle and Smith, 2005). Field spectroradiometers have been used from short distances of a few centimetres to longer distances of a few meters. For example, Zhang *et al.* (2005) measured lichens using the bare end of the fibre of an ASD FieldSpec FR which was centered one centimetre from the target. Price (1994) used a boom truck with a cherry-picker to raise a spectroradiometer to heights between 7 m – 10 m to measure crops for endmember production. The versatility of field spectroradiometers has also allowed them to be used as components of other devices employed in remote sensing applications. An example is the integrating of a field spectroradiometer with a portable goniometer for measuring bidirectional reflectance in field operations (Coburn and Peddle, 2006; Coburn and Noble, 2009).

1.4 Endmembers

Pixel values in remotely sensed airborne and satellite image data are the results of radiance from multiple components. The term endmember is used to describe the reflectance spectrum representing a unique scene component (Bateson and Curtiss, 1996; Tompkins *et al.*, 1997). Henceforth in this thesis, “spectrum” and “spectra” will refer to a reflectance spectrum and to reflectance spectra, respectively.

Pixels are frequently extracted from airborne and satellite images for use as endmembers and the rest of the image is classified based on these endmember pixels. However, the lower the spatial resolution of satellite imagery, the less likely a pixel is to be made up of a single component since the pixel encompasses a larger area. The use of a single pixel to generate an endmember does not truly conform to the theoretical definition of an endmember due to the likelihood that the pixels are still mixtures, whereas a true endmember would be the reflectance spectrum of a single component and not a mixture (Tompkins *et al.*, 1997).

Spectroradiometer data are also used in developing endmembers. Spectra are taken from samples of scene components in a laboratory setting or *in-situ*, a specific mineral or tree species for example, and stored together in a library (Roberts *et al.*, 1998; Peddle and Smith, 2005; Zhang *et al.*, 2005). The library is then usable with hyperspectral classifiers, such as spectral mixture analysis, to estimate sub-pixel quantities of the endmembers included in the analysis.

The majority of plants undergo seasonal and imposed changes: they flower, get eaten, get harvested, senesce, lose leaves, etc. Logically, a plant should have at least two endmembers to classify it, one for the stage at which it is fully green and one for the fully

senesced stage. If using field endmembers, flowers or fruits on the plant may require a third endmember (Price, 1994).

There are other inputs to consider when thinking about target separability. Target structure can have a significant effect on reflectance spectra (e.g., light transmission through or shadow from the target's own leaves, moisture content, etc.) to the point where two different species have reflectance spectra with so few differences as to make them spectrally inseparable, opening the way to ambiguous classification (Price, 1994).

The definition for a true endmember is highly unlikely to be satisfied when considering vegetation as a target. Vegetation endmembers are capable of evolving along with the conditions that affect the reflectance spectrum of a plant at any given time (Price, 1994; Dennison and Roberts, 2003).

1.5 Spectral Mixture Analysis

Spectral mixture analysis (SMA), or spectral unmixing, has been used successfully in different vegetation mapping applications, such as mapping stress caused by lack of moisture in wheat crops (Lelong *et al.*, 1998), detection of invasive species (Parker Williams and Hunt, 2004) and wetland monitoring (Schmid *et al.*, 2004). SMA is often used in the interpretation of hyperspectral data, which estimates the fractional abundances of a target material within a pixel. This is based on the concept of linear mixing in digital imaging; the spectral signature of a pixel is most often the amalgamation of the reflectance spectra of two or more components within the area that the pixel represents. There are two mixing models used when analysing remotely sensed data: linear mixing and non-linear mixing. When treating a spectrum as a linear mixture, it is regarded as the

combination of direct reflectances from the components found within the view area as well as an error term.

Accordingly a linear mixture is mathematically described as follows:

$$R_b = \sum_{i=1}^m f_i r_{bi} + e, \quad (2)$$

where:

$$\sum_{i=1}^m f_i = 1.0 \quad \text{and} \quad 0 \leq f_i \leq 1, \quad (3)$$

R_b is the total pixel reflectance in a band (b), $f_i r_{bi}$ represents the reflectance (r_b) of component (endmember) i taking up a fraction (f_i) of the pixel, m is the total number of components and e_b is the error term (Staenz *et al.*, 1999). Equation 3 represents a constrained linear model. Non-linear unmixing is less straight-forward as the concept rests upon radiated energy taking an indirect route before being measured at the sensor (Borel and Gerstl, 1994) or sub-pixel components with a spectral response having a disproportionate effect on pixel values (Foody *et al.*, 1997). Due to the difficulties encountered when a non-linear model is employed, linear unmixing is widely used as it is much easier to compute and provides accuracies that are adequate in many applications (Dennison and Roberts, 2003).

Rangeland areas have proven to be difficult to monitor as they are often highly variable in the types and species of vegetation covering a given area. This difficulty extends to the use of remotely sensed data to identify endmembers within a pixel (Asner *et al.*, 2000; Asner and Heidebrecht, 2002). SMA assumes that all materials have unique spectral characteristics and, thus, a specific spectroradiometric response. Classification is further complicated when one or more components (such as vegetation) can have several

possible spectroradiometric responses resulting from structural and/or chemical changes within the target, such as plant growth or senescence (Shaw and Burke, 2003).

Therefore, more than one endmember should be collected for these materials in order to properly account for different reflectances from the same component types.

1.6 Spectral Library

The information included in data collected for land cover studies ranges from spectral measurement files to manual measurements to digital photographs of collection sites. It is necessary to develop a method of storing these data in a way that is both efficient and easy to use. In the remote sensing and spectroscopy community, digital libraries are created to store and organize spectral data, in a way similar to a database and are also referred to as spectral databases (Hueni *et al.*, 2007). These data may be spectra collected from naturally occurring samples (*in-situ*) and from samples prepared and measured in a laboratory setting, as well as endmembers derived from imagery.

Although the libraries are similar in their organizational use to a database, not all have the functionality of a database as is discussed at the end of this sub-section.

One of the most extensive spectral libraries open for public use is the United States Geological Survey (USGS) spectral library (Clark *et al.*, 2007). As the entries in this library are often used in unmixing exercises, much research has gone into acquiring pure endmember spectra and their associated metadata for a number of natural and man-made substances. Metadata additions include digital images, coordinates of sample location, chemical formulas (for mineral samples), and measurement environment (for vegetation samples). The online USGS spectral library includes spectra, ASCII files

listing reflectances, and metadata describing the samples and sampling methods; a few samples include digital photographs. However, as large as the online USGS library is, its main focus is on mineral spectra; the section containing vegetation spectra is populated by only a few examples of vegetation spectra. Moreover, the online USGS library is inconvenient to use as it requires manual searching for desired targets within an extensive listing of all available spectra.

Other publicly available spectral libraries found online include the ASTER Spectral Library³ (Hook, 1998) and a spectral library hosted by the Mars Space Flight Facility (MSFF) at Arizona State University (ASU)⁴ specifically intended for endmembers found in the Martian landscape. Both of these libraries also focus on mineral spectra, containing little or no spectral information on plants. These examples illustrate the need for extensive research and development of spectral libraries dedicated to the collection of data for use in vegetation studies. Creating a spectral library database specifically for vegetation spectra would be a more difficult process than it is to build one for minerals as plants undergo physical changes in response to changes in local weather and as they age (Ustin *et al.*, 2004). To account for the condition of vegetation at the time of data acquisition, increased attention to metadata, such as recent precipitation or other weather events, may be necessary to fully explain the spectral responses of samples. To properly represent the variation in plant spectra, more measurements would be required to produce endmembers for individual species at different phenological stages (Dennison and Roberts, 2003).

³ Hook, S.J. (1998). "Aster Spectral Library." Retrieved March 4, 2010 from <http://speclib.jpl.nasa.gov/>.

⁴ "Spectral Library: Version 1.0." Retrieved March 4, 2010 from <http://speclib.asu.edu/>.

If researchers cannot find the data they need from one of these online sources, the next alternative is to build their own library. The University of Zurich has developed a spectral library program called SPECCHIO using Java and MySQL (Hueni *et al.*, 2009). SPECCHIO can be accessed online and a user can extract data from an existing library or build their own library with their own collection of data. As SPECCHIO is built on a database platform, it includes database functionality allowing automated data queries as well as the ability to perform a handful of simple adjustment calculations, such as the application of reference panel coefficients.

1.7 Phenology

Plant phenology is the study of the lifecycle of vegetation. Contributors to the phenological process include available moisture and nutrients, sunlight and temperature, and plant age (Dickinson and Dodd, 1976). In their research, Dickinson and Dodd (1976) found that, although there are some species that can be grouped together in a similar phenological sequence, there are many that cannot be easily grouped, having a variety of responses to changes in local climate and nutrient availabilities. These changes also affect the attributes of plant spectra over the course of the plant's growth and senescence stages. Figure 1.3 is an example of this change typical in vegetation.

Studies investigating methods for vegetation monitoring strongly suggest the importance of including plant phenology as an integral classification parameter. Vanamburg *et al.* (2006) tested the effects of phenology on the estimation of green biomass from images taken using a digital camera. They found that the omission of

phenological interaction in their classification model resulted in significantly less accurate biomass estimations.

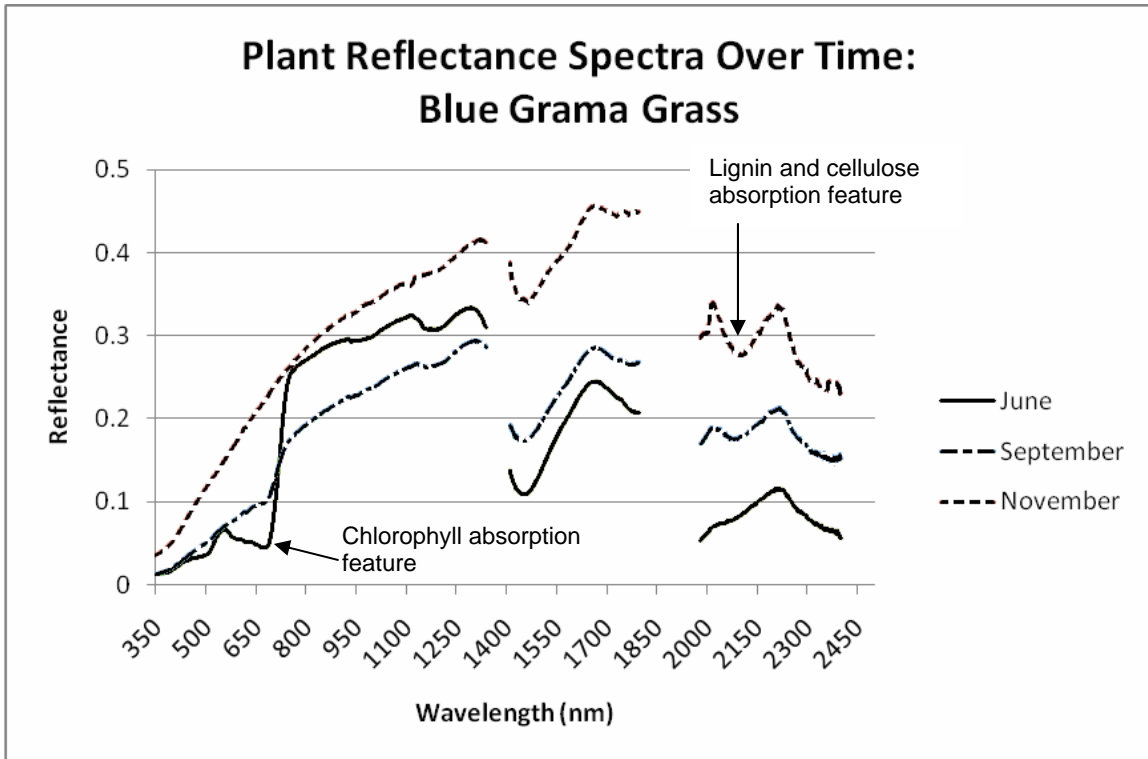


Figure 1.3: Changes to blue grama reflectance spectra as a result of its phenological progression. The green peak (530 nm) and the chlorophyll absorption trough (670 nm) are lost as the plant senesces and reflectance increases across all portions of the spectrum. Also visible is the appearance and increase of the cellulose and lignin absorption feature around 2100 nm, resultant of decreased plant moisture.

As the phenological stages of a plant do not follow a rigid schedule, differing stages of the same plant type exhibiting different spectral properties may be present in the same image. It is then logical that integrating endmembers that appropriately reflect the phenological stage of targeted vegetation in an analysis would result in a more effective classification model. Dennison and Roberts (2003) explored the effects of phenology on mapping chaparral in southern California, using imagery from five different dates in order to recognize where patterns of class confusion change over time. By introducing

multi-temporal data to the classification model, a greater amount of land cover area was classified with up to 90% accuracy. The images used by Dennison and Roberts were spread over five years with one image per year. Although the image data were from different years, there were two images obtained in May, one obtained in June, and two in September. Even with the split in years, the differences caused by the phenological stages for each month are visible in the endmembers extracted from each image.

Classification using SMA may be confused by the apparent spectral similarity between plant types during certain periods when attempting to classify vegetated areas. However, the introduction of a time series to the process allows plant phenology information to lessen the confusion of plant type in a classification model as certain plants grow and senesce differently in relation to each other (Dickinson and Dodd, 1976; Dennison and Roberts, 2003; Karnieli, 2003; Delalieux *et al.*, 2009).

1.8 Objectives

The objectives of this thesis were to collect data for the establishment of a spectral library and to assess the separability of some of the more prominent rangeland plant species common to southern Alberta based on *in-situ* measurements of their reflectance characteristics. In assessing the separability of rangeland species, the species samples were compared at the peak of the season (when all the plants were green). Samples taken throughout the season were then compared to discover what effect phenology would play on the ability to separate them by their reflectances. The separability of scene components is a necessary step in designing a method to distinguish and map rangeland

using multispectral and hyperspectral imagery alike. In this case, the focus is on species separability using hyperspectral data.

1.9 Hypotheses

There are two main hypotheses tested in this thesis. The first is that sample species of rangeland plants are separable by reflectance spectra from data collected *in-situ*. The second is that the phenological characteristics of rangeland species can help reduce confusion when classifying rangeland plant species.

2. METHOD

2.1 Species Selection

Information about the grasses existing in southern Alberta was found using field guides produced by Alberta Sustainable Resource Development (ASRD) (Adams *et al.*, 2003 and 2004). These guides list all native plant species and their abundances within the mixed-grass (40 survey areas) and foothills fescue (30 survey areas) regions of Alberta. Species to be considered for this study were chosen based on the frequency with which they appeared at the ASRD survey sites and their abundances at those sites. Nine rangeland plant species were studied for this thesis including western wheatgrass (*Agropyron smithii*), blue grama (*Bouteloua gracilis*), Idaho fescue (*Festuca idahoensis*), June grass (*Koeleria gracilis*), needle-and-thread grass (*Stipa comata*), silver sagebrush (*Artemisia cana*), snowberry (*Symphoricarpos occidentalis*), wild rose (*Rosa acicularis*), and crested wheatgrass (*Agropyron cristatum*). While the others are native to Southern Alberta, crested wheatgrass is a wide-spread invasive species and has been the subject of other studies focused on invasive species detection (Heidinga and Wilson, 2002; Zhou, 2007) and was chosen for separability comparison.

There were three sample species measured at three study areas. Sample photographs of the plant species chosen are given in Figure 2.1. A summary of measurements with all dates, solar zenith angle ranges, and comments can be consulted in Appendix A.

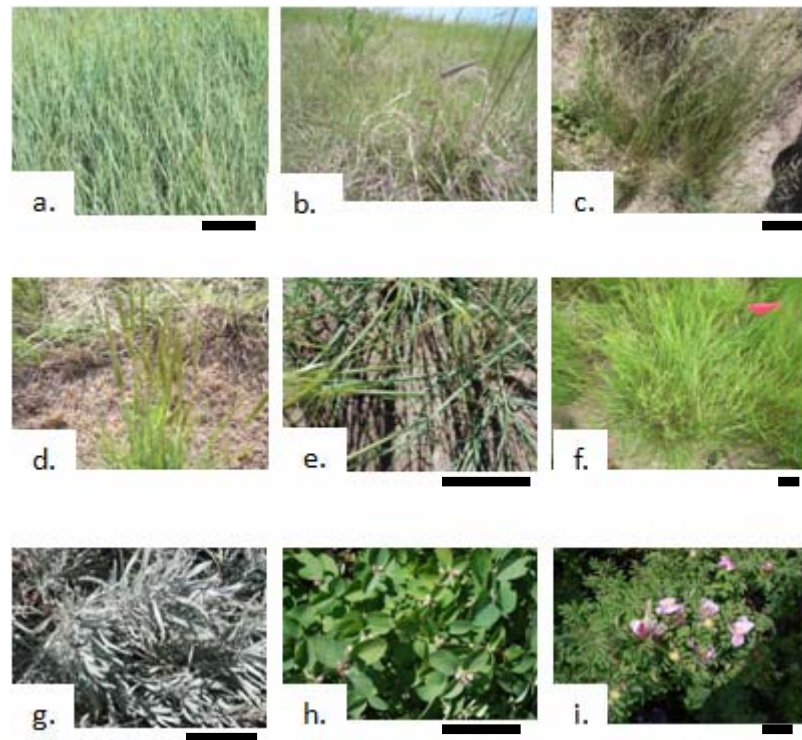


Figure 2.1: The nine plant species studied for this thesis include a. *Agropyron smithii* (western wheatgrass), b. *Bouteloua gracilis* (blue grama), c. *Festuca idahoensis* (Idaho fescue) d. *Koeleria gracilis* (June grass), e. *Stipa comata* (needle-and-thread grass), f. *Agropyron cristatum* (crested wheatgrass, an invasive species), g. *Artemisia cana* (silver sagebrush), h. *Symphoricarpos occidentalis* (snowberry), and i. *Rosa acicularis* (wild rose). Images photographed from overhead (length of black bars to lower right of images represents 10 cm) except b and d which were photographed to detail seed heads.

2.2 Study Area

The sites chosen for measurement purposes included one area containing planted native grass plots under the care of the Agriculture and Agri-Food Canada's Lethbridge Research Centre (LRC; 49°41'45.29"N, 112°45'57.65"W), another area containing planted native grass plots formerly used by the Lethbridge College (LC; 49°42'5.17"N, 112°44'14.67"W), and a third site containing growths of the three shrubs close to the Galt Museum in Lethbridge (49°41'33.12"N, 112°50'51.67"W) (Figure 2.2). The general soil type for the area encompassing the study areas is Dark Brown Chernozemic with a clay loam texture.

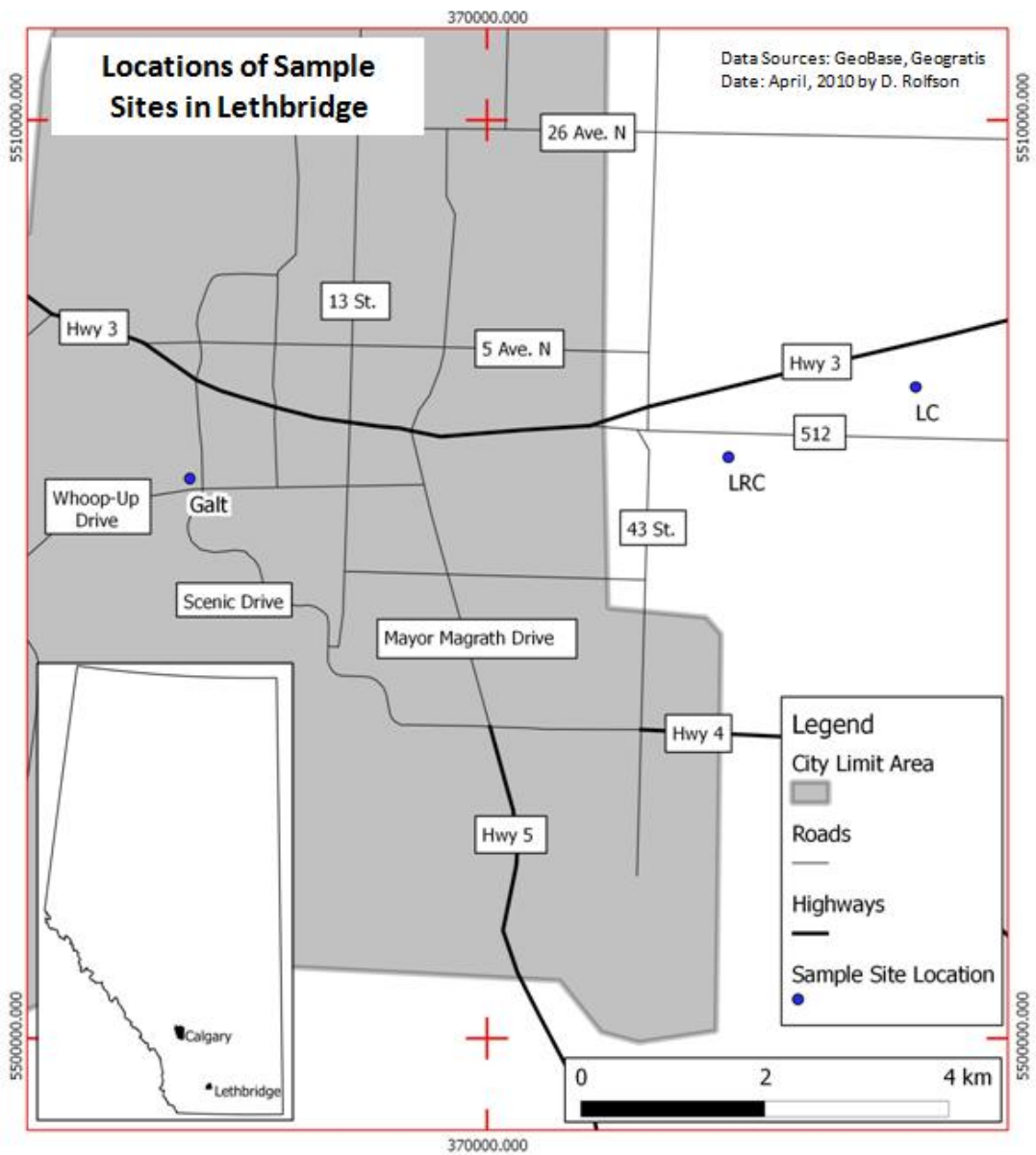


Figure 2.2: Locations of sample sites used for collection of spectra in the vicinity of Lethbridge, Alberta.

The LRC and LC sites were both located on open prairie land. However, the presence of rangeland grasses at the sites was obviously planned and the ground was cultivated and seeded to raise the grasses of interest to the institution’s purpose.

Although these sites were chosen because they had, at one time, been planted as homogeneous plots, the LC site (Figure 2.3) had not been tended in a number of years, and the more aggressive plants had spread throughout all of the plots. The LRC site (Figure 2.4) was still tended and minimal encroachment had occurred. As there had been encroachments of other plant species into the plots, spectra were measured from single plants or small bunches to reduce the influence of the other plant species.



Figure 2.3: LC study area.

The plants at the Galt site were naturally occurring (Figure 2.5). The site was 30 m to the west of the Galt Museum building. As a result, some morning measurements could not be completed in the fall as the building blocked the sun at the time.

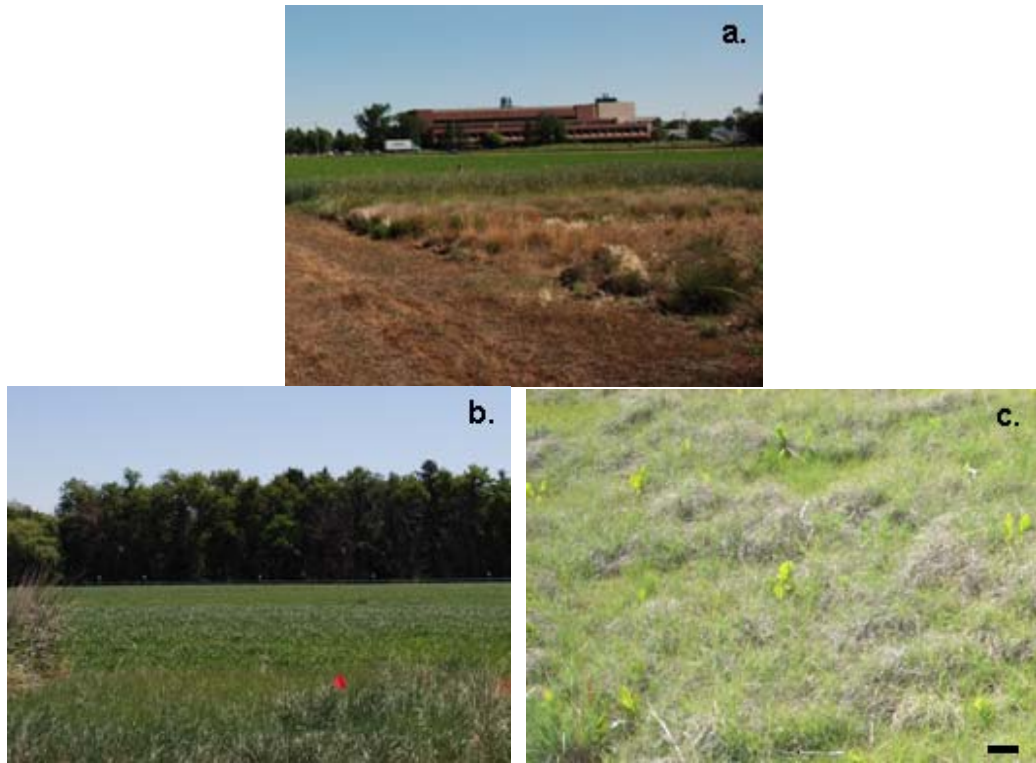


Figure 2.4: Looking north-east and east respectively on LRC study plots showing (a) the Idaho fescue plot, (b) western wheatgrass plot, and (c) blue grama (the black bar represents 10 cm ground distance).



Figure 2.5: The Galt site, showing some silver sagebrush branches in the foreground and snowberry bushes.

2.3 Materials and Measurement Method

2.3.1 Equipment and Software

The Analytical Spectral Devices FieldSpec 3 (ASD, 2007), as shown in Figure 2.6, was used to collect the spectra of the sampled plants. The instrument's FOV was circular, simplifying the initial placement of the assembly for measuring an area with as little background (soil) as possible within the FOV. It has a wavelength range of 350 nm to 2500 nm and a spectral resolution of 3 nm in the VNIR portion of the spectrum and 10 nm in the SWIR portion. Reference measurements of reflected irradiance were collected using a Spectralon™ sintered polytetrafluoroethylene (PTFE) reference panel to estimate downwelling irradiance and convert the target radiance to reflectance (Figure 2.7).



Figure 2.6: The ASD FieldSpec 3 was used for all field measurements. It features wireless communication with controlling laptop, fibre optic cable directly integrated with the sensor, and a 25° FOV (may be modified using different foreoptics).

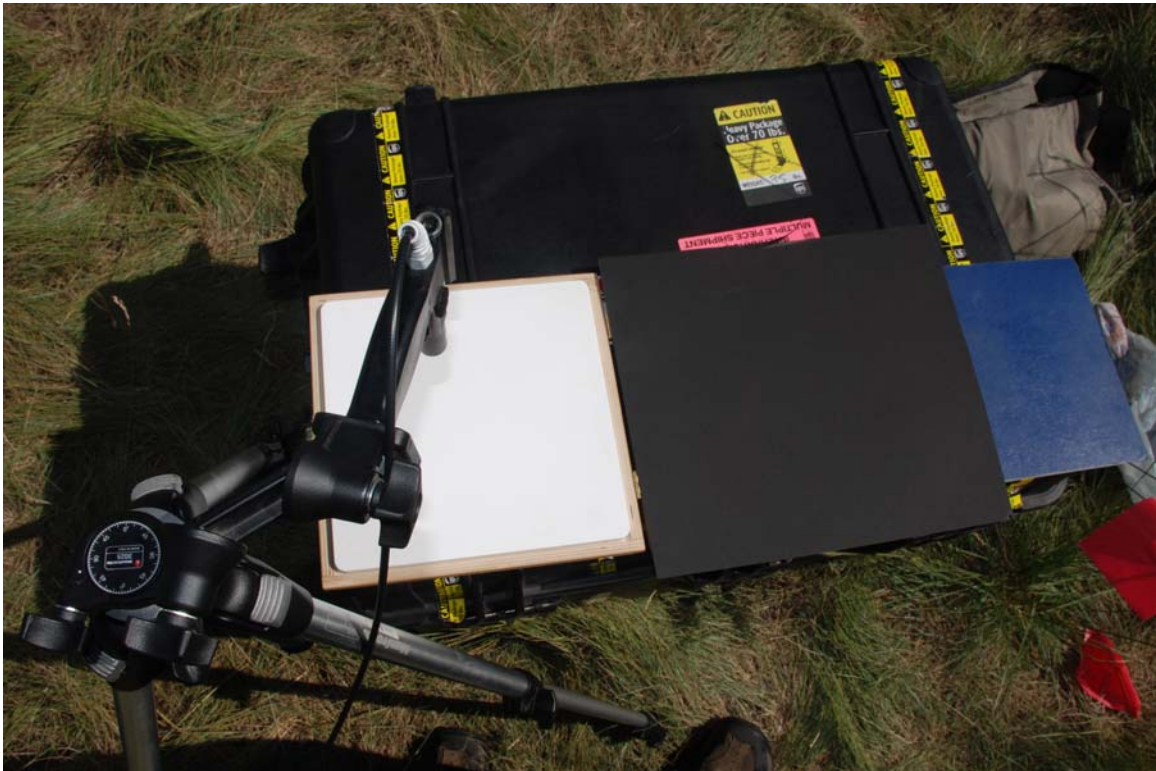


Figure 2.7: A SpectralonTM panel measurement was collected before and after each measurement interval, which took place at predetermined times based on the solar zenith angle.

To account for changes in solar position and intensity, and to determine if these changes had a significant effect on the results of the separability measures used, measurements were made at pre-determined solar zenith angles. Sample measurement occurred when the solar zenith angle was a multiple of five over the duration of a field visit. In order to measure at the chosen angles, the times that they occurred were required for each day of sample measurement.

Time of day information for pre-determined solar zenith angles was calculated using the Sun Position Calculator (SPC) version 1.2 as shown in Figure 2.8 (Volkan-Kasco and Neda, 2003). Results were checked for accuracy against the National Oceanic

and Atmospheric Administration (NOAA) Sun Position Calculator (NSPC; Cornwall *et al.*, 2008). The SPC would not have been necessary if the NSPC had the ability to calculate the time of day from a given solar zenith angle, but it was only programmed to use the day and time as input to calculate the solar zenith. Adjustments were made to any differences between the two results with a bias toward the NSPC as it has been continually maintained and updated. Measurement times were rounded to the nearest minute. Accuracy of calculated solar zenith times was also verified at random intervals using the clinometer functionality of a Brunton Eclipse 8099 compass. Clinometer accuracy was $\pm 3^\circ$ of slope.

Solar azimuth would also influence spectral readings by altering the amount and distribution of shadow that the sample casts on itself. However, as similar effects would also be introduced with sample movement by winds between and during spectral captures and as incoming solar energy is more greatly affected by solar zenith angle, the solar azimuth was disregarded.

For collecting *in-situ* spectral measurements, the ASD was carried on a backpack with the fibre inserted in the pistol grip, which was mounted on a tripod. Depending on the FOV of the foreoptic, and the basal area of the sample, the tripod height was adjusted to maximize the fraction of the target plant while maintaining a minimum amount of background material (soil) within the FOV, which resulted in different distances from canopy to foreoptic. Hence, the distance from canopy to foreoptic at each sample was measured and recorded (Table 2.1) and the FOV at the canopy (CFOV) was calculated. The ground to foreoptic distance was kept the same within each species group (for example the same tripod height was used for all measurements of blue grama grass) to

keep the same ground FOV (GFOV). Some of the CFOV sizes (Table 2.1) seemed to be on the small side. However, lighting and shade visible in subsets of the sample images used for unmixing (Chapter 3.2) were good approximations of sample conditions observed in the field.

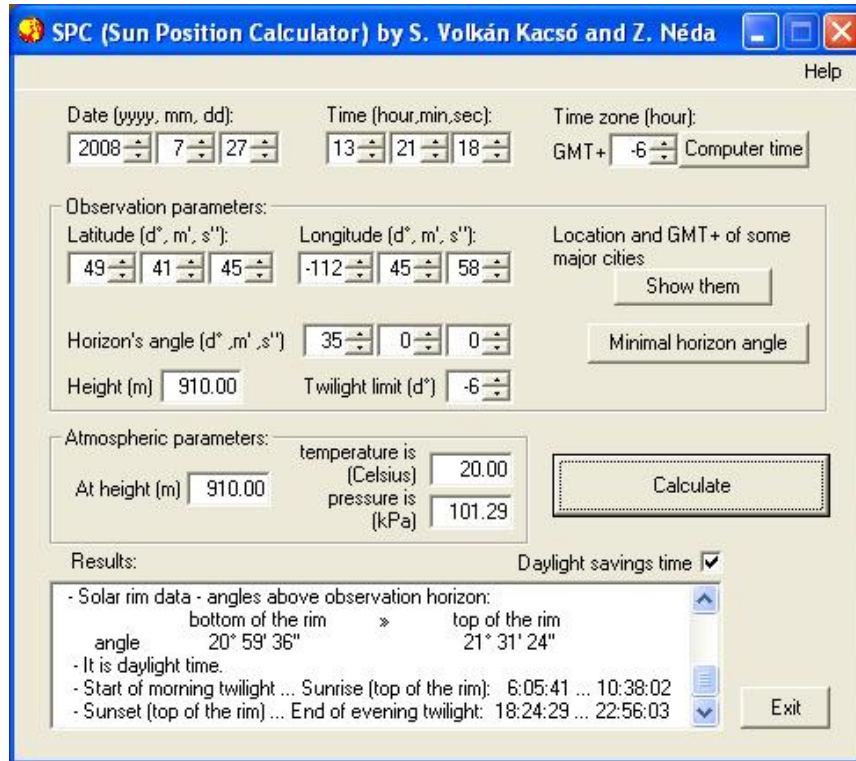


Figure 2.8: Sun Position Calculator (SPC) interface used to determine measurement times. The desired solar zenith angle is entered in the "Horizon's angle" area (along with Date, Time zone, Latitude and Longitude, etc.). The times are printed in the "Results" box (not corrected and corrected for refraction). In this example, on July 27, 2008, a solar zenith angle of 55° takes place at 10:38 and 18:24.

Table 2.1: Rangeland species used for this study, FOV foreoptic used (in brackets), distance to the target and the resulting CFOV.

Target name (FOV)	Distance to target (cm)			CFOV diameter (cm)		
	Sample 1	Sample 2	Sample 3	Sample 1	Sample 2	Sample 3
<i>Western wheatgrass</i> (8°)	22	23	--	9.8	10.2	--
<i>Crested wheatgrass</i> (8°)	30	38	39	13.3	16.8	17.3
<i>Blue grama</i> (8°)	27	27	28	12.0	12.0	12.4
<i>June grass</i> (8°)	37	41	40	16.4	18.2	17.7
<i>Idaho fescue</i> (8°)	19	21	20	8.4	9.3	8.9
<i>Needle-and-thread</i> (8°)	45	40	--	20.0	17.7	--
<i>Snowberry</i> (25°)	16	34	26	7.1	15.1	11.5
<i>Silver sagebrush</i> (25°)	27	23	17	12.0	10.2	7.5
<i>Wild rose</i> (25°)	14	--	--	6.2	--	--

As each site held a number of samples, it was necessary to move the instrument between samples to get a measurement for each predetermined solar zenith at each sample. To reduce the error introduced by the rotation through samples, 25-cm spikes were marked with surveyor's tape and driven into the ground at the points where the tripod feet rested after its height and positioning were established and remained until the end of the season (Figure 2.9). The length of the tripod legs and the height of the centre column were also determined and remained constant for each sample site. Thus, the tripod could be set up multiple times throughout the season to measure the same GFOV area for each sample.

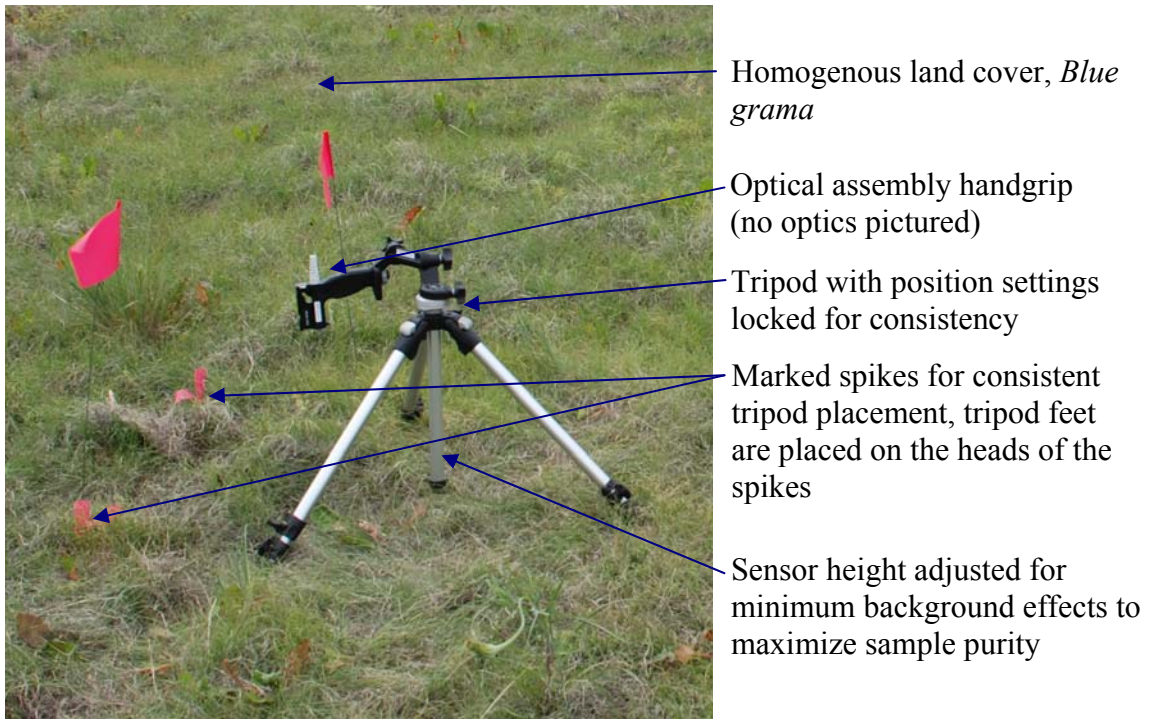


Figure 2.9: Example of the tripod and optical assembly set-up.

2.3.2 Sampling Procedure

At the commencement of the data collection period, samples were identified and marked with survey flags. Each sample was prepared by removing all vegetation not of the same species as well as all senesced material in and around the sample (Figure 2.10). Throughout the remainder of the season, any new growth not immediately attached to the sample was removed before measuring, and the samples were allowed to senesce and the senesced material was left intact.



Figure 2.10: June grass after all other vegetation and litter is cleared in preparation for measurement. The circled area represents the CFOV. Being sample 1, the CFOV is 16.4 cm in diameter (Table 2.1).

As the objective was to measure all plants as closely to the calculated times as possible, a specific route of travel was established to move the equipment between each sample site as quickly as possible. A reference spectrum (reflected irradiance) was obtained using a SpectralonTM near-Lambertian reference panel as the target before and after a cycle of measurements. At each sample site, the tripod with foreoptic was placed on the position marked by the spike heads. The instrument arm holding the foreoptic was adjusted and levelled using the built-in level on the pistol grip so that the measurements were made at nadir. Five spectral readings were taken at each sample location as there was often a breeze that would move the grass/shrub during measurement, effectively

adding an averaging effect to the measurements. The distance from the foreoptic to the target canopy was measured and recorded (Table 2.1). After the five spectra were collected a photograph was taken of the sample site. The camera was positioned to centre the lens on the vertical axis of the foreoptic cable. The tripod assembly was then removed for an unobstructed view of the sample from nadir and a photo was taken with its corresponding image identification number (ID) manually recorded with the five spectrum IDs. The equipment was then moved to the next sample spot. After each cycle of measurements another reading of the SpectralonTM panel was taken. One cycle normally took approximately 20 minutes.

The 8° FOV foreoptic was used for the grass samples and the bare fibre (25° FOV) for the shrub samples. The foreoptic was used on grass samples as its smaller GFOV allowed measurement from above the canopy without capturing too much of the surrounding vegetation and soil. The bare fibre was used to measure the shrubs as they covered enough ground that the larger angle FOV did not pose a problem with including unwanted components.

Data collection was only carried out on days with less than 10% cloud cover, totalling 18 days. As only one study area could be covered in a day, the field collection days had to be divided between the three locations. Accordingly, each area was visited at least five times throughout the field season from June 27 to November 10, 2008.

The GFOVs were calculated using references in the photographs such as the distance between the marked spikes, upon which the tripod legs were positioned, or the distance across the head of one spike (where only one was visible in the photo) (Figure 2.11). These reference distances were recorded for each site. In later trips to the field

sites, photographs were taken at the samples with a tape measure clearly visible as a reference. Using these references, the pixel distance in the photographs was calculated and also used to mark the edges of the GFOV within the images. Image distances were then converted to pixel distances using the ENVI measurement tool. Thus, reference distances not orthogonal to the pixel alignment were automatically calculated in fractions of pixels.



Figure 2.11: Photo of sample containing reference marks of spike heads (circled) to the left and right of the sample marked with strips of surveyor's tape.

In most cases, the centre of each photo coincided with the centre of the GFOV. To find the edges of the GFOV, each GFOV radius (Table 2.1) was measured from the centre of the image using the ENVI measurement tool. The center of the GFOV was also verifiable in some of the images using measurements from the spike heads to the GFOV center. Other points of reference found in the images were also employed in a similar manner to verify that the calculated GFOV had acceptable accuracy and to better

calculate it in the earlier photographs for comparison with the later ones. The FOV at the canopy level was calculated for shrub samples, since the ground could not be seen. Accordingly, the GFOV is equivalent to the canopy FOV of the shrub samples.

Spectral measurements were started during the time of peak greenness in the growing season. Soil spectra were taken at each site for use as endmembers in the classification analyses of the sample plants.

Other spectra were taken for inclusion in the spectral library as time and measurement conditions permitted, including other plant species, some plant mixtures, soils, and some completely shaded portion of the samples mentioned. Some of the targets included were downy brome (*Bromus tectorum*), a thistle (species not identified), foxtail (*Hordeum jubatum*), green needle grass (*Stipa viridula*), a red shale walking path, and grass mixtures.

2.4 Spectral Database

The spectral database program SPECCHIO (Hueni *et al.*, 2009) was chosen as the storage database for the collected sample spectra. SPECCHIO was developed by the Remote Sensing Laboratory at the University of Zurich. Its functions are programmed using the Java language, and it employs MySQL as the storage database. SPECCHIO provides the primary function of data storage, but adds to that function a more dynamic platform allowing for further analysis of the data it contains. The features that take advantage of the more dynamic database include data plotting, application of reference panel coefficients for corrections, and automatic generation of metadata (including sun angle calculation). Further improvements include the ability of SPECCHIO to read

spectral information saved in the file types used by some of the different brands of spectroradiometers. Moreover, it allows for data to be imported from certain types of text files (.csv for example) following a specified format.

2.4.1 Database Organization

The SPECCHIO database required a degree of preparation before populating the database. A hierarchy of folders was created to efficiently organize the spectra collected with the ASD. The hierarchy used a species-date-sample structure (Figure 2.12). This seemed to provide the most user-friendly organization of the data as a species type would likely be the most common discriminating factor. SPECCHIO was then set to read in the data from the file structure making up the hierarchy.

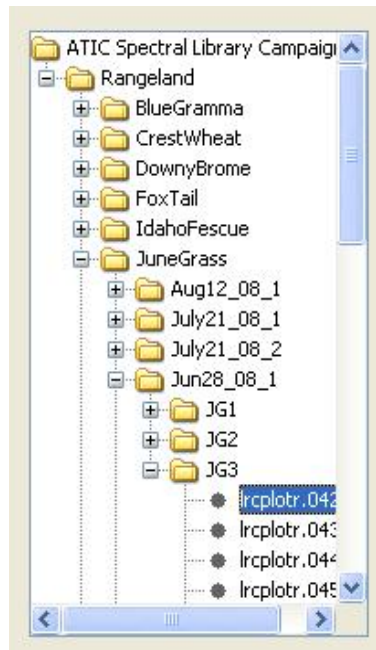


Figure 2.12: The organization of the database file structure for a specific land cover type, species, date, sample and individual spectrum.

With data read into the SPECCHIO structure there remained a number of items to be entered manually as they were not recordable by the ASD. These ancillary data included sample type, sample coordinates, illumination type, and instrument used. In a next step, the digital photographs of the samples were matched to the spectra. To save space, only one image was used per sample per collection day.

SPECCHIO includes the ability to apply certain corrections or adjustments to metadata for all spectra or for specified groups. Applied to these data were two of these adjustments. In a first step, as the program expects temporal information in Coordinated Universal Time (UTC), there is a function included to adjust the time stamp originating with the instrument used during data collection. This was used to align the data collection times to UTC. Secondly, the program was able to calculate the solar zenith angle for each measurement (which confirmed the time-of-day calculations made when planning the field measurements).

2.5 Endmember Creation

There was some deliberation on the question of how endmembers in this study should be defined as discussed in Chapter 1.5. However, to satisfactorily test the hypothesis that phenological data could assist with separability of rangeland species, it seemed most logical to get spectra from the same plant samples throughout the season in order to obtain a more realistic data set to illustrate phenological progression. This meant that plant structure would remain intact and would change as the plants matured.

The data resulting from all of the components of the target plant were treated as the endmember for that species. However, since the measurements were conducted *in*

situ to include the structural properties of each sample species, there existed spaces between leaves and stems where other target materials such as soil may have contributed to the spectral signature of a species sample. Also, there were two endmembers desired for each plant – green and fully senesced. Having these two extremes as endmembers is necessary for spectral mixture modeling and analysis. Some of the measurements taken for green vegetation were carried out a little late in their phenological cycle, resulting in the presence of a few senesced components in the FOV. This was minimized by removing as much of the senesced plant and litter as possible from in and around the samples before measurement commenced on the first day at each site.

Photographs of the measurements were then analyzed to calculate the fractions of the individual components within the GFOV. Spectra were adjusted to isolate green endmembers by subtracting the effect of the background soil component (covered in Chapter 2.5.1). Only four samples had fully senesced before the arrival of the year's first snow covered all of the sample sites.

Since the averages of species spectra were compared, statistical confidence levels were calculated to ascertain whether the mean spectra used were within the error ranges of the each species group. The range of the confidence interval gives an estimate of the upper and lower limits for where the actual mean might be. Using the statistical computing package, [R]⁵, 0.95 and 0.99 confidence intervals, upper and lower limits were calculated for the mean reflectance at each spectral wavelength for each species for each day of measurement. Accordingly, the average of the confidence intervals of the reflectances at each wavelength was calculated for the various measurements, providing

⁵ The R Project for Statistical Computing, www.r-project.org.

one confidence interval per wavelength per species reflectance mean. Finally, the average confidence intervals of reflectances of all wavelengths for each species reflectance mean were calculated, resulting in a single confidence interval for each of the nine species.

2.5.1 Digital Image Classification

The classification of digital images was carried out using the ITT Corporation⁶ digital image analysis software, ENVI. Circular subsets reflecting the sensor GFOV were extracted from the photographs of measured samples. Using the Support Vector Machine (SVM; Brown *et al.*, 1999) classifier – a learning machine classifier in which input vectors are mapped in a non-linear, high-dimensional space (Cortes and Vapnik, 1995) – the image subsets were classified into the two categories of soil and vegetation.

As the area in the subsets to be classified was circular, areas of no data existed in the corners of the ENVI image window and were masked for the image classification. The percentage cover of each class was used as the background fraction in unmixing the background reflectance from the original reflectance ($S_{species}$) according to the following unmixing equation:

$$S_{species} = \frac{(S - f_{soil}S_{soil})}{f_{species}}, \quad (4)$$

where S is the sample reflectance, $(f_{soil}S_{soil})$ is the contribution of the soil reflectance and $f_{species}$ is the fraction taken up by the sample species. Classification accuracy was

⁶ Formerly International Telephone and Telegraph

completed by comparing known regions of interest (ROIs) with the classification results in a confusion matrix.

2.5.2 Spectra Pre-processing

For storage in the SPECCHIO spectral library, the collected spectra were translated into ASCII text file format using the ASD desktop software, ViewSpec Pro. Reflectance data were retrieved from the spectral library using SPECCHIO's query function. Spectra were imported into Microsoft Excel to be sorted, averaged and corrected. These data were then prepared for unmixing and similarity measure calculations by appending all data into a single text file. The text files were required for input in the calculations, which were completed using the [R] statistical program (Venables and Smith, 2009).

Spectrum averages were calculated from the reflectance data and each average was labelled with the site ID, date, raw spectrum numbers and solar zenith angles. The average was calculated for every instance of the five spectra collected per sample per measurement cycle. Reflectance spectra were adjusted using wavelength-specific correction coefficients based on the reflectance levels of the SpectralonTM panel (Labshere, 2007).

As the solar zenith angle changed from $< 1^\circ$ over the duration of measurements taken at solar noon to $< 3^\circ$ during the first and last measurement cycles of a day, the spectra collected were adjusted to compensate for this effect. The difference between start time and finish time reference spectra acquisitions was determined for each

measurement cycle. Assuming a linear rate of change, a temporal adjustment coefficient (TAC) was calculated as follows:

$$TAC = \frac{t_{sm} - t_{start}}{t_{end} - t_{start}}. \quad (5)$$

where $(t_{end} - t_{start})$ is the time the measurement cycle took to complete and $(t_{sm} - t_{start})$ is the time difference from the starting reference panel measurement to when the sample was measured.

The new coefficients were then used to adjust the spectra taken during the interval times as follows:

$$\vec{s}_f = \vec{s}_{sm} + (\vec{s}_{ps} - \vec{s}_{pe}) \times TAC \quad (6)$$

where \vec{s}_f is the resulting reflectance spectrum, \vec{s}_{sm} is the sample spectrum, and $(\vec{s}_{ps} - \vec{s}_{pe})$ is the difference between the cycle start and end reference measurements.

Some of the spectra displayed a noticeable jump at 1000 nm, which is where the break between the VNIR and the SWIR 1 sensors occurs. The amplitude of the jump was inconsistent in its value from one spectrum to the next and raised concerns over the accuracy of any future analyses involving these data. To ensure that the spectra were more consistent, the data were adjusted to negate the difference in amplitude occurring at 1000 nm. Simply moving one side or the other of an affected spectrum often resulted in negative reflectances.

To limit the frequency of negative values resulting from this adjustment, the spectrum values in the 350 nm-1000 nm range and the spectrum values beyond 1000 nm were moved half the difference toward each other, eliminating the difference in

amplitude while limiting the number of spectra with negative reflectance values (Figure 2.13). Spectra that ended up with negative values were removed from the data set.

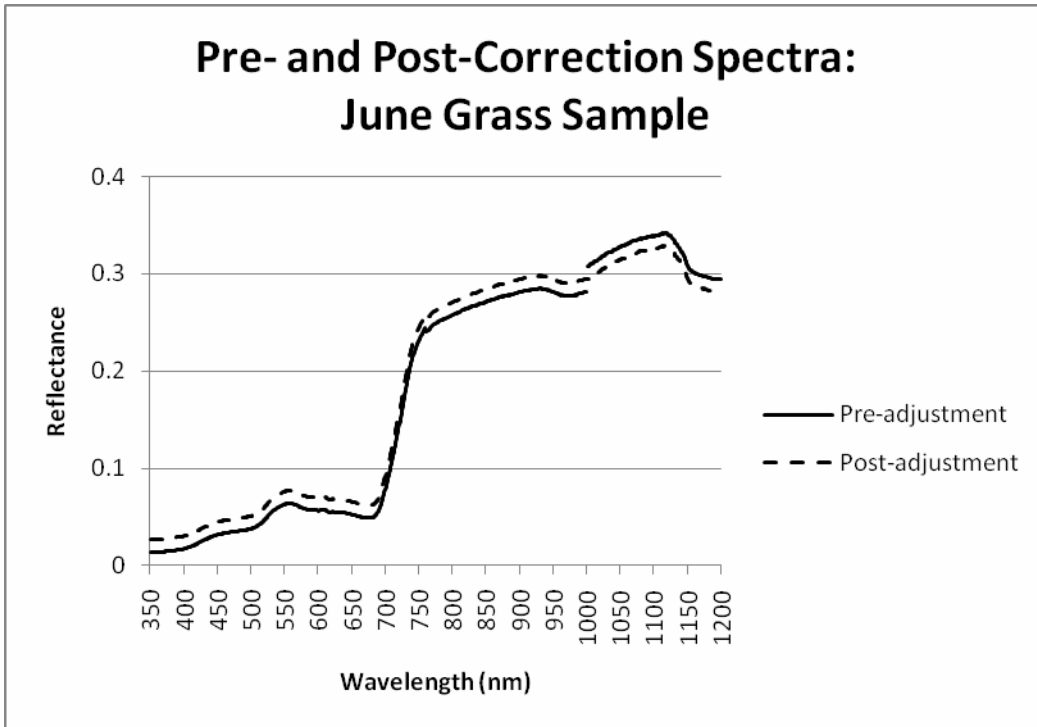


Figure 2.13: Example of jump in spectra at 1000 nm between the VNIR and SWIR sensors (in blue) and the result of its adjustment (in red).

2.6 Separability Analysis of Green Plant Spectra

Data from the first measurement day at each study site were used to compare green plant reflectance spectra as they were relatively free of senescent portions and, thus, were most representative of “pure” endmembers for green plants. Three similarity measures were used – Euclidean distance, spectral angle mapper, and correlation – to test the prepared spectra for separability between samples of the same and differing species.

2.6.1 Euclidian Distance

The Euclidean distance is the calculation of a straight-line distance between two points on a plane using the horizontal and vertical differences between their coordinates. This measure is often used to illustrate differences in multiple data series (Yool *et al.*, 1997). As described by Danielsson (1980), the Euclidean distance, d_e , is calculated using the following equation:

$$d_e((h,i),(j,k)) = \sqrt{(j-h)^2 + (k-i)^2}, \quad (7)$$

where (h,i) and (j,k) are coordinate pairs.

The results were then normalized by dividing each value by the maximum value of all the distances calculated. This ensured that the resulting values were between 0 and 1 to be comparable with the results from the two other measures used and is referred to as the Normalized Euclidean Distance (NED) for the duration of the thesis.

2.6.2 Correlation Similarity Measure

The correlation similarity measure (CSM) is used for describing the similarity between two spectra and is based on Pearson's correlation coefficient calculation as presented in Staenz *et al.* (1999) by:

$$CSM = \left[\frac{M - n \bar{t} \bar{r}}{(n-1)\sigma_t \sigma_r} \right]^2, \quad (8)$$

where n is the number of wavelength bands used in the comparison, \bar{r} and \bar{t} are the means of the reflectance values of a reference species (r) and a test species (t), respectively, σ_t and σ_r are the corresponding standard deviations of the means. M is the sum of products of each spectral band b in the two spectra and can be written as follows:

$$M = \sum_{b=1}^n t_b r_b . \quad (9)$$

The result is a value between 0 and 1, where 1 is an exact match between the reference and the test spectra and 0 indicates no match at all.

2.6.3 Spectral Angle Mapper

The spectral angle mapper (SAM; Kruse *et al.*, 1993) rapidly maps the similarity of the spectra from an image to a reference spectrum. The equation uses n-dimensional vectors of each spectrum to calculate the angle between the lines drawn through each point (reflectance at each band) and the origin in the n-dimensional space. This measure can be calculated by the following formula:

$$SAM = \cos^{-1} \left(\frac{M}{\sqrt{\sum_{b=1}^n t_b^2 \sum_{b=1}^n r_b^2}} \right) . \quad (10)$$

The result of this measure is an angle in radians. When the angle is calculated using SAM, the smaller the angle at the origin is, the closer the match is between the reference spectrum and the spectrum to be compared. This measure is often used in spectral similarity measures because it is not affected by changes in intensity (Park *et al.*, 2007).

Stanz *et al.* (1999) also described modifying the results of the spectral angle mapper (MSAM) to form an output between 0 and 1 in order to be comparable to the results of the CSM as follows:

$$MSAM = 1 - \frac{2SAM}{\pi} . \quad (11)$$

The results were output to a table for plotting purposes. The plots are important as a visual illustration of separability.

2.7 Separability Analysis Incorporating Phenology

The NED measure was then used to compare the spectra measured during the remainder of the growing season. A separability analysis was carried out for samples collected within two weeks of each other in an attempt to minimize the possibility of a high degree of phenological change between sample dates. Where sample days were more than two weeks apart and missing species for comparison, or where the two-week comparison times overlapped, a day was shared (Table 2.2).

The species reflectance spectra collected may have differed as a result of being measured during different solar zenith angles. In response to this possibility, steps were taken to ensure that only data collected during the same solar zenith angle range were compared to each other. Spectra were divided into comparison groups made up of measurements collected within a range of 10° solar zenith angle. As a check, these groups were applied in 5° overlap every five degrees of change in solar zenith angle. This meant, for example, that a spectrum collected at a solar zenith angle of 47° was used when comparing spectra collected between 40° - 50° and between 45° - 55° solar zenith angle range.

Table 2.2: Measurement days arranged by comparison groups. The rows show which measurement dates were compared in the analysis of phenological effects. The 15th of August (orange) and the 26th of September were included in the analysis of both the groups above and below them in the table.

Date	27-Jun		28-Jun		08-Jul	
Species Sampled	Western Wheat Grass	Blue Grama	Idaho fescue	crested wheat grass	June grass	needle-and-thread
Date	14-Jul		17-Jul		21-Jul	
Species Sampled	snowberry	silver sagebrush	Wild Rose	Western Wheat Grass	Blue Grama	Idaho fescue
Date	25-Jul		12-Aug			
Species Sampled	Western Wheat Grass	Blue Grama	Idaho fescue	crested wheat grass	June grass	needle-and-thread
Date	15-Aug					
Species Sampled	snowberry	silver sagebrush	Wild Rose			
Date	16-Sep					
Species Sampled	crested wheat grass	June grass	needle-and-thread	Western Wheat Grass	Blue Grama	Idaho fescue
Date	26-Sep					
Species Sampled	snowberry	silver sagebrush	Wild Rose			
Date	29-Sep		30-Sep		01-Oct	
Species Sampled	snowberry	silver sagebrush	Wild Rose	crested wheat grass	June grass	needle-and-thread
Date	27-Oct		10-Nov			
Species Sampled	crested wheat grass	June grass	needle-and-thread	Western Wheat Grass	Blue Grama	Idaho fescue
					needle-and-thread	
					Blue Grama	
					Western Wheat Grass	
					Idaho fescue	

3. RESULTS

3.1 Collected Spectra and Spectral Library

The total number of spectra, including target species and soil, collected during the field campaigns was just over 4000. Table 3.1 gives the upper and lower limits of error for each species from the mean measurement used in each case. Both 0.95 and 0.99 confidence levels were calculated along with the average reflectance value for each species spectrum.

Table 3.1: Confidence levels of sample spectra collected in the field. This table shows the differences above and below the sample means. 'N' is the number of bands used, and 'n' is the total number of measurements for each species.

N = 1625	Spectral Mean	Confidence Interval (0.95)		Confidence Interval (0.99)	
		Upper	Lower	Upper	Lower
<i>Blue grama</i> (n=926)	0.1914	0.0073	0.0074	0.009	0.010
<i>Crested wheatgrass</i> (n=915)	0.2490	0.0167	0.0028	0.019	0.022
<i>June grass</i> (n=730)	0.1989	0.0004	0.0230	0.018	0.009
<i>Needle-and-thread</i> (n=721)	0.2035	0.0306	0.0539	0.006	0.026
<i>Idaho fescue</i> (n=1021)	0.1918	0.0166	0.0168	0.019	0.006
<i>Western wheatgrass</i> (n=671)	0.2041	0.0148	0.0057	0.070	0.014
<i>Snowberry</i> (n=645)	0.2463	0.0633	0.0211	0.027	0.058
<i>Silver sagebrush</i> (n=773)	0.2231	0.0126	0.0127	0.016	0.017
<i>Wild rose</i> (n=311)	0.2381	0.0091	0.0092	0.012	0.012

The data collected in the field were stored in the SPECCHIO database in the raw file format produced by the ASD. SPECCHIO automatically extracted such data as spectral values and capture date and time (Figure 3.1). A small area showing the plotted

spectral profile was generated. The database included areas where other information was entered manually including, for example, ground coordinates (Figure 3.1), digital photographs of samples, and the instrument used (Figure 3.2). Other data included (not shown) were sensor zenith angle and sensor height above target.

The image shows a web-based data entry form for the SPECCHIO database. The form is organized into several sections:

- Capture date:** A date picker showing 2008, 6, 28, 16, 58, 12.
- Loading date:** A date picker showing 2009, 7, 24, 9, 27, 4.
- Is reference spectrum:** Radio buttons for Yes and No, with No selected.
- Required quality level:** A dropdown menu currently set to "None".
- Attained quality level:** An empty text input field.
- Spectral:** A line graph titled "Spectral plot". The y-axis is labeled "Reflectance" and ranges from 0.0 to 0.6. The x-axis is labeled "Wavelength [nm]" and ranges from 0 to 3000. The plot shows a blue line representing the spectral profile, with a prominent peak at approximately 2100 nm.
- Datalink:** A section with a dropdown menu and "New" and "Delete" buttons.
- Position:** A section with four text input fields:
 - Latitude: 49.701437
 - Longitude: 112.737409
 - Altitude [m]: (empty)
 - Location: Southern Applied Research Association

Figure 3.1: Detail of the SPECCHIO data input form. Shown are date and location information along with a plot of the sample reflectance.

Names

-spectrum_name- June Grass (Common) Koeleria gracilis (Latin)	<input type="button" value="Add"/> <input type="button" value="Edit"/> <input type="button" value="Remove"/>
---	--

Target type

-target_type- 	<input type="button" value="Add"/> <input type="button" value="Edit"/> <input type="button" value="Remove"/>
-----------------------	--


Sensor and Instrument Data

Sensor: <input type="text" value="ASD F5 FR-3"/>	FOV [deg]: <input type="text" value="NIL"/>
Name: <input type="text" value="ATIC ASD_1"/>	<input type="button" value="Show Instrument Info"/>

Reference Data

Reference name: <input type="text" value="NIL"/>	<input type="button" value="Show Reference Info"/>
--	--

Pictures



June Grass: Sample 1

Figure 3.2: Detail of the SPECCHIO metadata form showing areas for sample name, information about the sensor used and a picture of a sample.

3.2 Classification of Digital Images

The SVM classification map results, of which some examples are given in Figure 3.3, were used to extract the soil fractions from the digital photographs for each of the measured spectra. An assessment of the classification results showed an average 98.59% overall accuracy achieved (Table 3.2).

Table 3.2: Confusion between the classes of vegetation and background using the SVM classifier.

Confusion Matrix Results:		
	Overall Accuracy	
Sample	Pixels Correct	Percent Correct
Jun27_BG1gmSVM	(757/762)	99.34%
Jun27_BG2gmSVM	(699/701)	99.71%
Jul17_BG3gmSVM	(657/704)	93.32%
Jul21_CW2gmSVM	(567/581)	97.59%
Jun27_IF2gmSVM	(731/733)	99.73%
Jun27_IF3gmSVM	(480/480)	100.00%
Jul21_NT1gmSVM	(1229/1250)	98.32%
Jul21_NT2gmSVM	(1489/1489)	100.00%
Jul21_JG1gmSVM	(975/975)	100.00%
Jul21_JG2gmSVM	(820/826)	99.27%
Jul21_JG3gmSVM	(1001/1030)	97.18%

As mentioned, soil measurements were collected at the sample sites for use as endmembers. After image classification, the soil fraction was used with the collected soil endmembers to calculate the amount of influence soil had on the sample spectra. Using the unmixing formula in Equation 2, the reflectance spectra were unmixed to produce plant and soil fractions. After unmixing, the plant fraction showed an increase in reflectance values of up to 2% from the sample spectra. The only exception was crested wheatgrass, where a difference in amplitude of 10% was observed in the near infra-red (NIR) spectrum range. It was in the NIR that the greatest difference in reflectance amplitude took place. In any of the soil extraction results there were no changes to spectral shape that could be perceived.

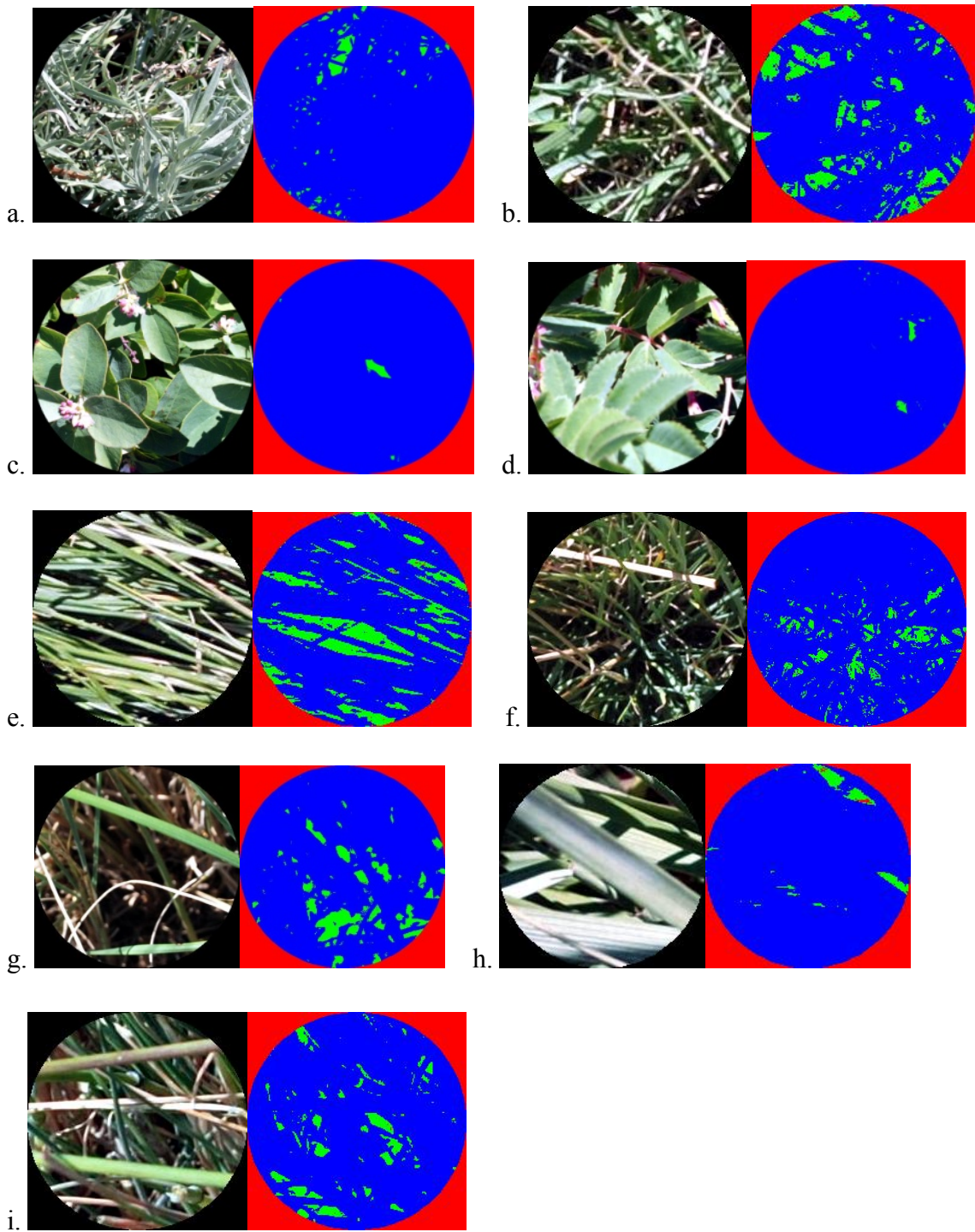


Figure 3.3: Classification examples using the SVM classification: a. silver sagebrush, b. blue grama, c. snowberry, d. wild rose, e. crested wheatgrass, f. June grass, g. needle-and-thread, h. western wheatgrass, i. Idaho fescue. Image pairs show the FOV from the sensor foreoptic on the left and the classification maps of the FOV on the right, where blue is vegetation, green is background material (soil), and red is mask.

3.3 Species Endmember Separability

Figure 3.4 shows a comparison of the species endmembers that were derived for and included in the study. For convenience in analysis procedures, species names were abbreviated (Table 3.3).

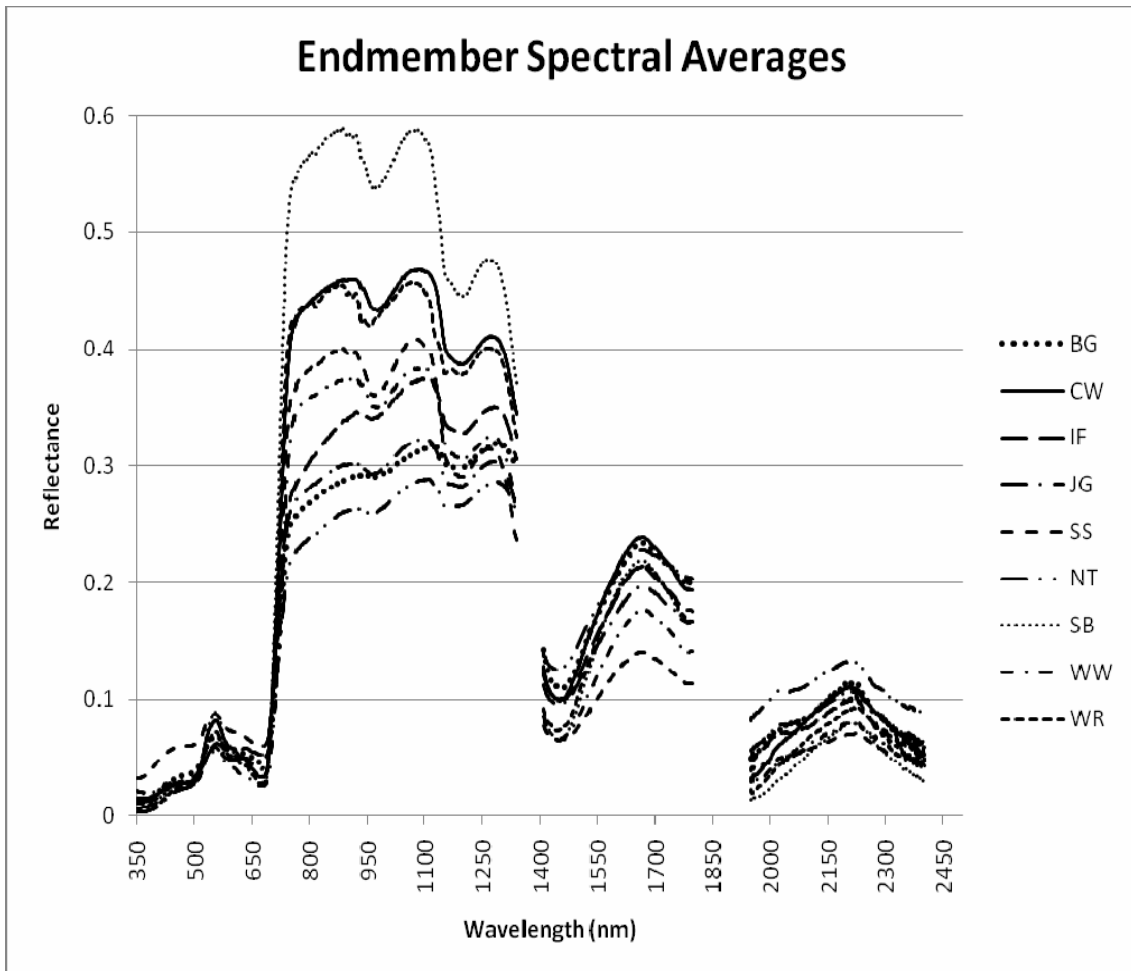


Figure 3.4: Comparison of endmembers derived from the averages of spectral reflectances (species n values in Table 3.1).

The three measures – CSM, MSAM and NED – were used and compared to study their sensitivity to spectral differences when comparing rangeland plants, i.e. what the difference was between the results. Also, the three separability measures allowed cross-checking of the results to make sure that separability results were consistent. All

measurements made throughout the day were used to calculate the average spectral curve for each species. The separability test results indicated that the solar zenith angle did not significantly affect the ability to identify multiple reflectances from the same species as being from the same species.

Table 3.3: Name abbreviations used for identifying species in separability plots.

Abbreviation	Common Name	Latin Name
BG	blue grama	<i>Bouteloua gracilis</i>
IF	Idaho fescue	<i>Festuca idahoensis</i>
JG	June grass	<i>Koeleria gracilis</i>
NT	needle-and-thread	<i>Stipa comata</i>
WW	western wheatgrass	<i>Agropyron smithii</i>
CW	crested wheatgrass	<i>Agropyron cristatum</i>
SB	snowberry	<i>Symphoricarpos occidentalis</i>
SS	silver sagebrush	<i>Artemisia cana</i>
WR	wild rose	<i>Rosa acicularis</i>

In general, all three separability measures returned the same results in relation to separability between species. CSM was able to separate the different species, but required a comparatively high threshold of 0.992 (Figure 3.5). MSAM had a lower threshold of separability of 0.970 (Figure 3.6). NED separated the sample spectra with a similar separability threshold of 0.950 (Figure 3.7). 0.99 confidence limits for the mean spectra used are included as vertical error bars in Figures 3.5-3.7.

Comparisons are presented in columns (Figures 3.5-3.7). The symbol for the reference species, the one being compared to all others, is found at the bottom of the column (on the x-axis) with its abbreviation identifier. The symbol is also found at the top of the column with a value of 1, signifying an exact match. The symbols for the species being compared are arranged along the column. The greater the distance of a

symbol from 1, the more separable its represented species is from the reference species. Error bars represent the upper and lower confidence limits calculated for each species (0.99 confidence). Species symbols are offset horizontally for clarity.

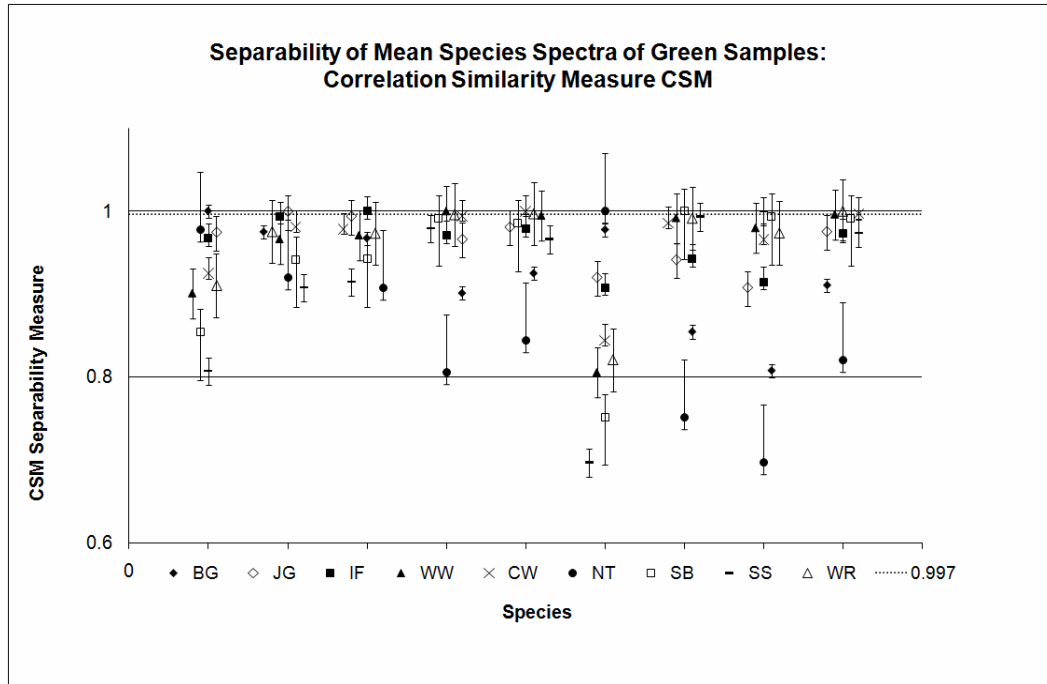


Figure 3.5: CSM separability analysis results. Error bars reflect the average degree of error calculated for the mean of each species spectrum at a confidence level of $p=0.99$. The dotted line indicates the threshold of separability.

Of significant concern were the confidence intervals as shown in Figures 3.5, 3.6 and 3.7 as the actual mean may be anywhere in the range of the intervals. As seen in the case of CSM (Figure 3.5), the confidence intervals have a lot of overlap between species. Moreover, species endmembers are also quite close to the separability threshold line, which in turn is quite close to 1, which is an exact match. While CSM and MSAM returned the same general patterns of separability (Figures 3.5-3.7), NED outputs different results (Figure 3.7). Using NED, all but two of the species endmembers tested were clearly separable from each other.

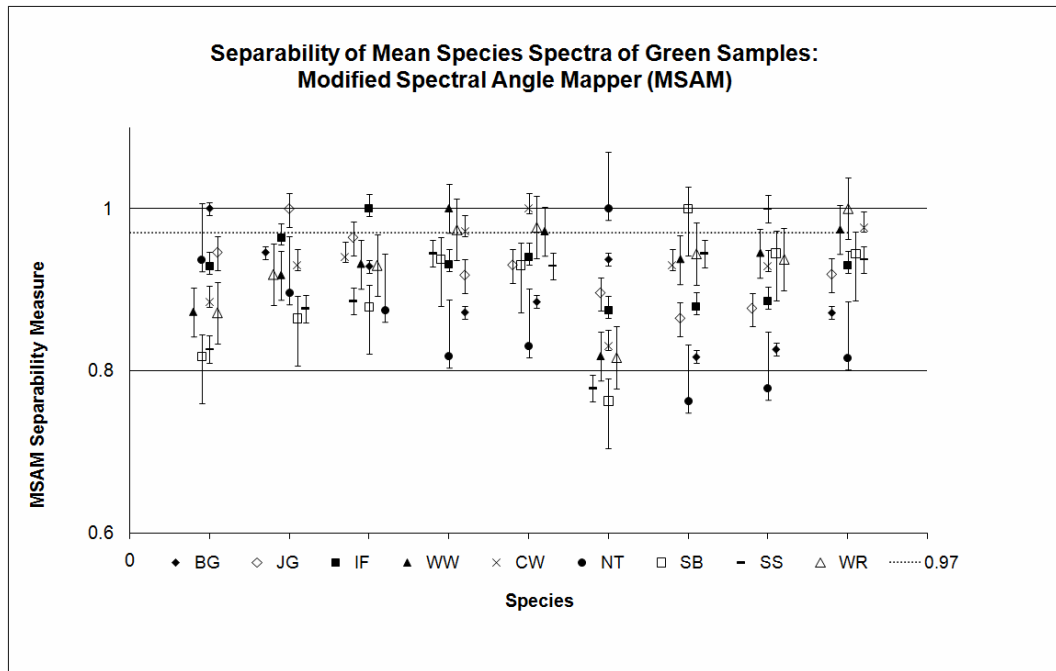


Figure 3.6: MSAM Separability analysis results. Error bars reflect the average degree of error calculated for the mean of each species spectrum at a confidence level of $p=0.99$. The dotted line indicates the threshold of separability. According to MSAM, wild rose (white triangle), western wheatgrass (black triangle) and crested wheatgrass (the 'X') spectra are similar to each other.

Assuming that plant structure plays a significant role in canopy spectral response and, therefore, spectral separability of plants, the apparent similarity of western wheatgrass and crested wheatgrass with the wild rose shrub was an unexpected result. While there is a similarity in the shapes of the spectra for these plants, there are definite differences in reflectance amplitude in the VNIR (Figure 3.8).

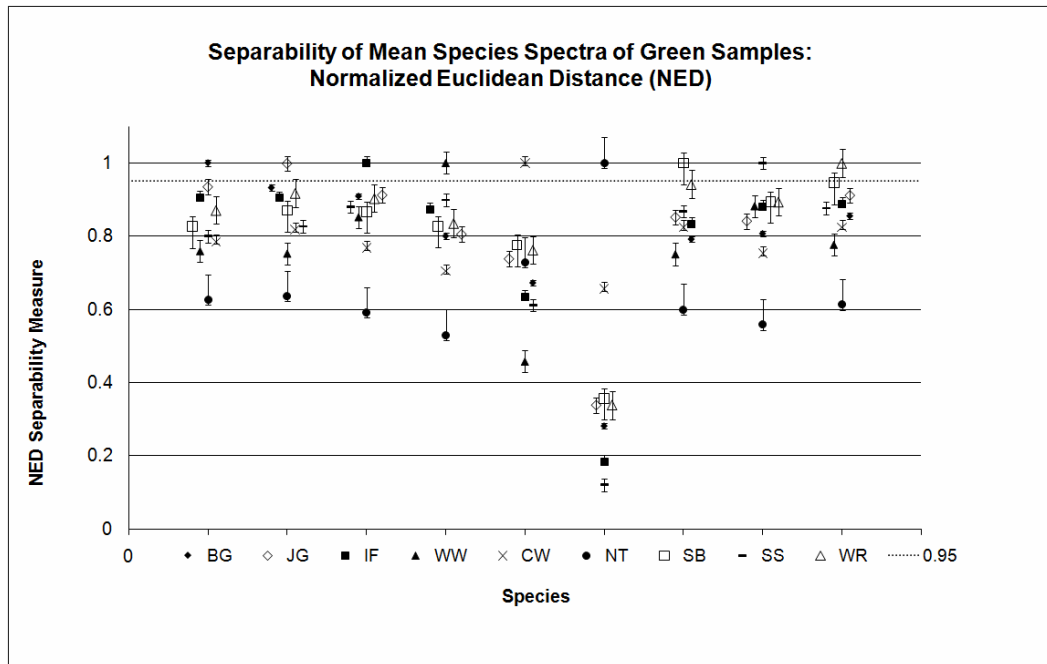


Figure 3.7: NED separability analysis results. Error bars reflect the average degree of error calculated for the mean of each species spectrum at a confidence level of $p=0.99$. The dotted line indicates the threshold of separability. NED shows a different ability to separate species spectra, only two shrubs are similar: snowberry (white square) and wild rose (white triangle).

Data gathered from samples of needle-and-thread were inconsistent. During initial separability tests where the solar zenith angle was included as a factor, needle-and-thread was separable from all of the other sampled species and approximately 50% of the time, from itself. None of the other species shared this result.

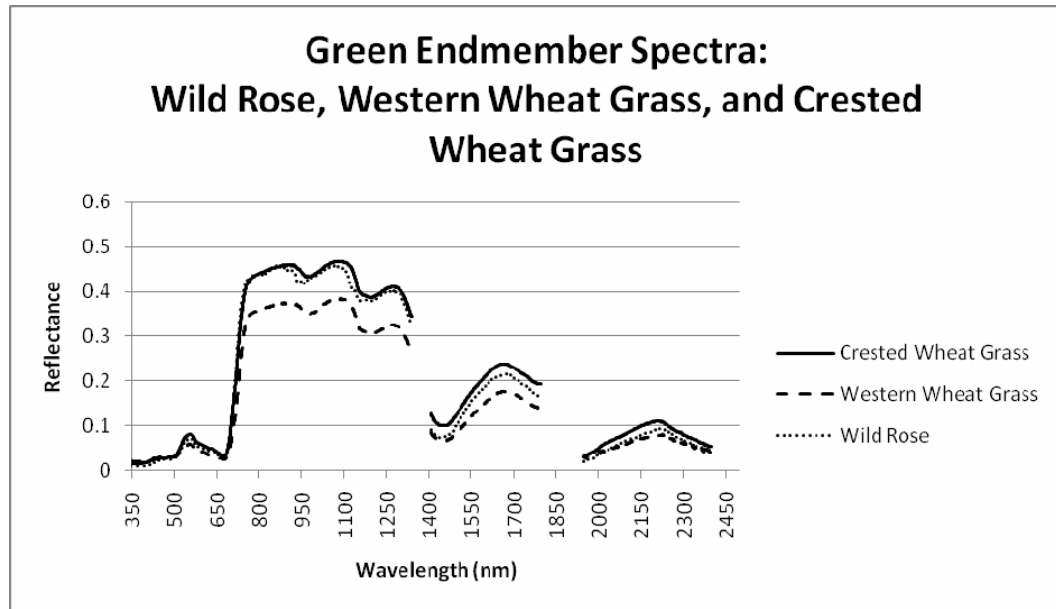


Figure 3.8: Comparison of the spectral response curves of wild rose, western wheatgrass, and crested wheatgrass. There is a clear similarity visible in the shape of the spectra. Thus separability must reside in amplitude of reflectance values.

3.4 Role of Phenology

Plant phenology is affected by a number of inputs. These include soil moisture, temperature, and sunlight, among other things. Lethbridge gets an average of 138 mm of rain from May through July, with most of it falling in June. The spring and summer of 2008 was wetter than normal, receiving 239 mm of rain over the three month period. The historical average daily temperatures for the same three month period (15°C) were also exceeded by 2008's three-month average of 21.5°C. Because of the higher-than-average conditions, it was generally observed that plants in the area stayed green longer than usual. Thus, the phenological timing of the sample species was altered in the same way.

Possibly as a result of the conditions discussed, only three grasses were completely senesced by the end of the season: blue grama, Idaho fescue, and crested wheatgrass. The other grasses and the shrubs sampled retained a large portion of green

plant matter further into the fall and were not fully senesced when snowfall began.

However, the leaves of the shrub wild rose did take on a more reddish hue towards the end of the season.

Comparison of spectra using NED showed Idaho fescue, June grass and blue grama to be similar (Figure 3.9). Later on, the spectra of crested wheatgrass began to resemble these three native grasses. The samples of these species then became separable later in the season.

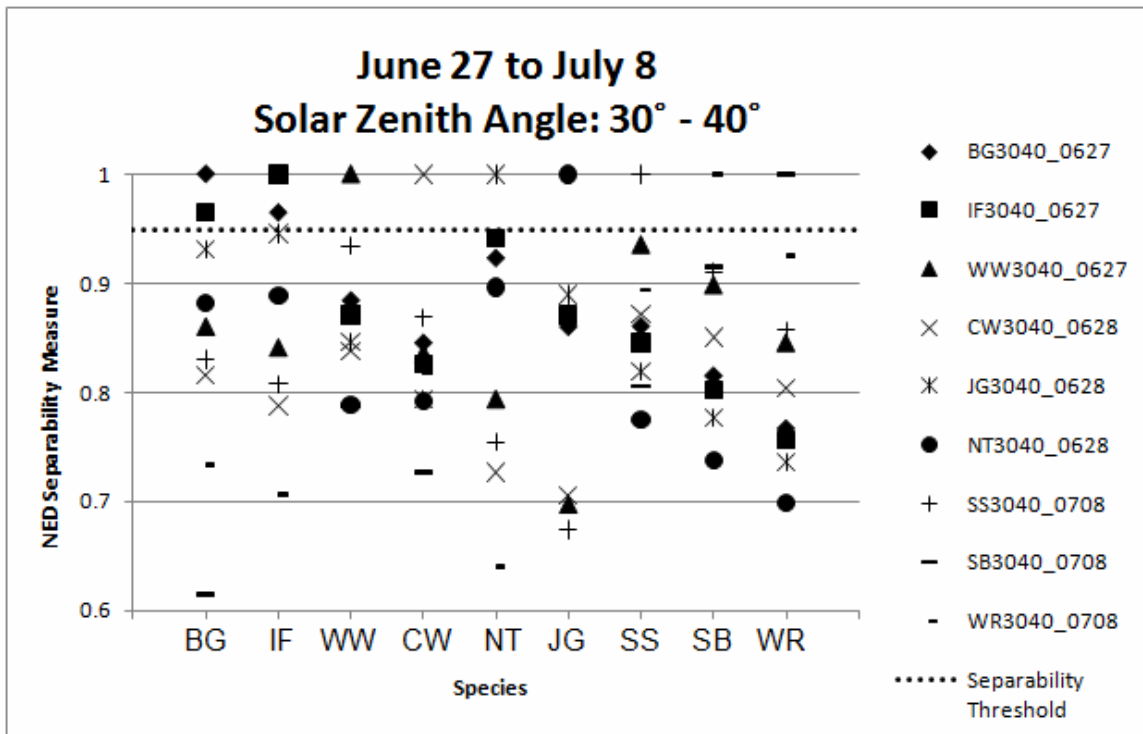


Figure 3.9: A summary of the separability of the species in the early stages of measurement at the highest solar zenith. The x-axis shows reference species symbols. (The full series of plots may be found in Appendix B.)

Two of the factors of most value to finding separability of the measured plant spectra are the change over time of the chlorophyll absorption feature (660 nm) and changes in the spectral response in the SWIR, especially in the cellulose/lignin absorption area around the 2100 nm band. Figure 3.10 shows the phenological effects on reflectance

at the chlorophyll absorption band, 660 nm, and the cellulose/lignin absorption band, 2100 nm, of these four plants through the season. The plots in this figure exhibit the requirement of multiple bands when looking for features that contribute to the ability to spectrally separate vegetation. For example, June grass remains extremely close to blue grama in the chlorophyll absorption feature (660nm) over the season. However, its reflectance at 2100 nm becomes more significant as a separating feature. Judging by their progression, all four grasses seemed to be the most separable by the latter end of July.

Crested wheatgrass, western wheatgrass and wild rose endmembers were not separable using MSAM and CSM (Figures 3.5 and 3.6). Continuing with reflectance data averages using all solar zenith angle measurements, isolating a phenological window where differences may be found was still possible, using reflectance values in the SWIR. Where these species only vary in amplitude at 660 nm by less than 5% throughout the season, a larger difference is apparent in the 2100 nm band (Figures 3.11 a and b). The amplitude change at 300908 in Figure 3.11 b suggests the importance of phenological timing when separating vegetation spectra, along with the inclusion of SWIR bands in the analysis. Contrary to the results of the first analysis, crested wheatgrass, western wheatgrass, and wild rose are separable using data from the same range of solar zenith angles.

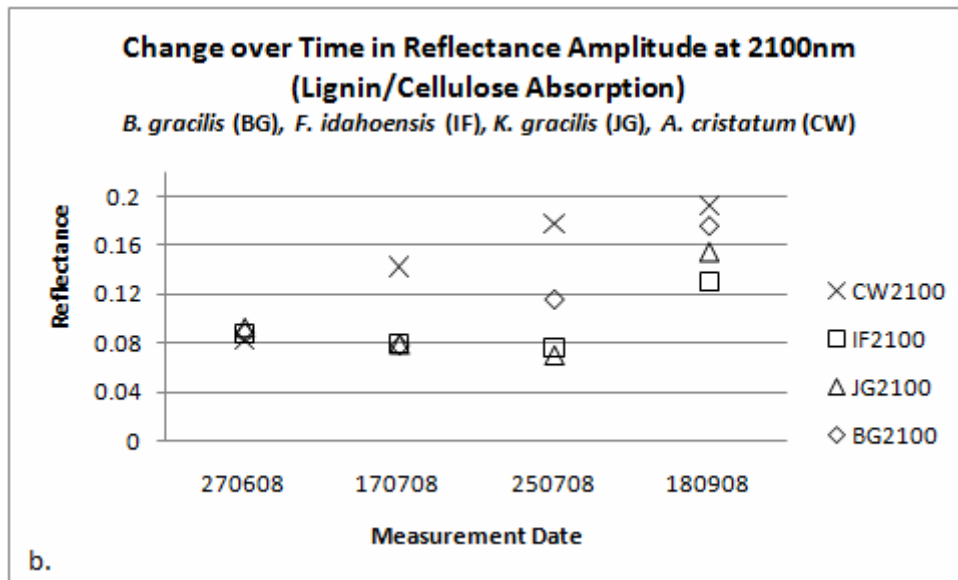
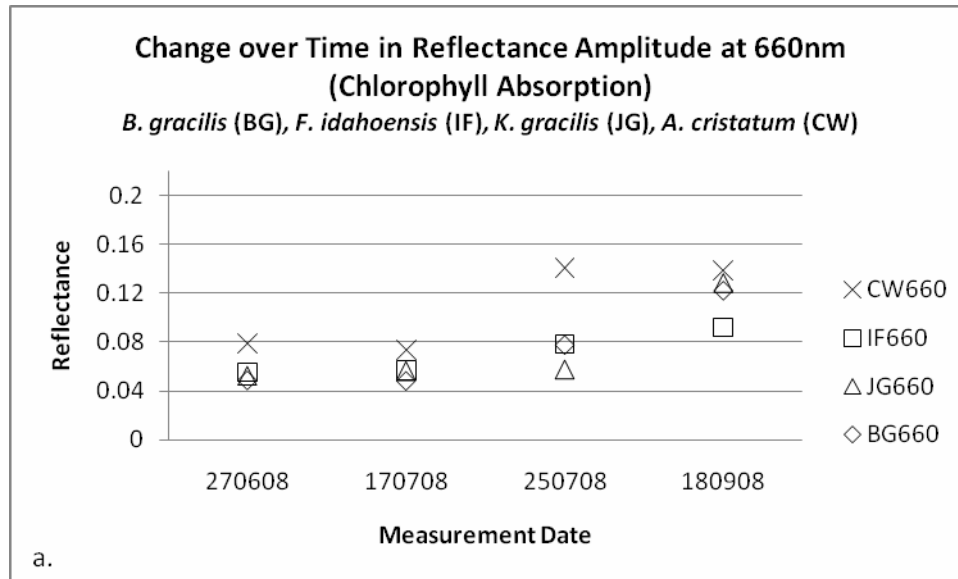


Figure 3.10: Comparison of band amplitudes of blue grama, Idaho fescue, June grass, and crested wheatgrass at (a.) 660 nm and at (b.) 2100 nm. The intervals along the x-axis reflect dates (ddmmyy) on which the samples were measured. These two examples show the importance of using SWIR2 bands in species separability as senescence starts to affect reflectance.

The month of September showed the highest capability of the separability measures to distinguish between species. Everything was separable using NED except for blue grama and crested wheatgrass, which by this point were both completely

senesced (Figure 3.12). Although plant spectra were collected in late October and early November, they were not used as not all species could be included. Only one to two measurements were obtained per sample, and tripod set-up spikes were either removed or buried at the Galt site as they could not be located.

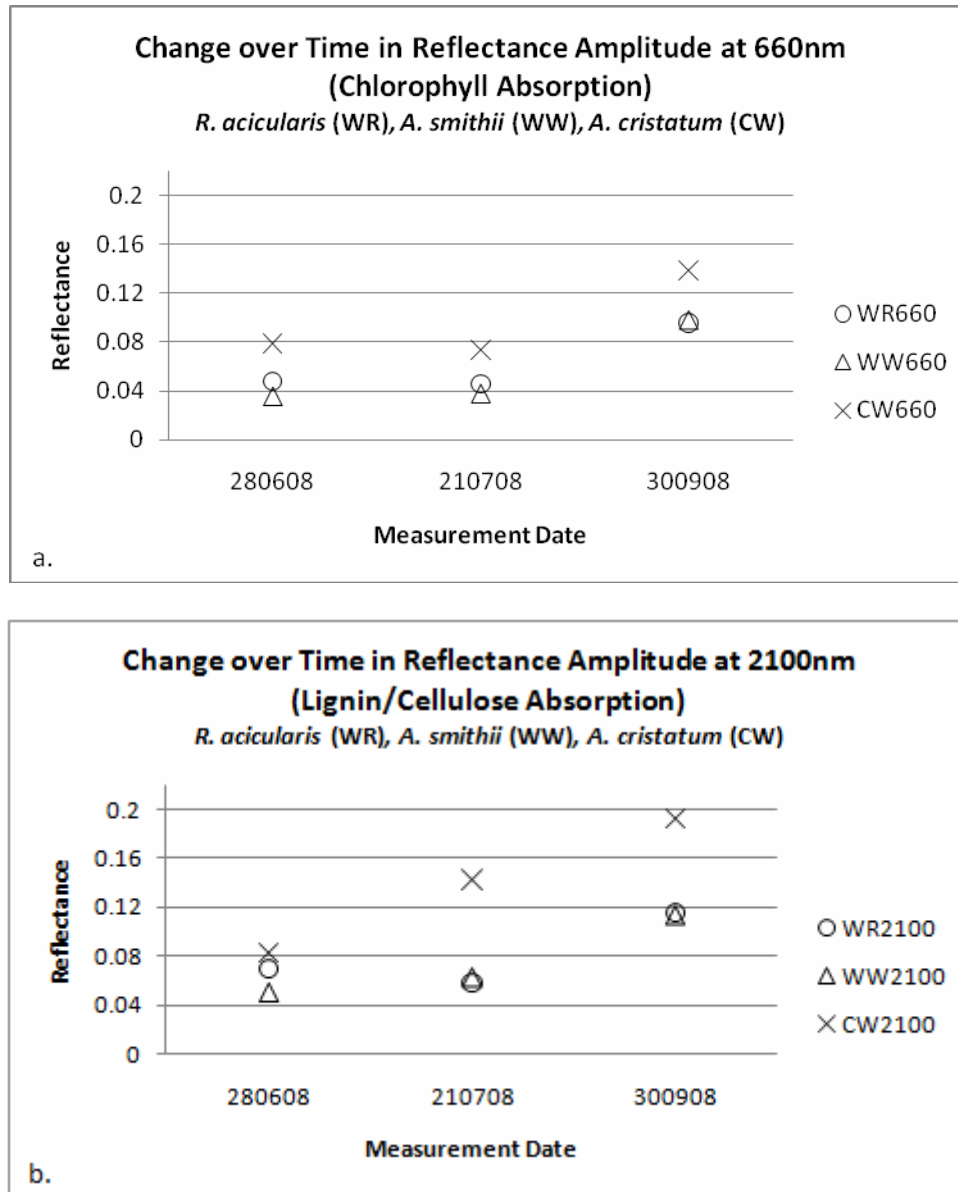


Figure 3.11: Comparing band amplitude over time of wild rose, western wheatgrass, and crested wheatgrass at (a) 660 nm and (b) 2100 nm which both show similar spectral responses. The intervals along the x-axis reflect dates (ddmmyy) on which the samples were measured.

Silver sagebrush and snowberry were found to be spectrally separable from all sample species throughout the measurement period. The silver sagebrush spectral curve showed a greater amplitude in the visible range on either side of the green peak. Snowberry had a much higher reflectance in the NIR than any of the other species.

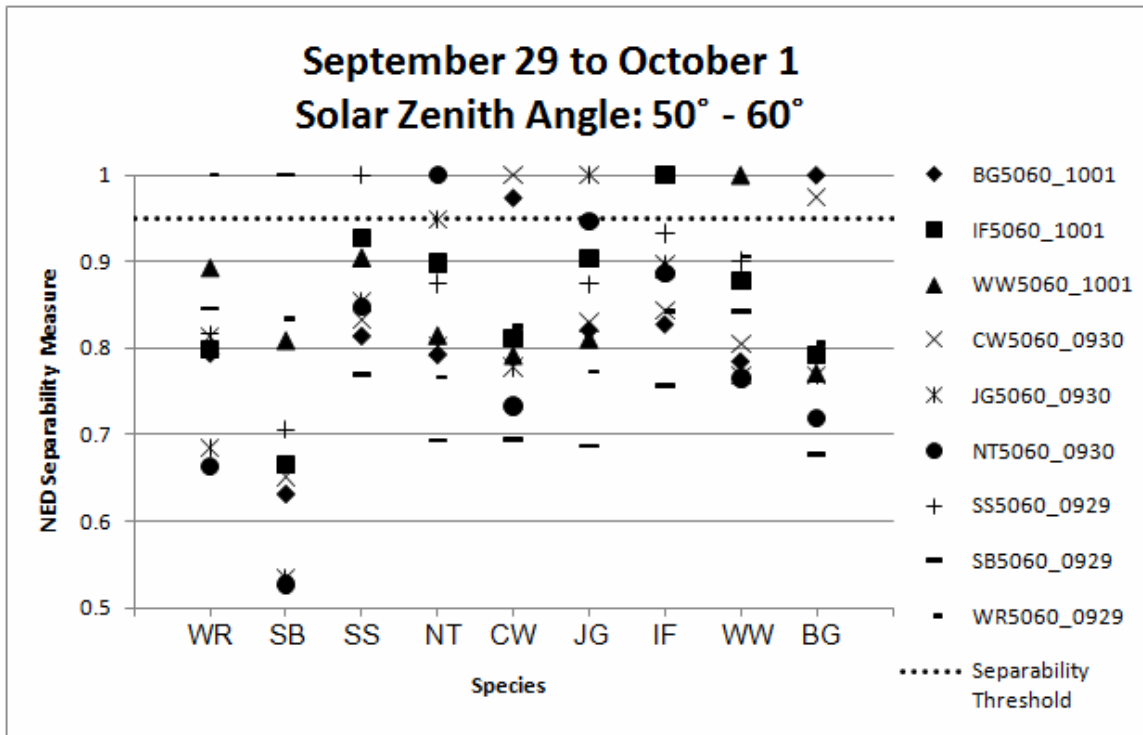


Figure 3.12: Separability of the grass species toward the end of the measuring period. As it is late in the season, some previously separable species are no longer separable due to increasing similarity in the latter stages of senescence.

4. DISCUSSION

4.1 Endmembers

The definition of an endmember is a cause for debate. There are different factors to consider in its definition. One that affected how endmembers were defined for this thesis was whether physical structure is important, leading to the question of shadows: whether an endmember can include the shadow that comes with leaving the structure intact, or if it is better to use a flat sample with minimal shadow for one endmember and assign another endmember for shadow. Another factor is the scale at which endmembers are measured, or what the sensor “sees”, for example, considering the endmembers collected at ground level for this thesis versus those extracted as pixels from an AVIRIS image. The two may or may not be interchangeable. It was in thinking about how a sensor, such as AVIRIS, “sees” vegetation targets in their natural setting that the decision was made to measure the plant samples *in-situ*.

4.2 Performance of Separability Measures

Van der Meer (2006) tested the performances of SAM and Euclidean distance as measures of separability and found that there was little difference between them. The results in this thesis did not agree with his findings as the pattern of the plotted separability values between the SAM and NED showed a different result in separability patterns; i.e., species similar to one measure, were separable by the other (Figures 3.6 and 3.7). CSM did not perform as a useful method of testing the separability of rangeland species due to its comparatively narrow spread between an exact match and the separability threshold.

4.3 Spectral Separability

These results have yet to be tested with image data. However, some of the endmembers collected during the fieldwork for this thesis were employed in a preliminary study that looked at endmembers derived with different methods and the resulting accuracy of image classifications involving these different generated endmembers⁷. Laboratory measurements of leaves, endmembers generated with canopy models, and *in-situ* endmembers from this thesis were compared in the study. Shrubs, litter, green and yellow grasses, and soil endmembers were used to classify a Compact High Resolution Imaging Spectrometer (CHRIS)⁸ hyperspectral image. The results were then compared to fractional cover estimates made in the field using a Daubenmire frame (Bonham *et al.*, 2004). The preliminary study concluded that all of these methods for endmember derivation had a low rate of agreement with the fractional cover estimates when used to classify a CHRIS hyperspectral image. The *in-situ* endmembers achieved the lowest accuracies. However, it should be noted that the accuracy of cover estimation using a Daubenmire frame is subject to the abilities of the person doing the estimation. Another factor of concern in this case is the difference in scale. The frame covered an area of 0.2 m x 0.5 m, while a CHRIS pixel (in this case) covered an area of 34 m x 34 m.

Despite the results from the preliminary study, the apparent ability to distinguish plant species using endmembers from *in-situ* measurements is promising for future studies and applications. One item to note is that the CHRIS sensor is limited to the

⁷ Rochdi, N. (2009). Monitoring Rangeland Community/Health Using Multispectral and Hyperspectral Data. Unpublished Presentation. Alberta Terrestrial Imaging Corporation.

⁸ Compact High Resolution Imaging Spectrometer (CHRIS) is an instrument on board the PProject for On-Board Autonomy (Proba) satellite.

VNIR spectral range. The results of this thesis suggest that the separation of plant species based on spectral response is possible. Since the results from the CHRIS image analysis differ, separability may be dependent on spectral responses in the SWIR bands, as well as those in the VNIR.

With further research, the ability to locate troublesome populations of invasive weeds may be improved, saving resources usually spent on invasive species detection by municipal and state/provincial and federal governments. More detailed information on plant populations (percent coverage) may improve the ability to map or monitor carbon uptake and/or releases by rangelands. Incorporating these results into larger scale operations may require refinement of the separability analysis procedure. Possible avenues toward a usable method might include further investigations into the abilities of separability measures (those discussed in this thesis and/or others) to achieve similar results using the spectral band configurations of available and/or upcoming hyperspectral sensor data, such as AVIRIS, Hyperion, or Environmental Mapping and Analysis Program (EnMAP; Stuffer *et al.*, 2007). Thus, it is possible to create a practical and usable commercial product.

The observation of western wheatgrass, crested wheatgrass, and wild rose suggests a spectral similarity between these wheatgrasses and wild rose. This is interesting in the fact that the wheatgrasses have a growth structure that is completely different from the shrub, wild rose. The results point to the possibility that, in some cases, targets of differing structure may have quite similar reflectance properties. Price (1994) came to the same conclusion while conducting an experiment on spectral

signature uniqueness, stating that some spectral reflectances were likely governed by small physical and chemical characteristics, including plant structure and water content.

The separability of all plant samples and silver sagebrush is likely due to the differences visible in both their colour and their structure. As both are shrubs, their differences from grass species in texture, structure and leaf shape and size would be expected to contribute towards their spectral separability. In detail, silver sagebrush has a paler leaf appearance than all of the other plants sampled. Its leaves also have hairs on them that reduce the amount of sunlight reaching the leaf, thereby reducing the total irradiance that may be reflected (Jensen, 2007). Snowberry, on the other hand, has broad leaves, which would also reflect solar radiation in a different pattern than grass leaves.

The confusion achieved by CSM and MSAM of two of the native species, western wheatgrass and wild rose, with an introduced species, crested wheatgrass, predicts similar complications in invasive species classifications that employ only one image (one acquisition date). As was shown in the results, the separability of these three plants became more pronounced over time. This supports the need for research into phenology patterns before an image is acquired or purchased to ensure an accurate classification result.

The result of MSAM spread the species further away from the separability threshold in plotting the calculated separability. This accomplished two things: the separability threshold moved further away from 1 and the confidence intervals have less overlap across species. NED spreads the species even further away from the separability threshold.

4.4 Phenology

Dickenson and Dodd (1976) grouped rangeland species according to similarities in their phenological patterns (Table 4.1). This knowledge may improve analyses of rangeland species by providing a guide to help estimate the best time to separate one species from the rest in a field operation.

Table 4.1: Phenology grouping of rangeland species and their indicators (two of which were sampled in this study) (from Dickenson and Dodd, 1976).

Group	Species	Indicator	Time of flowering
1	<i>Carex eleocharis</i> , <i>Oxytropis sericea</i> , <i>Senecio tridenticulatus</i>	<i>Carex eleocharis</i> (CAEL)	Late April-Mid-May
2	<i>Lepidium densiflorum</i> , <i>Vulpia octoflora</i> , <i>Cryptantha minima</i>	<i>Lepidium densiflorum</i> (LEDE)	Mid-May-Early June
3	<i>Stipa comata</i> , <i>Sitanion hystrix</i>	<i>Stipa comata</i> (STCO)	June
4	<i>Agropyron smithii</i> , <i>Buchloe dactyloides</i> , <i>Aristida longiseta</i>	<i>Aristida longiseta</i> (ARLO)	June-July
5	<i>Bouteloua gracilis</i> , <i>Sphaeralcea coccinea</i>	<i>Bouteloua gracilis</i> (BOGR)	July-August
6	<i>Artemisia frigida</i> , <i>Gutierrezia sarothrae</i> , <i>Chrysothamnus</i> <i>nauseosus</i>	<i>Artemisia frigida</i> (ARFR)	Late August- Early September

The non-separability of the grasses, June grass and Idaho fescue, may have been aided by the observed similarity in growth structure as both plants grow in clumps. crested wheatgrass was also observed to grow in clumps, but larger ones than June grass and Idaho fescue. Structural similarities cannot explain the initial similarity of blue grama to June grass and Idaho fescue. blue grama was observed growing in a more carpet-like pattern and has a more slender leaf. However, the changes undergone by these plants, as observed in this study, suggest that they will be separable late in the growing season.

Since the plants sampled seemed more separable as they senesced, it is likely that the best time to achieve a satisfactory result from a classification point-of-view is later in their phenological cycle. As this cycle is dependent on changing growing conditions, more research would be required to narrow the window in which data should be acquired. More research akin to that of Dickenson and Dodd (1976) would provide valuable information for classification studies where phenology may be a concern.

5. CONCLUSIONS

The use of remote sensing technology in discriminating specific plant species is useful in monitoring rangeland health for planning and improvement in both economic and social uses. Applications that require discrimination of rangeland areas are often in need of appropriate data for accurate classifications. When classifying using hyperspectral remotely sensed data, endmembers are required for estimating the abundances of target materials within a scene. Hyperspectral image analysis methods that use a collection of endmembers, such as SMA, can give accurate quantitative results describing how much of a certain component exists in a pixel. A spectral library is often employed to provide efficient access to endmembers, but must be built using spectra collected from samples of the target being detected.

The thesis goals were to collect *in-situ* data to obtain plant species reflectances for the creation of endmember spectra, test the separability of the species endmembers during peak greenness, and to test the effects of phenology on the separability of the collected sample spectra. Nine plant species were investigated, eight of which were native to Southern Alberta, western wheatgrass, blue grama, Idaho fescue, June grass, needle-and-thread grass, silver sagebrush, snowberry, and wild rose. The remaining species sampled was crested wheatgrass, an invasive species. Reflectance data were generated from irradiance and radiance data using an ASD FieldSpec 3 field spectroradiometer over the course of the summer and fall of 2008. Over 4000 spectra were collected for the creation of endmembers and for separability comparison.

A spectral library database was created using the SPECCHIO program developed at the University of Zurich. It was populated using the plant sample spectra collected

during this research. The SPECCHIO spectral library proved to be easy to use after the initial set up, the most time consuming process being the initial organization of spectra into a suitable hierarchy. The data hierarchy needs to be detailed enough to effectively use the metadata entry required by SPECCHIO. However, it may easily become too detailed and inefficient if the user is not careful. If data need to be changed in the hierarchical structure, the changes are only made to the file tree in the operating system's explorer window, which can be read by SPECCHIO again.

Plant spectra extracted from the spectral database were used to create species endmembers. These were then tested for separability from each other using the separability measures NED, MSAM, and CSM. All measures produced very similar results, the only difference between them being the difference between the threshold of separability and zero separability. The greatest spread between zero separability and the threshold of separability was achieved using the NED.

Given the results of the species endmember separability tests, the first hypothesis, that green plant species are spectrally separable, is partially accepted. All but three of the species sampled were spectrally separable. The finding that crested wheatgrass, western wheatgrass, and wild rose were not separable affirms that endmembers of different plant species can, in fact, appear quite similar.

Since the senescent patterns of the plants sampled differed in their timing, the data collected from them suggest that they are more separable by their spectral characteristics during specific times in the growing season. The data also suggest that the differences between some species become more apparent later in the season. The second hypothesis, that phenological analysis can improve the ability to separate rangeland plant species, is

also accepted as species separability based on reflectance was observed to fluctuate throughout the growing season.

Preliminary results of a comparison of endmembers collected and/or created using different methods suggest that endmembers collected *in-situ* may be of limited reliability when used for classifying a hyperspectral image. Further research in this direction would produce a sounder conclusion.

6. FUTURE OUTLOOK

Hyperspectral remote sensing has been in use in land cover studies for a number of years. Practical operational availability is only just beginning with the scheduled launches of space borne sensor platforms such as Germany's EnMAP and Italy's PRISMA (PREcursore IperSpettrale della Missione Applicativa; Labate *et al.*, 2009). As space borne hyperspectral technologies improve in spatial and spectral resolution, the quality of analyses performed using these and airborne sensors should improve. With a greater availability of data from space borne sensors and with the larger coverage (over that of airborne sensors), it is likely that hyperspectral remote sensing will become a more affordable data source than it currently is. Affordability and availability, coupled with the ability to separate plant species in a highly variable vegetation cover environment (e.g., rangelands), hyperspectral image analysis may prove to be a more labour- and cost-efficient mapping method than manual techniques, increasing the accuracy and efficiency of monitoring programs.

Development of endmember collection is as important a requirement for hyperspectral analysis as the improvement of sensor and detector performance. Some possible directions might be the development of a standardized file format for spectroradiometer data output, research into the question of scale differences between field measurements and image data, and further research on defining what a vegetation endmember is. The latter is the most difficult. The definition of a vegetation endmember will need to take into account such questions as what is seen by sensors, how important structure is, and whether it is better to model or measure. Phenological characteristics and timing will also be important to improving analysis of vegetation using hyperspectral

data. Building on the amount of data already available will likely be another important undertaking for a good deal of time.

The functionality and intuitive design of the SPECCHIO database allows for an easy-to-use system for spectral data storage. SPECCHIO offers a few basic analysis tools to its users. However, future iterations of this program or the creation of other libraries are sure to include more analysis options along with the database itself. Another possibility that would increase efficiency in data storage and analysis might be a fusion of a spectral library database with powerful image analysis software such as ENVI. Such a partnership would increase efficiency by reducing or eliminating some of the issues that are currently encountered in the use of two separate programs, such as compatibility and data transfers.

7. REFERENCES

- Adams, B. W., Ehler, R., Moisey, D. and McNeil, R. L. (2003). *Rangeland Plant Communities and Range Health Assessment Guidelines for the Foothills Fescue Natural Subregion of Alberta*. Rangeland Management Branch, Public Lands Division, Alberta Sustainable Resource Development, Lethbridge: 85.
- Adams, B. W., Poulin-Klein, L., Moisey, D. and McNeil, R. L. (2004). *Rangeland Plant Communities and Range Health Assessment Guidelines for the Mixedgrass Natural Subregion of Alberta*. Rangeland Management Branch, Public Lands and Forests Division, Alberta Sustainable Resource Development, Lethbridge: 101.
- ASD. (2007). *Fieldspec 3 User Manual* (Rev. F ed. Vol. 2007). Boulder, Colorado: Analytical Spectral Devices Inc.: 110.
- Asner, G. P. and Heidebrecht, K. B. (2002). Spectral unmixing of vegetation, soil and dry carbon cover in arid regions: comparing multispectral and hyperspectral observations. *International Journal of Remote Sensing*, 23(19): 3939-3958.
- Asner, G. P. and Lobell, D. B. (2000). A biogeophysical approach for automated SWIR unmixing of soils and vegetation. *Remote Sensing of Environment*, 74: 99-112.
- Asner, G. P., Wessman, C. A., Bateson, C. A. and Privette, J. L. (2000). Impact of tissue, canopy, and landscape factors on the hyperspectral reflectance variability of arid ecosystems. *Remote Sensing of Environment*, 74: 69-84.
- Bateson, A. and Curtiss, B. (1996). A method for manual endmember selection and spectral unmixing. *Remote Sensing of Environment*, 55: 229-243.
- Bennouna, T., Nejmeddine, A., Lefevre-Fonollosa, M. J., Lacombe, J. P., Kaemmerer, M. and J.C., R. (2004). Detection of change in Moroccan Rangelands with Multitemporal SPOT imagery. *Arid Land Research and Management*, 18: 229-240.
- Bonham, C. D., Mergen, D. E. and Montoya, S. (2004). Plant cover estimation: a contiguous daubenmire frame. *Rangelands*, 26(1): 17-22.
- Booth, D. T. and Tueller, P. T. (2003). Rangeland monitoring using remote sensing. *Arid Land Research and Management*, 17: 455-467.
- Borel, C. C. and Gerstl, S. A. W. (1994). Nonlinear spectral mixture models for vegetative and soil surfaces. *Remote Sensing of Environment*, 47: 403-416.
- Brown, M., Gunn, S. R. and Lewis, H. G. (1999). Support vector machines for optimal classification and spectral unmixing. *Ecological Modelling*, 120: 167-179.
- Butterfield, H. S. and Malmstrom, C. M. (2006). Experimental use of remote sensing by private range managers and its influence on management decisions. *Rangeland Ecology and Management*, 59: 541-548.
- Castelli, O., Fent, L., McEwan, D., Adams, B., Orr, R. and McNeil, R. (2005). *Grassland Vegetation Inventory (GVI) Final Report*. GVI Committee, Lethbridge, Alberta: 1-67.
- Cheng, Y.-B., Tom, E. and Ustin, S. L. (2007). Mapping an invasive species, kudzu (*Pueraria montana*), using hyperspectral imagery in western Georgia. *Journal of Applied Remote Sensing*, 1: 1-11.
- Chevrel, S. (2002). *Assessing and monitoring the environmental impact of mining activities in Europe using advanced Earth Observation techniques*. Bureau de Recherches Géologiques et Minières, Orleans, France: 47.

- Clark, R. N., King, T. V. V., Ager, C. and Swayze, G. A. (1995). *Initial vegetation species and senescence/stress mapping in the San Luis Valley, Colorado using imaging spectrometer data*. Proceedings of the Summitville Forum '95, Summitville, Colorado, pp. 64-69.
- Clark, R. N., Swayze, G. A., Wise, R. A., Livo, K. E., Hoefen, T. M., Kokaly, R. F. and Sutley, S. J. (2007). USGS digital spectral library splib06a. *U.S. Geological Survey Data Series 231* Accessed May 4, 2010, from <http://speclab.cr.usgs.gov/spectral.lib06>
- Coburn, C. A. and Noble, S. D. (2009). *High performance field and laboratory goniometer for measuring hyperspectral bi-directional reflectance characteristics of various agricultural canopies*. Proceedings of the 30th Canadian Symposium on Remote Sensing, Lethbridge, Alberta, pp. 748-757.
- Coburn, C. A. and Peddle, D. R. (2006). A low cost field and laboratory goniometer system for estimating hyperspectral bidirectional reflectance. *Canadian Journal of Remote Sensing*, 32(3): 244-253.
- Cornwall, C., Horiuchi, A. and Lehman, C. (2008, June 10, 2009). Sun Position Calculator. Accessed November 9, 2008, from <http://www.srrb.noaa.gov/highlights/sunrise/azel.html>
- Cortes, C. and Vapnik, V. (1995). Support-vector networks. *Machine Learning*, 20: 273-297.
- Danielsson, P. (1980). Euclidean distance mapping. *Computer Graphics and Image Processing*, 14: 227-248.
- Delalieux, S., Somers, B., Verstraeten, W. W., Van Aardt, J. A. N., Keulemans, W. and Coppin, P. (2009). Hyperspectral indices to diagnose leaf biotic stress of apple plants, considering leaf phenology. *International Journal of Remote Sensing*, 30(8): 1887-1912.
- Dennison, P. E. and Roberts, D. A. (2003). The effects of vegetation phenology on endmember selection and species mapping in southern California chaparral. *Remote Sensing of Environment* 87: 295-309.
- Dickinson, C. E. and Dodd, J. L. (1976). Phenological pattern in the shortgrass prairie. *The American Midland Naturalist*, 96(2): 367-378.
- Dyksterhuis, E. J. (1955). What is range management? *Journal of Range Management*, 8(5): 193-196.
- Foody, G. M., Lucas, R. M., Curran, P. J. and Honzak, M. (1997). Non-linear mixture modelling without end-members using an artificial neural network. *International Journal of Remote Sensing*, 18(4): 937-953.
- Green, A., Berman, M., Switzer, P. and Craig, M. D. (1988). A transformation for ordering multispectral data in terms of image quality with implications for noise removal. *IEEE Transactions on Geoscience and Remote Sensing*, 26(1): 65-74.
- Hanson, J. D., Skiles, J. W. and Parton, W. J. (1988). A multi-species model for rangeland plant communities. *Ecological Modelling*, 44: 89-123.
- Harris, A. T. and Asner, G. P. (2003). Grazing gradient detection with airborne imaging spectroscopy on a semi-arid rangeland. *Journal of Arid Environments*, 55: 391-404.

- Heidinga, L. and Wilson, S. D. (2002). The impact of an invading alien grass (*Agropyron cristatum*) on species turnover in native prairie. *Diversity and Distributions*, 8: 249-258.
- Hirano, A., Madden, M. and Welch, R. (2003). Hyperspectral image data for mapping wetland vegetation. *Wetlands*, 23(2): 436-448.
- Hook, S. J. (1998). ASTER Spectral Library. Accessed December 5, 2007, from <http://speclib.jpl.nasa.gov/>
- Hueni, A., Nieke, J., Schopfer, J., Kneubuhler, M. and Itten, K. I. (2007). *2nd generation of RSL's spectrum database "SPECCHIO"*. Paper presented at the 10th Intl. Symposium on Physical Measurements and Spectral Signatures in Remote Sensing.
- Hueni, A., Nieke, J., Schopfer, J., Kneubuhler, M. and Itten, K. I. (2009). The spectral database SPECCHIO for improved long-term usability and data sharing. *Computers and Geosciences*, 35: 557-565.
- Hunt, E. R., Jr., Everitt, J. H., Ritchie, J. C., Moran, M. S., Booth, D. T., Anderson, G. L., Clark, P. E. and Seyfried, M. S. (2003). Applications and research using remote sensing for rangeland management. *Photogrammetric Engineering & Remote Sensing*, 69(6): 675-693.
- Hunt, E. R., Jr. and Parker Williams, A. E. (2006). Detection of flowering leafy spurge with satellite multispectral imagery. *Rangeland Ecology and Management*, 59: 494-499.
- Hutto, K. C., Shaw, D. R., Boyd, J. D., Jr. and King, R. L. (2006). Differentiation of turfgrass and common weed species using hyperspectral radiometry. *Weed Science*, 54: 335-339.
- James, L. F., Young, J. A. and Sanders, K. (2003). A new approach to monitoring rangelands. *Arid Land Research and Management*, 17: 319-328.
- Jensen, J. R. (2007). *Remote Sensing of the Environment: An Earth Resource Perspective* (2 ed.). Upper Saddle River, NJ: Pearson Education, Inc.:
- Julia, R., Holland, D. W. and Guenther, J. (2007). Assessing the economic impact of invasive species: The case of yellow starthistle (*Centaurea solstitialis* L.) in the rangelands of Idaho, USA. *Journal of Environmental Management*, 85: 876-882.
- Karnieli, A. (2003). Natural vegetation phenology assessment by ground spectral measurements in two semi-arid environments. *International Journal of Biometeorology*, 47: 179-187.
- Kerekes, J. P. and Baum, J. E. (2003). Hyperspectral imaging system modeling. *Lincoln Laboratory Journal*, 14(1): 117-130.
- Knapp, P. A., Warren, P. L. and Hutchinson, C. F. (1990). The use of large-scale aerial photography to inventory and monitor arid rangeland vegetation. *Journal of Environmental Management*, 31: 29-38.
- Kruse, F. A., Lefkoff, A. B., Boardman, J. W., Heidebrecht, K. B., Shapiro, A. T., Barloon, P. J. and Goetz, A. F. H. (1993). The Spectral Image Processing System (SIPS) Interactive Visualization and Analysis of Imaging Spectrometer Data. *Remote Sensing of Environment*, 44: 145-163.
- Kuemmerle, T., Roder, A. and Hill, J. (2006). Separating grassland and shrub vegetation by multivariate pixel-adaptive spectral mixture analysis. *International Journal of Remote Sensing*, 27(15): 3251-3271.

- Labate, D., Ceccherini, M., Cisbani, A., De Cosmo, V., Galeazzi, C., Giunti, L., Melozzi, M., Pieraccini, S. and Moreno, S. (2009). The PRISMA payload optomechanical design, a high performance instrument for a new hyperspectral mission. *Acta Astronautica*, 65: 1429-1436.
- Labshere. (2007). *Spectralon™ Calibration Report Panel No. # 52116-1-1*. Labsphere, Inc., North Sutton, New Hampshire: 1.
- Lass, L. W., Prather, T. S., Glenn, N. F., Weber, K. T., Mundt, J. T. and Pettingill, J. (2005). A review of remote sensing of invasive weeds and example of the early detection of spotted knapweed (*Centaurea maculosa*) and babysbreath (*Gypsophila paniculata*) with a hyperspectral sensor. *Weed Science*, 53: 242-251.
- Lawrence, R. L., Wood, S. D. and Sheley, R. L. (2006). Mapping invasive plants using hyperspectral imagery and Breiman Cutler classifications (RandomForest). *Remote Sensing of Environment*, 100: 356-362.
- Lelong, C. C. D., Pinet, P. C. and Poilve, H. (1998). Hyperspectral imaging and stress mapping in agriculture: A case study on wheat in Beauce (France). *Remote Sensing of Environment*, 66: 179-191.
- Lund, H. G. (2007). Accounting for the world's rangelands. *Rangelands*, 29(1): 3-10.
- Marsett, R. C., Qi, J., Heilma, P., Biedenbender, S. H., Watson, M. C., Amer, S., Weltz, M., Goodrich, D. and Marsett, R. (2006). Remote sensing for grassland management in the arid Southwest. *Rangeland Ecology and Management*, 59: 530-540.
- McClay, A. S., Fry, K. M., Korpela, E. J., Lange, R. M. and Roy, L. D. (2004). *Costs and Threats of Invasive Species to Alberta's Natural Resources*. Alberta Sustainable Resource Development, Edmonton, Alberta: 122.
- Miao, X., Gong, P., Swope, S., Pu, R., Carruthers, R., Anderson, G. L., Heaton, J. S. and Tracy, C. R. (2006). Estimation of yellow starthistle abundance through CASI-2 hyperspectral imagery using linear spectral mixture models. *Remote Sensing of Environment*, 101: 329-341.
- Mirik, M., Norland, J. E., Crabtree, R. L. and Biondini, M. E. (2005a). Hyperspectral one-meter-resolution remote sensing in Yellowstone National Park, Wyoming: I. Forage nutritional values. *Rangeland Ecology and Management*, 58: 452-458.
- Mirik, M., Norland, J. E., Crabtree, R. L. and Biondini, M. E. (2005b). Hyperspectral one-meter-resolution remote sensing in Yellowstone National Park, Wyoming: II. Biomass. *Rangeland Ecology and Management*, 58: 459-465.
- Mitchell, G. J. and Somoliak, S. (1971). Antelope range characteristics and food habits in Alberta. *The Journal of Wildlife Management*, 35(2): 238-250.
- Norse, D. and Tschirley, J. B. (2000). Links between science and policy making. *Agriculture, Ecosystems and Environment*, 82: 15-26.
- Ogden, J. A. E. and Rejmanek, M. (2005). Recovery of native plant communities after the control of a dominant invasive plant species, *Foeniculum vulgare*: Implications for management. *Biological Conservation*, 125: 427-439.
- Olsen, B. D. (1994). Alberta's prairie vegetation: past and present use. *Rangelands*, 16(2): 58-62.
- Owens, R. A. and Myres, M. T. (1973). Effects of agriculture upon populations of native passerine birds of an Alberta fescue grassland. *Canadian Journal of Zoology*, 51: 697-713.

- Park, B., Windham, W. R., Lawrence, K. C. and Smith, D. P. (2007). Contaminant classification of poultry hyperspectral imagery using a spectral angle mapper algorithm. *Biosystems Engineering*, 96(3): 323-333.
- Parker Williams, A. E. and Hunt, E. R., Jr. (2004). Accuracy assessment for detection of leafy spurge with hyperspectral imagery. *Journal of Range Management*, 57: 106-112.
- Peddle, D. R. and Smith, A. M. (2005). Spectral mixture analysis of agricultural crops: endmember validation and biophysical estimation in potato plots. *International Journal of Remote Sensing*, 26(22): 4959-4979.
- Pimentel, D., Lach, L., Rodolfo, Z. and Morrison, D. (2002). Environmental and economic costs of nonindigenous species in the United States. *Bio Science*, 50(1): 53-65.
- Price, J. C. (1994). How unique are spectral signatures? *Remote Sensing of Environment*, 49: 181-186.
- Pyke, D. A. and Herrick, J. E. (2003). Transitions in rangeland evolutions. *Rangelands*, 25(6): 22-30.
- Ramsey, E., III, Ragoonwala, A., Nelson, G. and Ehrlich, R. (2005). Mapping the invasive species, Chinese tallow, with EO1 satellite Hyperion hyperspectral image data and relating tallow occurrences to a classified Landsat Thematic Mapper land cover map. *International Journal of Remote Sensing*, 26(8): 1637-1657.
- Rasmussen, G. A. and Brunson, M. W. (1996). Strategies to manage conflicts among multiple users. *Weed Technology*, 10(2): 447-450.
- Roberts, D. A., Gardner, M., Church, R., Ustin, S., Scheer, G. and Green, R. O. (1998). Mapping Chaparral in the Santa Monica Mountains Using Multiple Endmember Spectral Mixture Models. *Remote Sensing of Environment*, 65: 267-279.
- Rosentreter, R. (2001). *Sagebrush Identification, Ecology, and Palatability Relative to Sage-Grouse*. Proceedings of the Sage-Grouse Habitat Restoration Symposium, Boise, Idaho, pp. 3-16.
- Schmid, T., Koch, M., Gumuzzio, J. and Mather, P. M. (2004). A spectral library for a semi-arid wetland and its application to studies of wetland degradation using hyperspectral and multispectral data. *International Journal of Remote Sensing*, 25(13): 2485-2496.
- Shaw, G. A. and Burke, H. K. (2003). Spectral imaging for remote sensing. *Lincoln Laboratory Journal*, 14(1): 3-27.
- Shibayama, M., Akiyama, T. and Munakata, K. (1986). A spectroradiometer for field use. *Japanese Journal of Crop Science*, 55(4): 427-432.
- Shibayama, M., Takahashi, W., Miorinaga, S. and Akiyama, T. (1993). Canopy water deficit detection in paddy rice using a high resolution field spectroradiometer. *Remote Sensing of Environment*, 45: 117-126.
- Smyth, A. J. and Dumanski, J. (1993). *FESLM: An international framework for evaluating sustainable land management*. Rome, Italy: Food and Agriculture Organization of the United Nations:
- Staenz, K., Schwarz, J., Vernaccini, L., Vachon, F. and Nadeau, C. (1999). *Classification of Hyperspectral Agricultural Data with Spectral Matching Techniques*.

- Proceedings of the International Symposium on Spectral Sensing Research (ISSSR 99), Las Vegas, Nevada, pp. 12.
- Stoddart, L. A. (1967). What is range management? *Journal of Range Management*, 20(5): 304-307.
- Stuffer, T., Kaufmann, C., Hofer, S., Forster, K. P., Schreier, G., Mueller, A., Eckardt, A., Bach, H., Penne, B., Benz, U. and Haydn, R. (2007). The EnMAP hyperspectral imager - an advanced optical payload for future applications in Earth observation programmes. *Acta Astronautica*, 61: 115-120.
- Sutter, G. C. and Brigham, R. M. (1998). Avifaunal and habitat changes resulting from conversion of native prairie to crested wheat grass: patterns at songbird community and species levels. *Canadian Journal of Zoology*, 76(5): 869-875.
- Tompkins, S., Mustard, J. F., Pieters, C. M. and Forsyth, D. W. (1997). Optimization of endmembers for spectral mixture analysis. *Remote Sensing of Environment*, 59(472-489).
- Underwood, E., Ustin, S. and DiPietro, D. (2003). Mapping nonnative plants using hyperspectral imagery. *Remote Sensing of Environment*, 86: 150-161.
- Ustin, S., Roberts, D. A., Gamon, J. A., Asner, G. P. and Green, R. O. (2004). Using image spectroscopy to study ecosystem processes and properties. *BioScience*, 54(6): 523-534.
- Van der Meer, F. (2006). The effectiveness of spectral similarity measures for the analysis of hyperspectral imagery. *International Journal of Applied Earth Observation and Geoinformation*, 8: 3-17.
- Vanamburg, L. K., Trlica, M. J., Hoffer, R. M. and Weltz, M. (2006). Ground based digital imagery for grassland biomass estimation. *International Journal of Remote Sensing*, 27(5): 939-950.
- Venables, W. N. and Smith, D. M. (2009). *An Introduction to R*. Unpublished manuscript.
- Volkan-Kasco, S. and Neda, Z. (2003). Sun Position Calculator (Version 1.2).
- Welk, E. (2004). Constraints in range predictions of invasive plant species due to non-equilibrium distribution patterns: Purple loosestrife (*Lythrum salicaria*) in North America. *Ecological Modelling*, 179: 551-567.
- West, N. E. (2003). Theoretical underpinnings of rangeland monitoring. *Arid Land Research and Management*, 17: 333-346.
- Yool, S. R., Makaio, M. J. and Watts, J. M. (1997). Techniques for computer-assisted mapping of rangeland change. *Journal of Range Management*, 50(3): 307-314.
- Zhang, J., Rivard, B. and Sanchez-Azofeifa, A. (2005). Spectral unmixing of normalized reflectance data for the deconvolution of lichen and rock mixtures. *Remote Sensing of Environment*, 95: 57-66.
- Zhou, W. (2007). *Assessing remote sensing application on rangeland insurance in Canadian Prairies*. University of Saskatchewan, Saskatoon, Saskatchewan: 105.

APPENDICES

Appendix A: Summary of Field Measurements

Summary of 2008 Field Measurements				
Date and Location	Species Sampled	Solar Zenith Range (degrees)	Sky Condition	Remarks
Jun-27 LRC	<i>Western wheatgrass</i> <i>Blue grama</i> <i>Idaho fescue</i>	27-45	clear	
Jun-28 LC	<i>Crested wheatgrass</i> <i>June grass</i> <i>Needle-and-thread</i>	27-45	clear	
Jul-08 Galt	<i>Snowberry</i> <i>Silver sagebrush</i> <i>Wild rose</i>	30-50	clear	Instrumentment problems during measurements at 14:36 Perceived general brightness variations despite cloudless sky
Jul-14 Galt	<i>Snowberry</i> <i>Silver sagebrush</i> <i>Wild rose</i>	29-45	clear	Light breeze increasing to light wind in the afternoon
Jul-17 LRC	<i>Western wheatgrass</i> <i>Blue grama</i> <i>Idaho fescue</i>	29-50	<10% cloud	Breezes in morning, some clouds moved in toward afternoon, then dispersed
Jul-21 LC	<i>Crested wheatgrass</i> <i>June grass</i> <i>Needle-and-thread</i>	30-45	clear	Windy enough to that plants were laying over in morning, decreasing in afternoon
Jul-25 LRC	<i>Western wheatgrass</i> <i>Blue grama</i> <i>Idaho fescue</i>	30-50	clear	
Aug-12 LC	<i>Crested wheatgrass</i> <i>June grass</i> <i>Needle-and-thread</i>	35-50	clear haze	Clear in the morning, haze moving in early afternoon, measurements ceased
Aug-15 Galt	<i>Snowberry</i> <i>Silver sagebrush</i> <i>Wild rose</i>	36-50	clear	AM measurements rejected: wrong foreoptic used

Summary of 2008 Field Measurements (cont'd)				
Date (Location)	Species Sampled	Solar Zenith Range (degrees)	Sky Condition	Remarks
Sep-16 LRC and LC	<i>Crested wheatgrass</i> <i>June grass</i> <i>Needle-and-thread</i> <i>Western wheatgrass</i> <i>Blue grama</i> <i>Idaho fescue</i>	48-60	clear haze	LC plots measured in the morning Attempted measurement of LRC plots in the afternoon, ceased due to haze
Sep-18 LRC	<i>Western wheatgrass</i> <i>Blue grama</i> <i>Idaho fescue</i>	48-60	clear	
Sep-26 Galt	<i>Snowberry</i> <i>Silver sagebrush</i> <i>Wild rose</i>	51-65	clear	Afternoon only
Sep-29 Galt	<i>Snowberry</i> <i>Silver sagebrush</i> <i>Wild rose</i>	52-65	clear	Samples shaded by museum during first measurement interval
Sep-30 LC	<i>Crested wheatgrass</i> <i>June grass</i> <i>Needle-and-thread</i>	52-65	clear breeze	Light breeze in the morning
Oct-01 LRC	<i>Western wheatgrass</i> <i>Blue grama</i> <i>Idaho fescue</i>	53-65	clear	Idaho fescue completely senesced
Oct-27 LC	<i>Crested wheatgrass</i> <i>June grass</i> <i>Needle-and-thread</i>	63-70	clear	Light wind bringing haze in morning, ceased measurements after first two intervals
Nov-10 LRC and LC	<i>Western wheatgrass</i> <i>Blue grama</i> <i>June grass</i> <i>Needle-and-thread</i>	77 77	clear windy	Western wheatgrass and blue grama completely senesced

Appendix B: Separability Over Time: Normalized Euclidean Distance Plots

This appendix contains scatter plots which illustrate the separability between the sample species over time. Each species has been assigned a marker shape and colour to aid in reading the plots. The symbols along the X-axis represent the species being compared against, or the reference species. Separability is then illustrated along the numbered columns, the further away a marker from the base species symbol at the bottom of the column, the more separable it is from the base species. For example, in column 1 of the first plot (Appendix Figure 1) the diamond (blue grama) is the reference species, from which the separability of the others is being measured. The short dash (wild rose) at the bottom of the column labelled IF is the most separable from the square (Idaho fescue) at the top while the asterisk (June grass) is the least separable. In fact, since the asterisk (June grass) is above the Separability Threshold (dotted line), it is considered to be spectrally similar to the square (Idaho fescue).

The dotted line in each plot is set at 0.95, which is the separability threshold calculated for the NED results. Thus, any symbol found below this line signifies that that species was found to be spectrally separable from the base species in the same column.

The series names are read as [species][illumination zenith]_[date]. The species abbreviations of their common names and their Latin names are listed in Appendix Table 1.

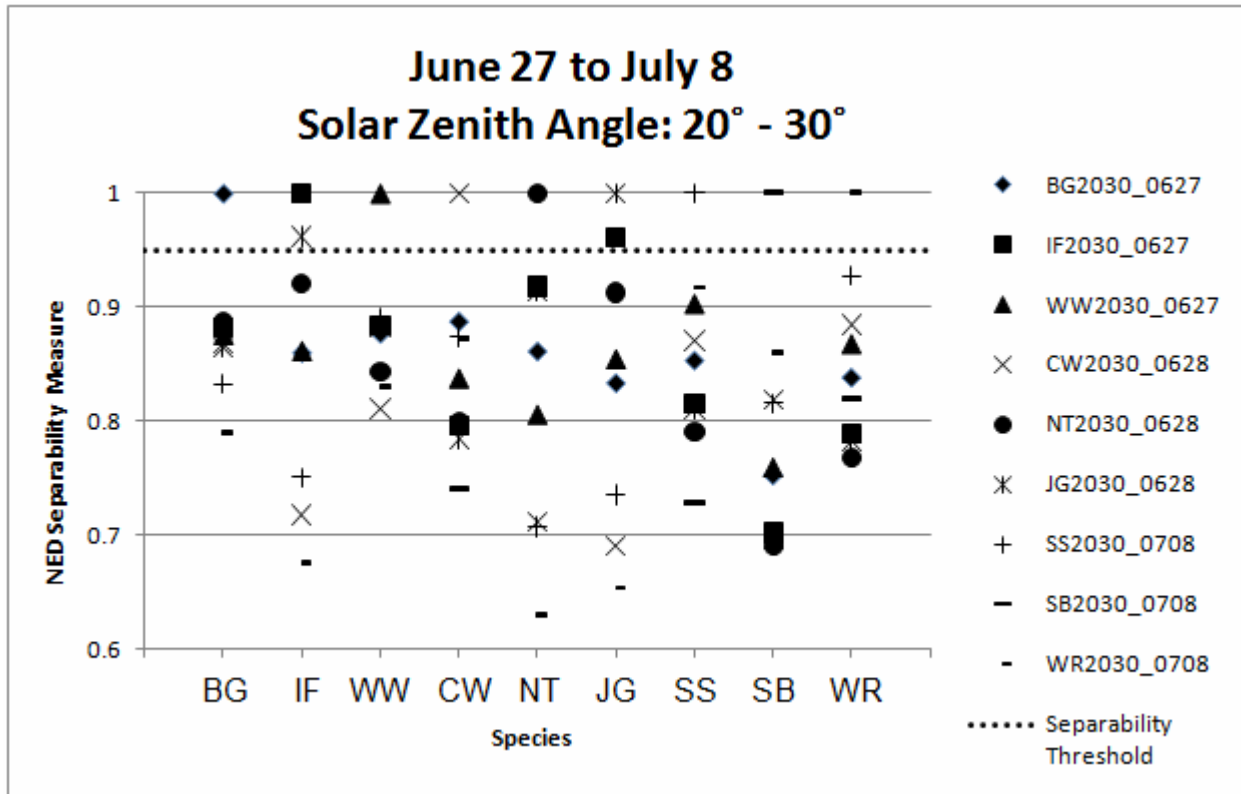
Reading series name example: BG2030_0717 reads as blue grama grass (BG), measured between 20° and 30° sun zenith angle (2030) on July 17 (0717). All measurements were taken in the year 2008.

These plots also track the impact of solar zenith angle on species separability. As Price (1994) pointed out, physical structure can have an impact on plant spectra. As the solar zenith

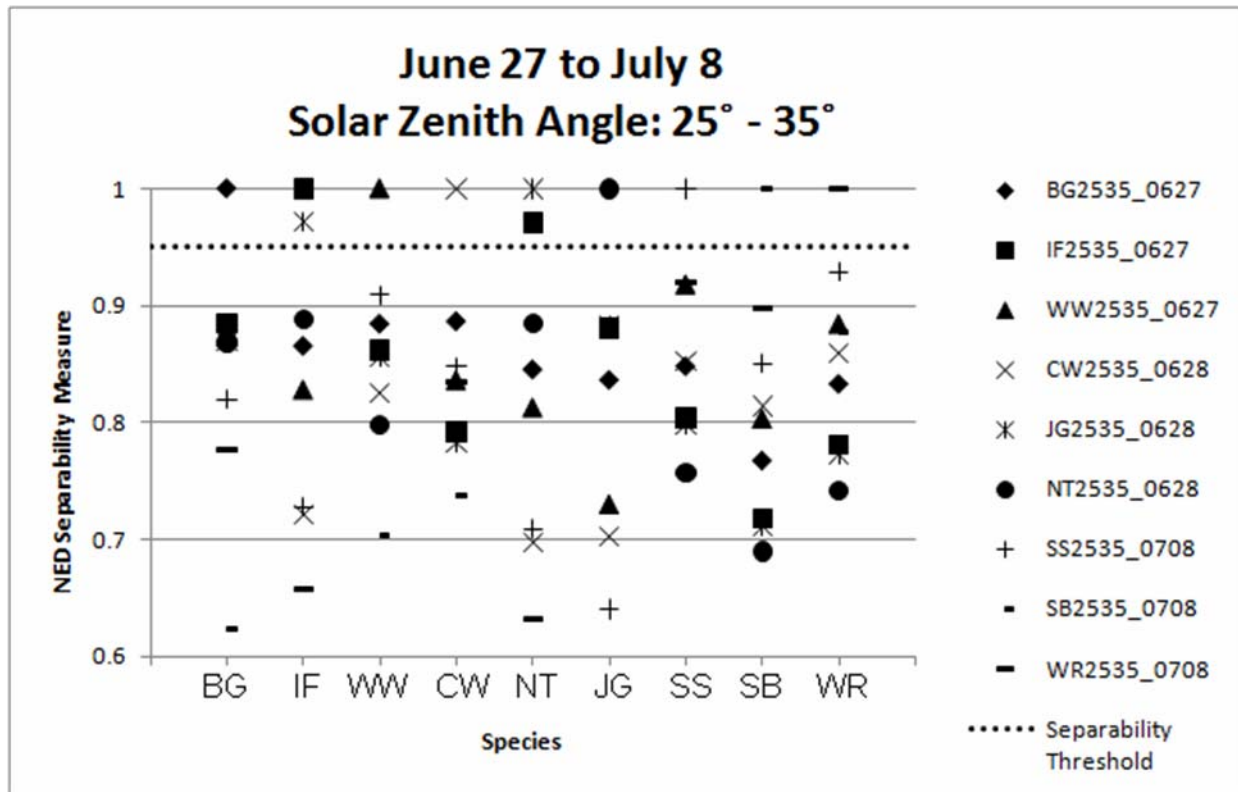
angle changes, differences in illumination direction and intensity cause changes in the amounts of sun-lit and shaded areas on the plant. The effect on separability can be seen in Appendix Figures 1 – 6. In Appendix Figures 1 and 2 (the lowest solar zenith angles measured), and in Appendix Figures 5 and 6 (the highest solar zenith angles measured), Idaho fescue and June grass spectra are similar. In Appendix Figures 3 and 4 blue grama is similar to Idaho fescue and June grass, respectively. It would appear, then, that the solar zenith angle does have an effect on separability when plant structure is left intact during measurement. Appendix Figures 7 – 12 and 13 – 15 display a similar case: a majority of the plots showing good separability between species interrupted by three instances of plant spectra being similar. From Appendix Figure 16 to 17 there is a decrease in the degree of species separability through the remainder of the season since the vegetation becomes more senescent. All of the appendix figures depict species separability for the time periods that they represent.

Appendix Table 1 (a copy of Table 3.3): Abbreviations used for identifying species in separability plots. Provided for ease of reference when using the Appendix Figures.

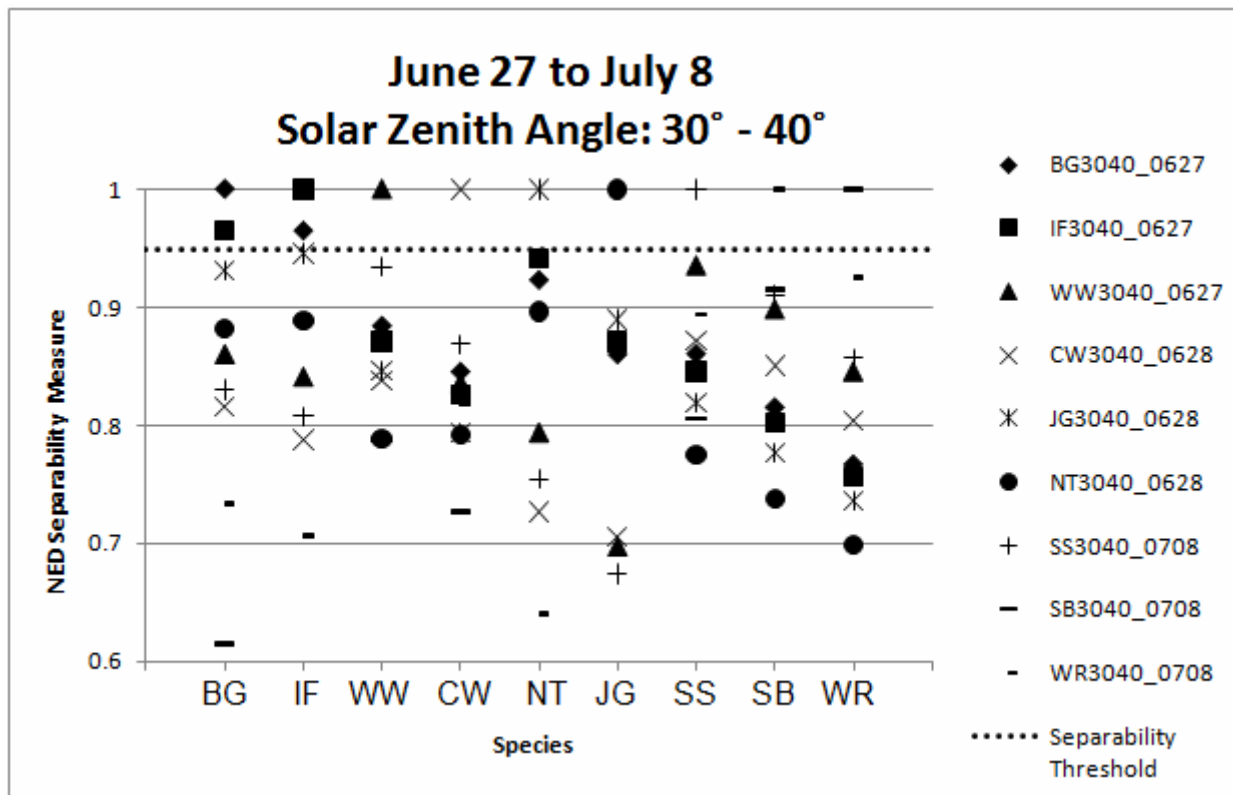
Abbreviation	Common Name	Latin Name
BG	Blue grama	<i>Bouteloua gracilis</i>
IF	Idaho fescue	<i>Festuca idahoensis</i>
JG	June grass	<i>Koeleria gracilis</i>
NT	needle-and-thread	<i>Stipa comata</i>
WW	western wheatgrass	<i>Agropyron smithii</i>
CW	crested wheatgrass	<i>Agropyron cristatum</i>
SB	snowberry	<i>Symphoricarpos occidentalis</i>
SS	silver sagebrush	<i>Artemisia cana</i>
WR	Wild rose	<i>Rosa acicularis</i>



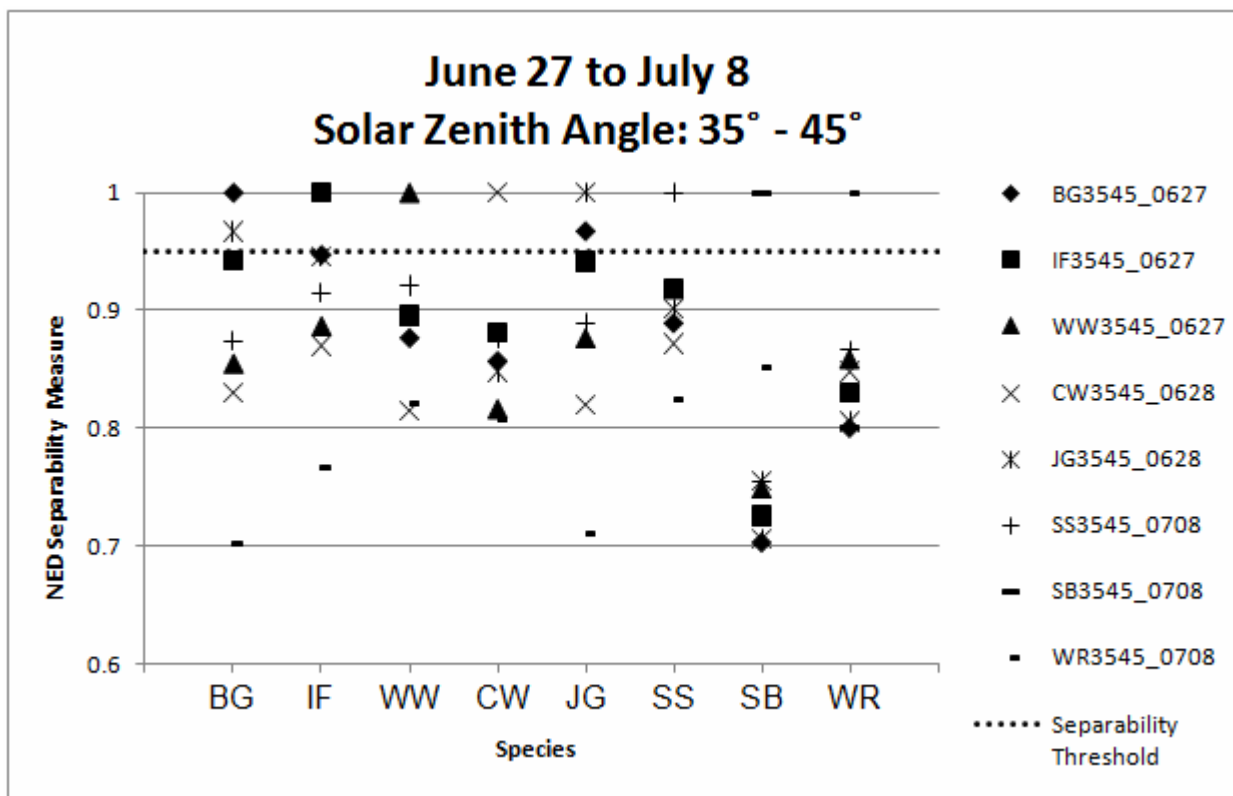
Appendix Figure 1



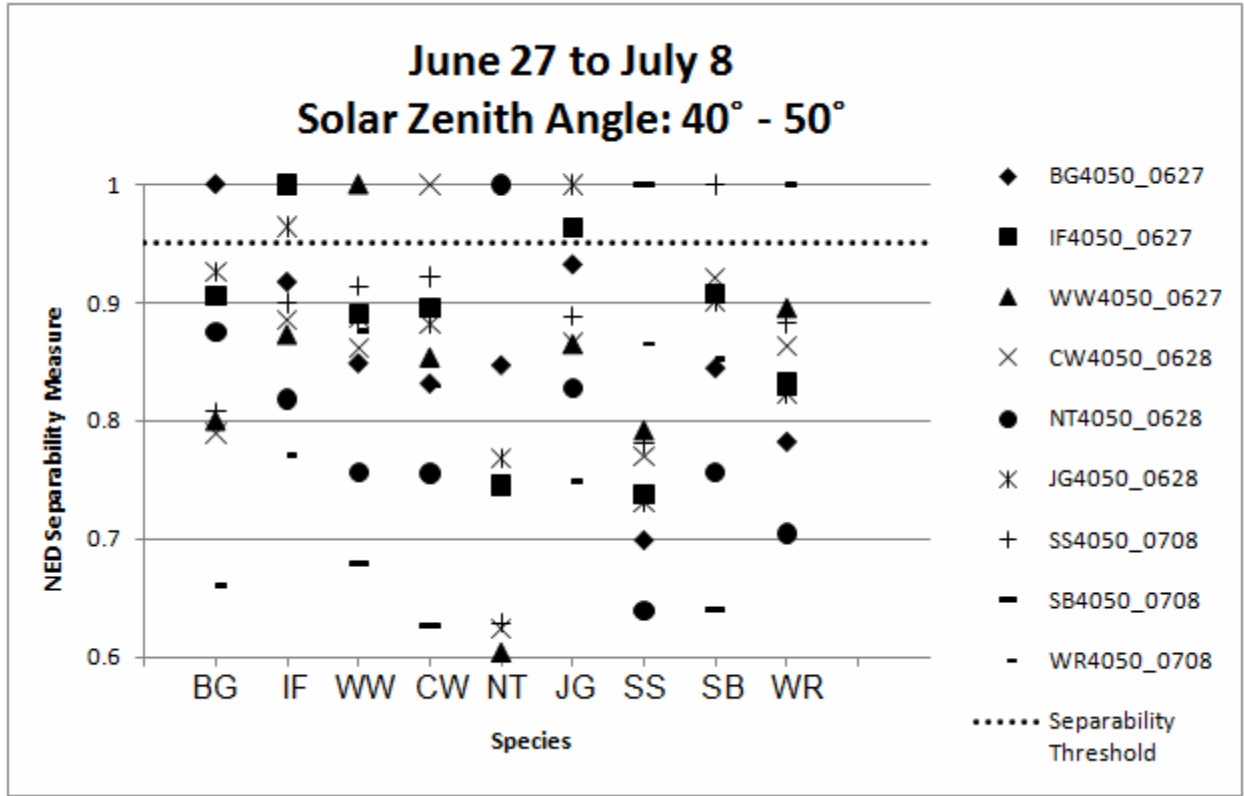
Appendix Figure 2



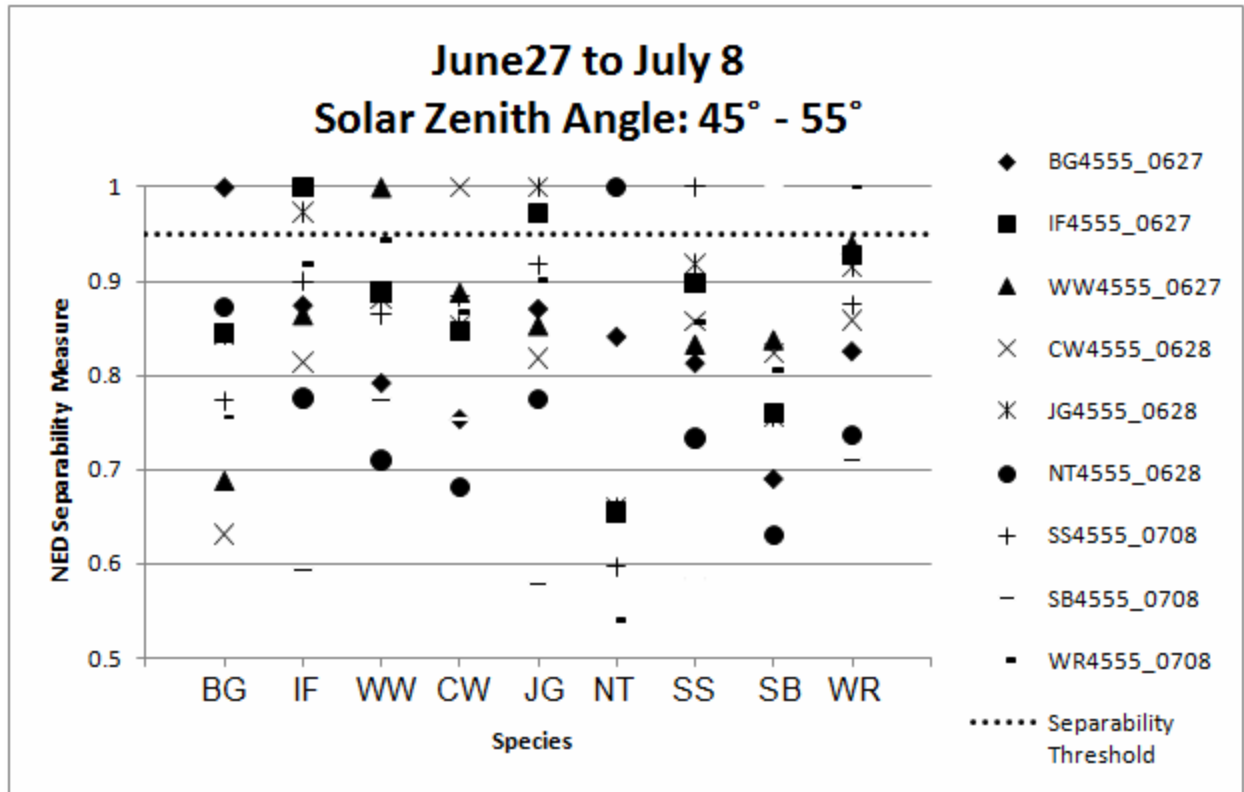
Appendix Figure 3



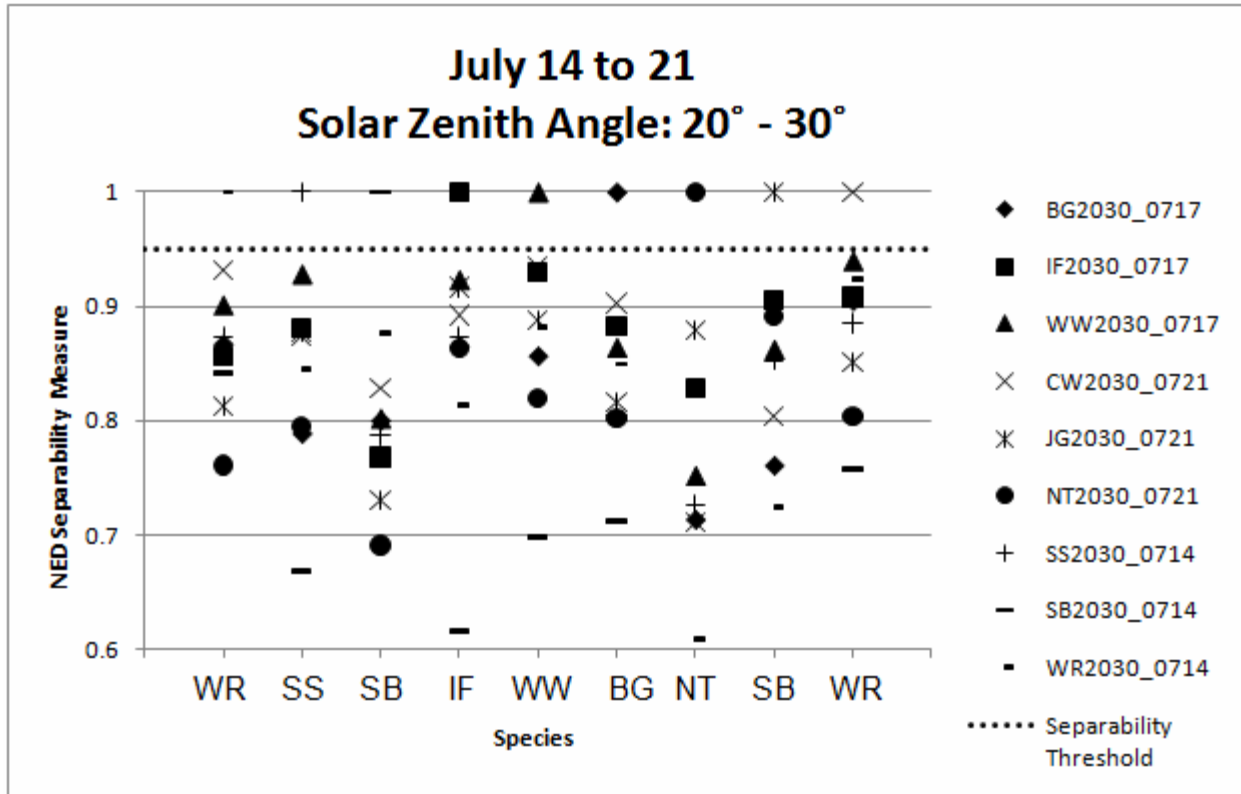
Appendix Figure 4



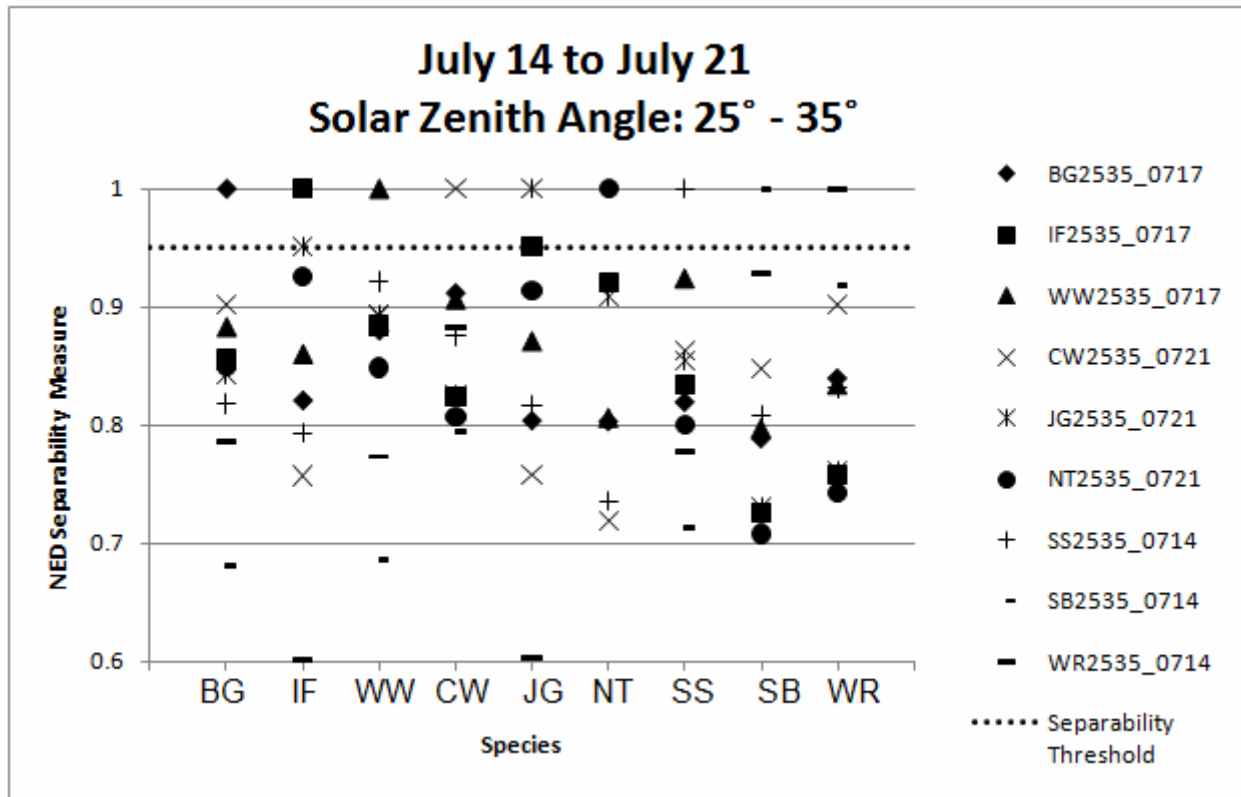
Appendix Figure 5



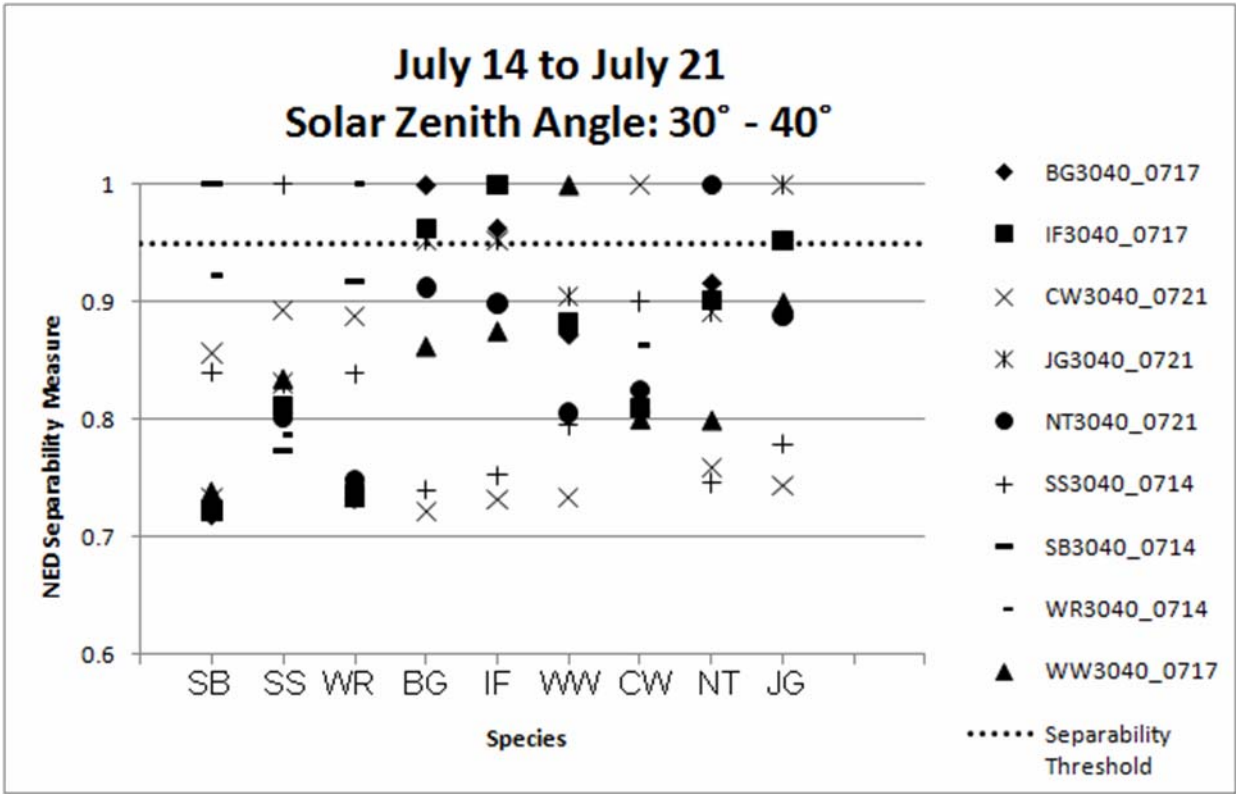
Appendix Figure 6



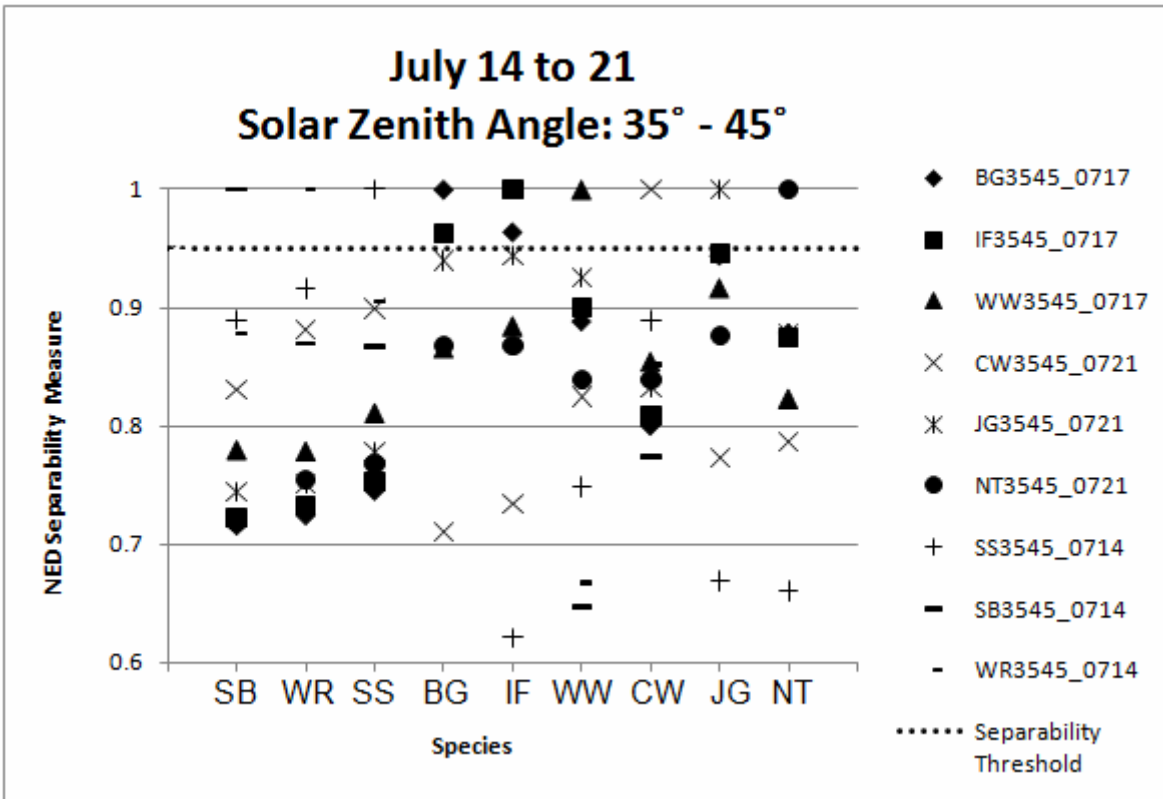
Appendix Figure 7



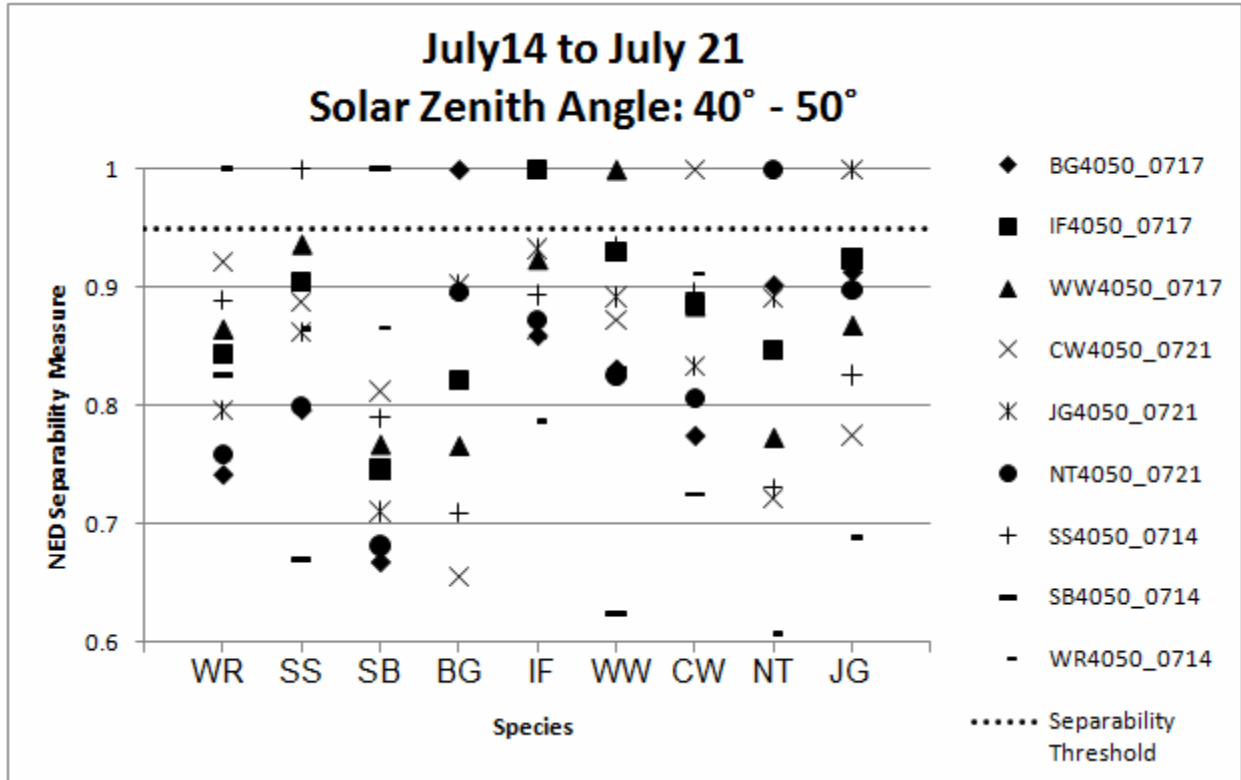
Appendix Figure 8



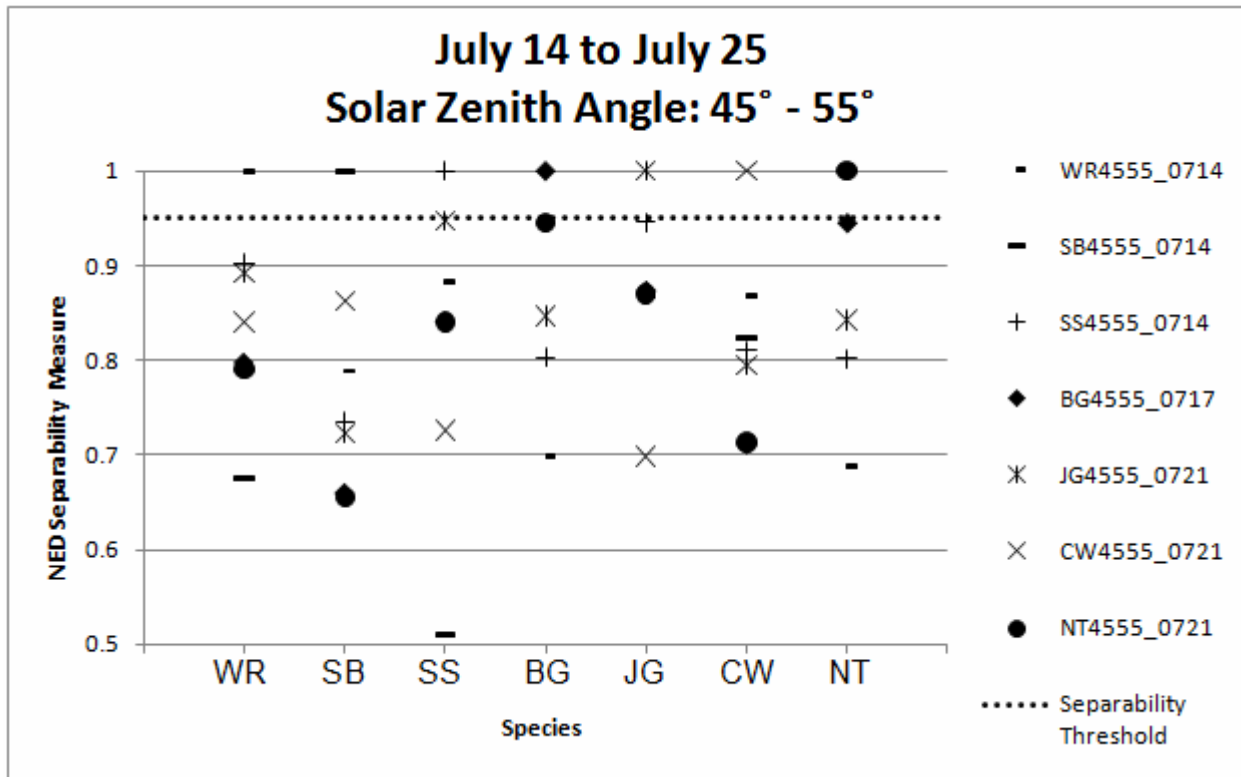
Appendix Figure 9



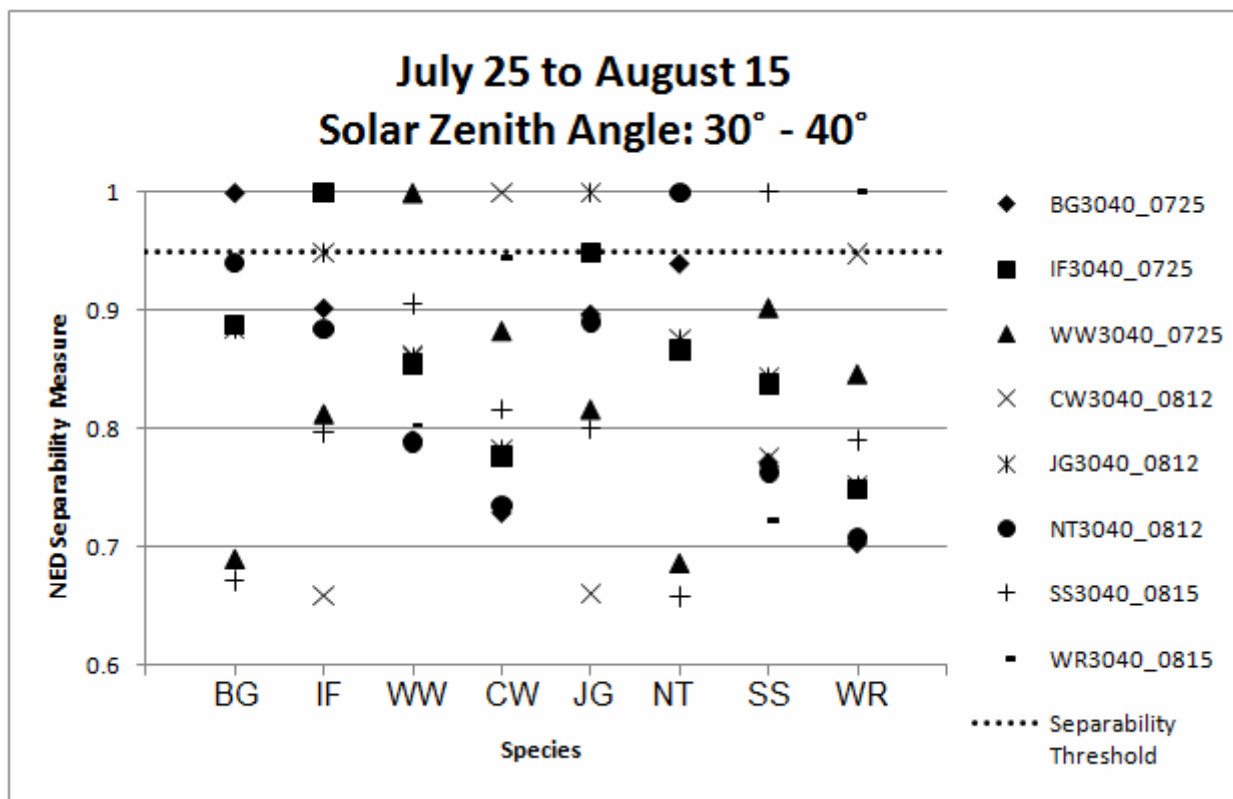
Appendix Figure 10



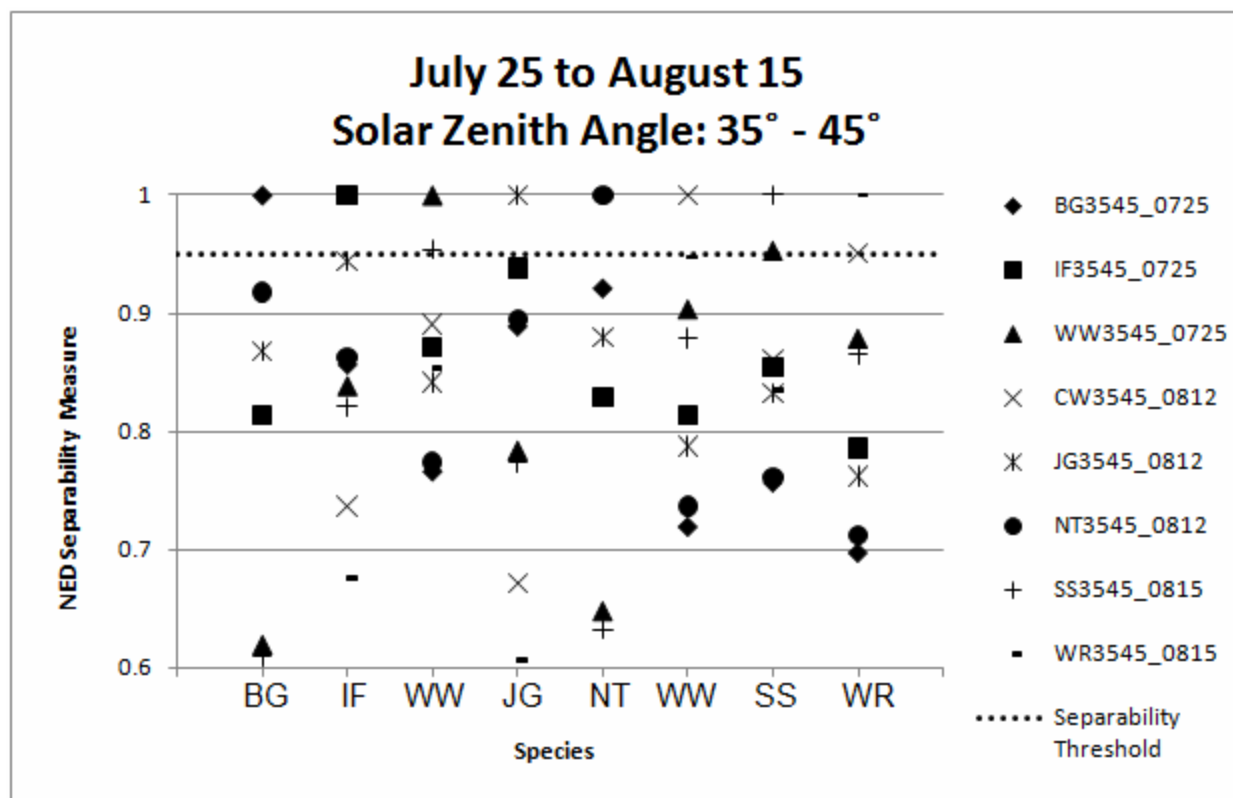
Appendix Figure 11



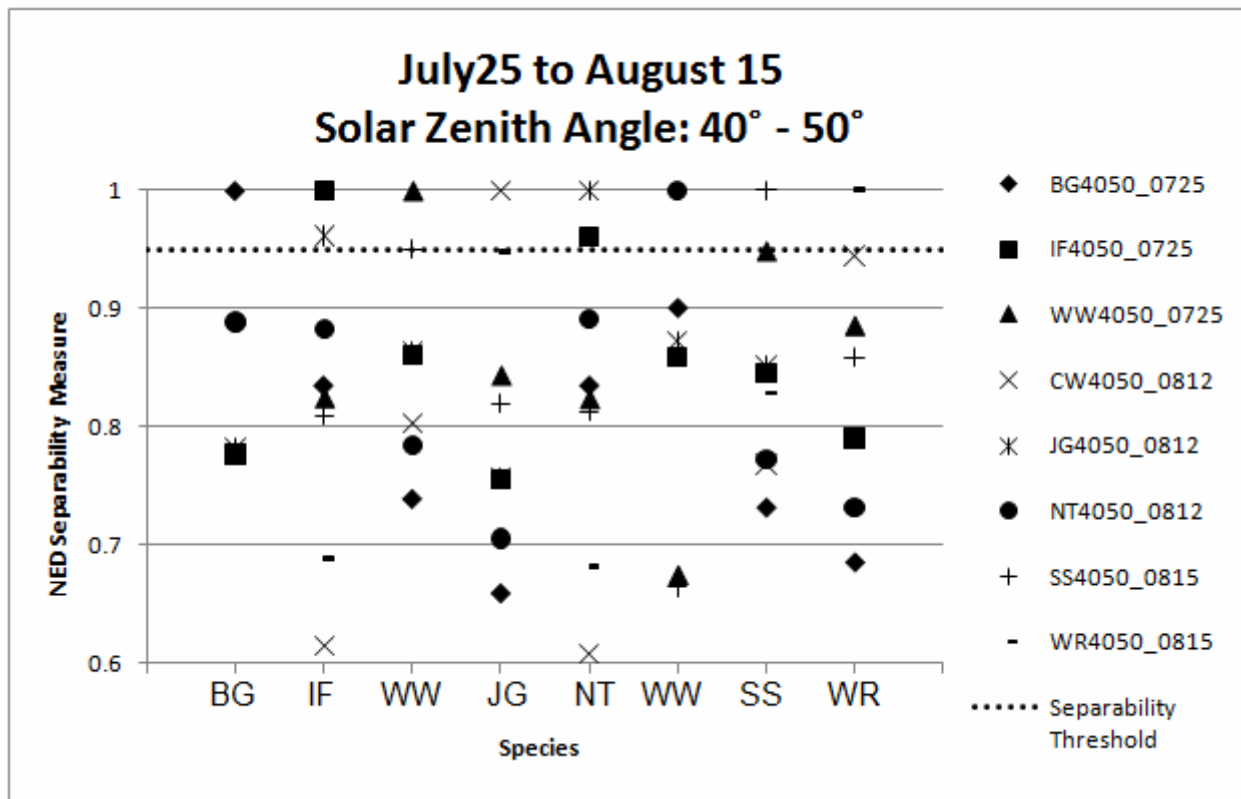
Appendix Figure 12



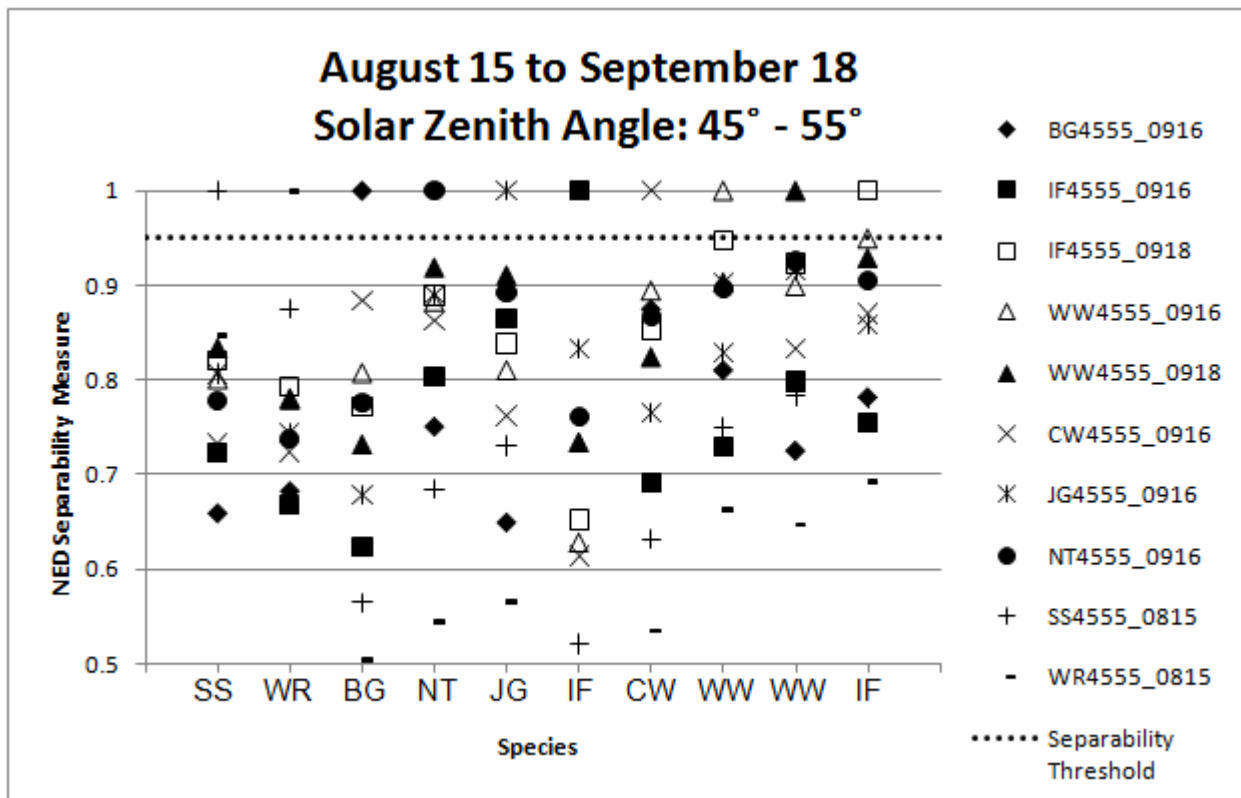
Appendix Figure 13



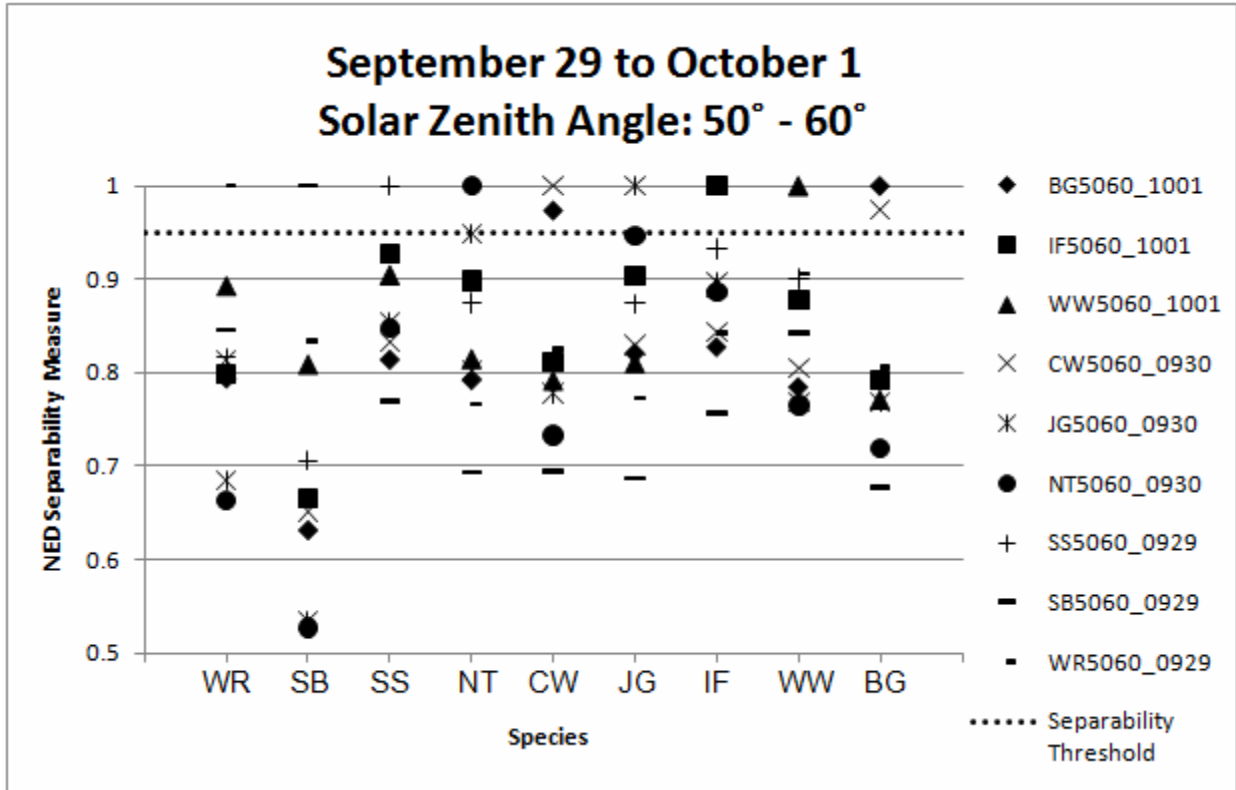
Appendix Figure 14



Appendix Figure 15



Appendix Figure 16



Appendix Figure 17